UNIVERSITY OF SOUTHERN QUEENSLAND

Development and characterisation of an ultra-long exposure UV dosimeter

A dissertation submitted by

Abdurazaq A. A. Amar

BSc. (Physics), MSc. (Applied Physics)

For the award of

Doctor of Philosophy

2014

Abstract

Excessive exposure to solar ultraviolet (UV) radiation is known to have detrimental effects on human health, some of which are cumulative in nature with impacts that may arise after years and decades of exposure. Therefore, it is important that the risk associated with prolonged UV exposure can be investigated; this requires long-term studies in which large-dose measurements can be accurately quantified.

Chemically-based UV dosimeters have been widely used to measure personal UV exposure since 1976. Despite the development of electronic UV dosimeters, chemical dosimeters maintain their suitability in human exposure research as versatile, labour- and cost-effective UV monitors that require no power. The main limitation of existing chemical dosimeters is their short dynamic measurement range, as they are saturated after relatively short exposure times. Consequently, prolonged personal UV exposures are estimated either from measurements spanning just a few days, with high uncertainty, or by the regular replacement of dosimeters on location, a practice that increases the cost and effort. A dosimeter that continuously measures longer periods would facilitate the task and provide more reliable estimates of prolonged UV exposures.

A new chemical UV dosimeter that meets this demand was developed and fully characterised in this study. The dosimeter, composed of unstabilised solvent cast polyvinyl chloride (PVC) in 16 μm thin film, is able to measure at least three weeks of full day exposure to solar UV radiation under clear sky conditions in summer at subtropical sites. This is twenty times the dose capacity of the most commonly used chemical UV dosimeter, a polysulphone based UV dosimeter.

The optimal parameters of the dosimeter's construction and its dosimetric properties were experimentally investigated and characterised. The results show that the proposed dosimeter is easy to prepare, inexpensive, physically robust and easily analysed using an FTIR spectrometer. It responds mainly to UVB radiation, and hence can be calibrated for quantifying erythemally effective doses for long-term personal exposure studies. The response of the dosimeter to solar UV radiation is independent of temperature and dose rate. It also, exhibits an acceptable angular-error (defined as the deviation of the dosimeter's relative response from the cosine function when the angle of incident beam is changed) and almost no dark reaction.

A field test was conducted to validate the proposed dosimeter with long-term personal UV exposure measurements. The erythemal UV exposures to selected anatomical sites on rotating head form manikins measured with the PVC dosimeter agreed well with the measurements obtained concurrently by a lower dose capacity chemical UV dosimeter, and are on a level with the results reported in earlier similar studies.

The characterised dosimeter is a valuable tool for research on the latent effects of cumulative UV exposure on human health. Measurements over longer periods will provide more reliable annual and lifetime exposure estimates as the larger the sample size (length of measurement period), the more accurately the sample will present the population (annual or lifetime UV exposure).

Certification of Dissertation

The research contained in this dissertation is the full documentation of the research results that are published and presented as

1. Amar, A & Parisi, AV 2012, 'Investigation of unstabilized polyvinyl chloride (PVC) for use as a long-term UV dosimeter: preliminary results', *Measurement Science and Technology*, vol. 23, no. 8, pp. 1-7.
2. Amar, A & Parisi, AV 2013, 'Spectral response of solvent-cast polyvinyl chloride (PVC) thin film used as a long-term UV dosimeter', *Journal of Photochemistry and Photobiology B: Biology*, vol. 125, pp. 115-20.
3. Amar, A & Parisi, AV 2013, 'Optical properties of a long dynamic range chemical UV dosimeter based on solvent cast polyvinyl chloride (PVC)', *Journal of Photochemistry and Photobiology B: Biology*, vol. 128, pp. 92-9.
4. Amar, A and Parisi, AV. (2012) *Investigation of unstabilized polyvinyl chloride (PVC) for use as a long-term UV dosimeter: preliminary results.* In: 37th Annual Conference of the Australasian Radiation Protection Society (ARPS 2012): Radiation Safety: Bridging the Gap, 14-17 Oct 2012, Sydney, Australia.

I certify that the ideas, experimental work, results, analyses, software and conclusions reported in this dissertation are entirely my own effort, except where otherwise acknowledged. I also certify that the work is original and has not been previously submitted for any other award, except where otherwise acknowledged.

_____ _____

Signature of Candidate Date

ENDORSEMENT

_____ _____

Signature of Principal Supervisor Date

_____ _____

Signature of Associate Supervisor Date

Acknowledgements

I would like to express my deepest gratitude and respect to my principle supervisor, Professor Alfio Parisi, for his excellent guidance, patience and care, and for providing me with valuable advice and suggestions throughout the research.

I would like to thank the Libyan Government through the Higher Education Ministry and Azzawia University for providing the scholarship for this research.

I would like also to thank my parents, brothers and sisters for all their love and support throughout the years. My endless love to my wife and our children: Riman, Abdurrahman and Raseel.

I would like also to express my thanks to a number of staff members of the Faculty of Health, Engineering and Sciences for various contributions made to this research:

- Associate Professor Brad Carter took the role of associate supervisor and made valuable contributions to the project design and provided valuable comments and suggestions;
- Dr Joanna Turner shared her experience in the field of UV dosimetery and contributed to the discussion regarding chemical UV dosimeters, and also assisted in proofreading and editing of the research proposal;
- Dr Nathan Downs provided valuable support in equipment training and calibration;
- Mr Oliver Kinder designed and constructed a number of precision mechanisms required for the experimental work;
- Mr Kim Larsen provided work space in the chemistry laboratory and assisted with the equipment required for the casting of the polymer films and also provided training and support relating to the FTIR spectroscopy; and
- Dr Kathryn Reardon-Smith contributed by proof reading and editing this dissertation and some of the related published papers.

Contents

Table of Figures

List of Tables

Chapter 1

Introduction

1.1 Introduction.

1.2 Objectives.

1.3 Dissertation outline.

1.1 Introduction

The sun is necessary for maintaining life on Earth. It provides the earth with the solar radiation required for all creatures and vegetation to survive. The infrared band of solar radiation warms the earth, while the light (visible band) is indispensable for visibility and the photosynthetic process in plants (Heisler & Grant 2000a). However, ultraviolet radiation (UV), the shortest waveband of solar radiation that reaches the earth, while it has some beneficial outcomes, has potentially deleterious effects on living organisms.

The effects of exposure to solar ultraviolet (UV) radiation on human health have long been an important subject of research. Moderate exposures to UV radiation are essential for cutaneous synthesis of vitamin D (Holick 2008; Juzeniene et al. 2011; Webb & Holick 1988) that plays a key role in skeletal health (Powers & Gilchrest 2012; Ross et al. 2011; Webb & Holick 1988). On the other hand, excessive exposure to solar UV radiation may result in acute and chronic health issues. Excessive exposure may cause acute sunburn that takes hours to days to develop following the exposure (Carli et al. 2008; Juzeniene et al. 2011). Other known acute effects are the development of the eye problems such as photokeratitis and photoconjunctivitis (O'Shea 1996). Fortunately, acute effects are short-lived and reversible. In contrast, large UV doses accumulated through long-term exposures have been shown to cause irreversible damage, the effect of which may become evident after years to decades of exposure to UV radiation (Juzeniene et al. 2011). For instance, cumulative UV exposures are associated with the development of skin cancer, photo ageing, and degradation of the eyes (Azzam & Dovrat 2004; Chang et al. 2010; Juzeniene et al. 2011; Rabe et al. 2006).

The assessment of individual solar UV exposure at any given time is, therefore, very important; particularly the estimation of doses accumulated through prolonged irradiation. In this regard, the World Health Organization has been encouraging researchers to develop and improve feasible techniques for personal UV exposure measurement (WHO 1979; 1994) to support studies relating UV exposure to human health. Measurements of personal exposure will help to better understand dose effect relationships and improve sun-protective strategies.

Monitoring personal UV exposure can be achieved through the use of electronic, biological or chemical UV dosimeters.

Miniaturised electronic dosimeters characterised by their reusability and high accuracy can be considered the optimum technique for personal exposure measurements. Some of these dosimeters have the ability to continuously register exposure for time periods up to several months of operation (Seckmeyer et al. 2012) with a response to UV radiation that matches the erythema action spectrum defined by the International Commission on Illumination (CIE) (CIE 1998). However, the high cost of electronic dosimeters often precludes their use in UV exposure research, especially for large scale anatomical measurements.

Biological dosimeters also provide a reliable means for quantifying UV exposures (Bérces et al. 1999; Munakata et al. 1996). Some bio-dosimeters are suitable for long-term measurements. However, the preparation of most bio-dosimeters involves complex procedures and the readout process often requires sophisticated techniques to determine the effect of exposure (Webb 1995).

Chemical dosimeters have long been the preferred method for measuring personal exposure to UV radiation as they are much cheaper than the electronic devices, and more simple and feasible than the biological dosimeters (Naggar et al. 1995). The principle of chemical UV dosimeters is to measure the change in optical density induced in thin films of synthetic polymers by UV radiation (Diffey 2002a). The measured changes are then calibrated against a UV recording instrument to estimate the UV exposure (Parisi 2004).

Several polymers have been characterised and employed in personal UV exposure measurements. At the top of the list come the polysulphone (PS) and polyphenlyne oxide (PPO) thermoplastics (Berre & Lala 1989; Davis et al. 1976). PS and PPO dosimeters have been successfully employed in a variety of personal UV exposure studies (e.g. Diffey et al. 1996; Moise et al. 1999; Parisi & Kimlin 2000; Schouten et al. 2010; Siani et al. 2009; Siani et al. 2011; Turnbull & Schouten 2008). The main disadvantage of these dosimeters is that they become saturated after a specific exposure time and therefore their ability to measure solar UV radiation over extended periods (e.g. one week) is limited.

Estimating long-term UV exposures using existing chemical UV dosimeters is conventionally undertaken by either frequently replacing the dosimeters before they saturate (Siani et al. 2008) or circulating (multiplying) the dose measured in a short period (e.g. one-day sun exposure) over a longer period (Moehrle et al. 2003). The first methodology is time consuming and labour intensive, while the latter increases the margin of error of estimated doses by ignoring the day-to-day variation in the solar spectrum, as the measured one-day sun exposure does not represent the general average daily sun exposure through a season or a year (Moehrle et al. 2003). A chemical dosimeter that is capable of recording a cumulative solar UV exposure over long periods (weeks) will provide more reliable estimations and will be of great benefit for studies of latent outcomes of exposure to UV radiation that are related to cumulative exposure throughout a lifetime.

This research intends to identify and characterise a photosensitive polymer with a greater dynamic measurement range than the known polymers employed as chemical UV dosimeters. The proposed polymer has to be inexpensive and commercially available and the dosimeter construction and readout processes should be simple and able to undertaken in a standard laboratory. Importantly, the new dosimeter should meet all the dosimetric and physical requirements of chemical UV dosimeters with the ability to measure UV exposure over an extended period of time.

1.2 Objectives

The overall objective of this research is to determine at least one polymer that satisfies the requirements for use as a long-term UV dosimeter. To reach this goal, the research also has the following subsidiary objectives:

1. Review the literature and conduct pilot studies in order to identify polymer(s) that seem to have the required basic properties of a long-term UV dosimeter. Once the best polymer(s) for this purpose have been identified, undertake the following tests.
2. Determine the optimal parameters for the dosimeter fabrication and the standard specifications of the dosimeter.
3. Investigate the dosimetric properties relevant to the quantification of solar UV radiation and listed in the literature. These properties are: film reproducibility, spectral response, angular response, dose-rate independency and temperature independency.
4. Investigate any possible impacts of the dark reaction and background material on the measured exposures.
5. Construct dose-response curves (calibration curves) of the dosimeter for each season of the year.
6. Employ the dosimeter in long term UV exposure experiments to compare and evaluate the results and estimate the measurement uncertainty of the proposed dosimeter.

1.3 Dissertation Outline

The approach of the research conducted to achieve the above-mentioned objectives is outlined as follows:

- Chapter 2 sets out the background to the study and presents a critical review of the relevant literature. This chapter defines ultraviolet radiation and provides details regarding its specific properties and quantities. The chapter also describes solar UV radiation, its origin and the factors impacting global solar UV on the earth's surface. The effects of human exposure to solar UV radiation and the necessity to quantify UV radiation are discussed. The three main categories of personal UV dosimetry outlined above are examined and the focus on chemically based UV dosimeters as a preferred tool justified. The dosimetric properties required for any chemical dosimeter are then reviewed in detail along with other practical requirements. The last point of this chapter is a review on the suitability of the polymer polyvinyl chloride (PVC) for long term UV measurements.
- The experimental research conducted in the development and characterisation of the PVC dosimeter is presented in Chapter 3. This chapter provides a detailed description of the instrumentation that was used and procedures that were followed to fabricate the dosimeter and investigate its properties and performance.
- Chapter 4 presents the results and analysis of research that was conducted based on methods described in Chapter 3.
- Chapter 5 presents and discusses the results of research conducted outdoors to measure long-term solar UV exposure of some anatomical sites using the new chemical UV dosimeter.
- The experimentally determined fabrication parameters, standardised specifications, dosimeteric properties and performance of the proposed PVC dosimeter are discussed in Chapter 6. This chapter concludes by suggesting some recommendations for future research.

Chapter 2

Literature review

2.1 Ultraviolet radiation (UV).

2.2 UV Quantities and units.

2.3 Solar UV radiation.

2.4 Effects of exposure to solar UV radiation on humans.

2.5 Measuring personal exposure to UV radiation.

2.6 Chemical UV dosimeter requirements.

2.7 Suitability of polyvinyl chloride (PVC) for long-term UV dosimetry.

2.8 Conclusion.

2.1 Ultraviolet radiation (UV)

Ultraviolet radiation is electromagnetic radiation with a wavelength (λ) shorter than that of visible light, but longer than X-rays, i.e., wavelengths from about 10 nm to 400 nm (Madronich 1993), corresponding to photon energies between 4 and 124 eV.

The full identification of UV radiation has been gradually achieved over about two centuries, coupled with the development of theoretical concepts and the improvement of devices for producing and quantifying radiation. The first major discovery was made by Ritter in 1801 who proved the existence of invisible radiation beyond the violet end of the light spectrum (radiation with shorter wavelength - higher energy- than 400 nm) (Hockberger 2002). Ritter dubbed the new radiation "deoxidizing rays" as it darkens silver chloride-soaked paper even more than visible light does. The term was later replaced by "chemical rays" to describe the UV-Violet-Blue region of the electromagnetic spectrum; this term remained in use during the 19th century until the term "UV radiation" was adopted specifically only for the invisible radiation beyond violet light (Hockberger 2002). By 1920, with improved knowledge of the concept, nature and properties of UV radiation, scientists were able to produce and quantify the entire band of UV radiation (Hockberger 2002).

UV radiation is emitted from the atoms of some materials during the relaxation process of core electrons excited to higher energy levels either by heating the material to an incandescent temperature, as is the case with solar UV, or by passing electrical current through specific materials as in artificial UV sources (Hockberger 2002). The emitted UV photons that have energies higher than 12 eV are capable of ionizing atoms and molecules when hitting a surface or passing through some materials (Persson 1991). Therefore, UV radiation is subdivided into ionizing UV (wavelengths < 100 nm) and non-ionizing UV (wavelengths > 100 nm). Ionizing UV is usually excluded from the UV spectrum and the UV band is considered to span the region from 100 nm to 400 nm (Diffey 2002b).

UV radiation is classified into three major categories on the basis of its physical properties (Hockberger 2002): Vacuum UV, Near UV and Far UV. Vacuum UV refers to wavelengths below 180 nm as these wavelengths are absorbed strongly by air and can only propagate in a vacuum. Near UV includes wavelengths between 290 nm and 400 nm; this is the entire band of solar UV radiation that reaches the earth's surface. Far UV describes wavelengths between 180 nm and 290 nm (i.e., wavelengths between vacuum UV and near UV).

In photobiology, where the effects of UV bands on biological systems are emphasised, UV radiation is subdivided into three main bands: UVC, UVB and UVA, representing the wavebands 100–280 nm, 280–315 nm and 315–400 nm, respectively (Sliney 2007). In this classification, UVC is designated for wavelengths that are very strongly absorbed by most biological systems, leading to severe damage

in living organisms (Sliney & Chaney 2006). Although UVC is energetically stronger than UVB, UVB is of greater importance for human health as it is the highest energy component of solar radiation that reaches the earth's surface as solar UVC is blocked by the atmosphere. UVA is the lowest energy per photon UV sub band; however, it spans a wider range of wavelengths and has penetration characteristics that enhance its effects on living organisms (Vázquez & Hanslmeier 2006). The boundaries between these three subdivisions, however, are somewhat arbitrary and vary according to disciplines. For instance, the wavelengths 290 nm and 320 nm are often used as boundaries between UVC/UVB and UVB/UVA, respectively (Diffey 1991; WHO 1994) while UVA may be subdivided into UVA1 and UVA2 at 340 nm (Diffey 2002b) as these play different roles in some biological processes.

In addition to the previous categories, there are also other conventions defining UV bands according to their use in different branches of science and technology. Figure 2.1 summarises the most common UV categories.

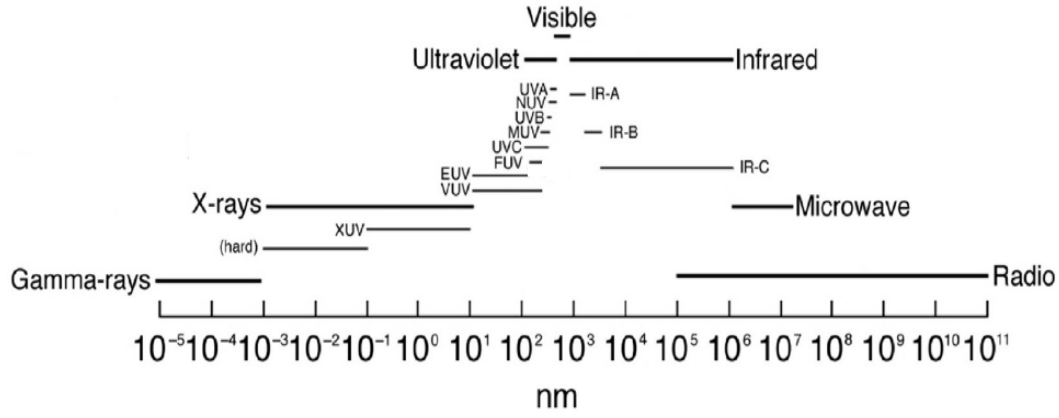

Figure 2.1: Electromagnetic radiation spectral categories from gamma-rays through radio wavelengths (ISO 2007).

In this research, the designations UVC, UVB and UVA indicate the spectral regions 100–280 nm, 280–320 nm and 320–400 nm, respectively.

2.2 UV Quantities and units

UV radiation, as an electromagnetic radiation, is a propagation of quanta of energy (photons) by the oscillations of the electromagnetic field. Each of these photons is characterised by the wavelength λ that determines its energy $e(\lambda)$, the fundamental quantity in radiometric measurements, according to Planck's law:

$$e(\lambda) = \frac{hc}{\lambda} = h\nu \qquad (2.1)$$

where $h = 6.626 \times 10^{-34}$ Joules.second (J.s) is Planck's constant, $c \approx 3 \times 10^{8}$ meters per second (m/s) is the speed of light in vacuum, $\nu = \frac{c}{\lambda}$ is the frequency in Hertz (Hz), λ is expressed in meters (m), and $e(\lambda)$ in Joules (J). The energy transported by n photons in a monochromatic beam of wavelength λ is then $ne(\lambda)$ and is called the spectral radiant energy $Q(\lambda)$. For a beam of radiation, the term "radiant energy" (Q) refers to the integration of energies over all wavelengths of the desired waveband (UV in this case) (Kohler 1998), i.e.,

$$Q = \int_{280}^{400} Q(\lambda) d\lambda \qquad \text{Joules (J)} \qquad (2.2)$$

while the radiant flux (power) (P) is the radiant energy passing through a point at a unit time (Kohler 1998), i.e.,

$$P = \frac{\int_{280}^{400} Q(\lambda) d\lambda}{dt} = \int_{280}^{400} P(\lambda) d\lambda \qquad \text{Watts (W)} \qquad (2.3)$$

where $P(\lambda)$ is the spectral power (spectral radiant flux).

For studies that are concerned with the effects of UV exposure, i.e. the interaction between the incoming UV radiation and received surfaces (e.g. human exposure to UV radiation), the most fundamental radiometric quantities are the irradiance, radiant exposure and the spectrally weighted quantities. Irradiance (E) is the incident radiant flux on a unit area of a receiver, and is expressed in Watts-per-square-meter (W/m^2) (McCluney 1994). Spectral irradiance $E(\lambda)$ is the irradiance for a single wavelength or narrow spectral band; it is measured by spectroradiometers which give the spectral power distribution (spectral irradiance distribution) in $W/m^2/nm$. The radiant exposure (H) is the radiant energy striking a unit surface area of an irradiated object over a specific period of time t. It can be calculated from the relationship:

$$H = \int_0^t \int_{280}^{400} \frac{Q(\lambda)d\lambda dt}{surface \quad area}$$

$$= \int_0^t \int_{280}^{400} H(\lambda)d\lambda dt \quad \text{J/m}^2 \qquad \text{(McCluney 1994)} \qquad (2.4)$$

In several UV-matter interaction processes, such as the absorption of UV radiation by biological macromolecules, the effects of UV radiation are strongly dependent on the wavelength of radiation, i.e. they depend on how the power is distributed with respect to wavelength (Diffey 2002b). To take this fact into account, action spectra and spectrally weighted UV quantities have been introduced into radiometric terminology (WHO 1994). An action spectrum $A(\lambda)$ is a function that reflects the relative effectiveness of UV radiation at different wavelengths in producing a certain biological effect (Vecchia et al. 2007). Examples of some action spectra are displayed in Figure 2.2: the erythema action spectrum (CIE 1998); the mammalian non-melanoma skin cancer action spectrum (De Gruijl & Van der Leun 1994); and the DNA damage action spectrum (Setlow 1974).

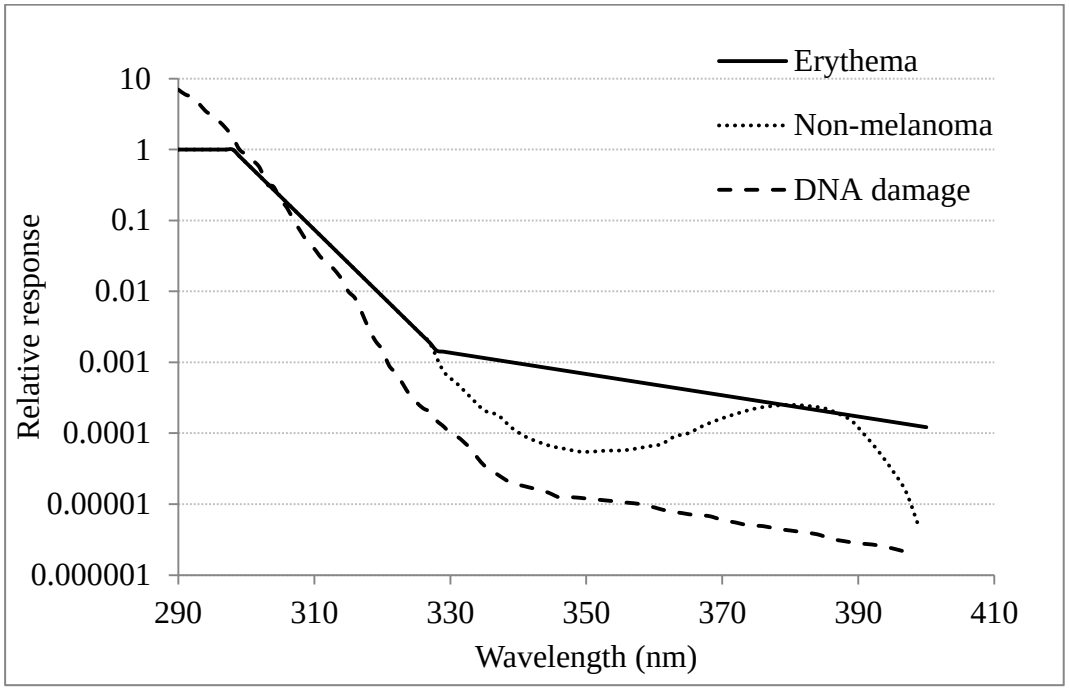

Figure 2.2: Action spectra of selected UV-related effects.

Specialized spectrally weighted quantities $X_{S.W}$ can be obtained by integrating the desired spectral quantity $X(\lambda)$ with an action spectrum of interest $A(\lambda)$ over the relevant wavelength range (CIE 2014; Tarrant 1989), i.e.

$$X_{S.W} = \int_{UV} X(\lambda)A(\lambda)d\lambda \tag{2.5}$$

Hence, spectrally weighted UV irradiance $E_{S.W}$ will be given by

$$E_{S.W} = \int_{UV} E(\lambda)A(\lambda)d\lambda \qquad \text{W/m}^2 \tag{2.6}$$

and spectrally weighted UV radiant exposure $H_{S.W}$ can be calculated by

$$H_{S.W} = \int_{UV} H(\lambda)A(\lambda)d\lambda \qquad \text{J/m}^2 \tag{2.7}$$

The weighted UV irradiance is usually referred to as "exposure dose-rate" or "dose-rate" and the weighted radiant UV exposure as "exposure dose" or "dose". It should be pointed out that the meaning of the term "dose" here is the radiant exposure accumulated on the external surface or interface (not the absorbed dose), unlike its concept in medicine, pharmacology and toxicology where it refers to the dose of a chemical agent that is actually absorbed by a target tissue (Sliney 2007).

Erythema (sunburn or reddening of the skin), which is an indicator of the excessive exposure to UV radiation and may be the beginning of subsequent skin disorders, is also wavelength dependent. The active radiant exposure in producing erythema (erythemally effective dose) (H_{ery}) is then calculated by

$$H_{ery} = \int_{UV} H(\lambda)A_{ery}(\lambda)d\lambda \qquad \text{J/m}^2 \qquad \text{(WHO 1994)} \tag{2.8}$$

where $A_{ery}(\lambda)$ is the erythemal action spectrum (CIE 1998). H_{ery} is expressed in J/m^2. Other units are the minimum erythema (MED) dose and the standard erythema dose (SED) (Diffey et al. 1997). MED is the minimum erythemally weighted radiant exposure required to produce a just noticeable erythema on previously unexposed fair skinned individuals 8–24 hours after irradiation; MED is estimated to be 200–300 erythemally weighted J/m^2 (WHO 1994). Due to its dependency on the receiver and the observer, MED is not a purely physical quantity and thereby the SED unit has been introduced to describe the erythemally weighted dose (ICNIRP 2004), where 1 SED = 100 J/m^2. In terms of this unit, the threshold for erythema for fair skins is about 2 SED (CIE 2014).

2.3 Solar UV radiation

Life on earth depends on the sun. Although the sun is about 150 million km away from the earth, it provides the earth with the radiant energy required to drive all physical and biological processes in the earth system. The sun, which can be considered as a black body radiator having a surface temperature of about 5800 K (Diffey 2002a), emits radiation throughout the electromagnetic spectrum from gamma-rays to radio waves. The wavelength of emitted radiation depends on both the radiative temperature of the emitting region and its height from the centre of the sun. Generally, shorter wavelength radiations originate higher in the solar atmosphere (Floyd et al. 2005). UV radiation of wavelengths between 300 nm and 400 nm originates in the solar photosphere, while shorter UV wavelengths originate up to 100 km higher in the solar atmosphere (Frederick et al. 1989). The calculated total solar irradiance on the sun's surface (Stefan-Boltzman law) is about 63 MW/m^2. Of this amount, only about 1.366 kW/m^2 reaches the top of the earth's atmosphere (Gueymard 2004). This value is known as the "solar constant" although it fluctuates within 3.3% of its mean value, depending on the 27-day apparent solar rotation, the earth-sun distance, which varies with an annual cycle, and the 11-year cycle of sunspot activity (Diffey 2002a; Frederick et al. 1989).

2.3.1 Extra-terrestrial solar UV irradiance

The solar constant is the integrated spectral solar irradiance measured at the upper end of the earth's atmosphere, extra-terrestrial solar irradiance, on a surface normal to the incident radiation. Figure 2.3 illustrates the extra-terrestrial solar spectral irradiance (Gueymard 2004) plotted along with the emission of a 5800 ºK blackbody as calculated from Planck's law.

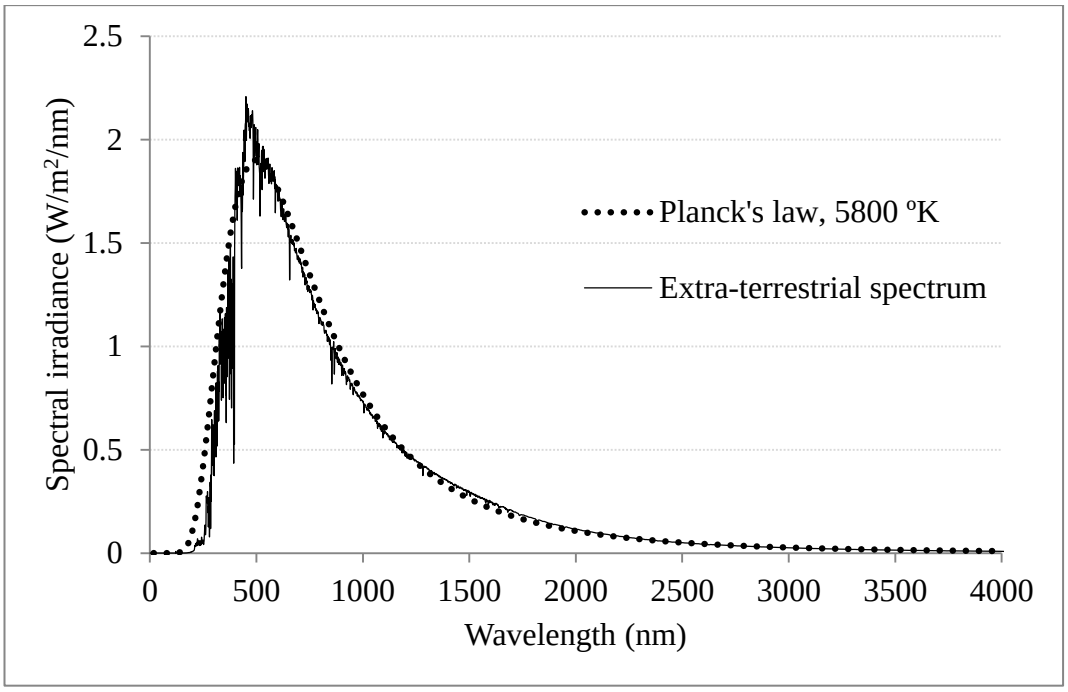

Figure 2.3: A comparison between the extra-terrestrial solar spectral irradiance and 5800 ºK blackbody emission.

In general, the solar spectral irradiance approximates the blackbody emission curve at this temperature (5800 ºK) with some superimposed line structures due to Fraunhofer absorption lines (Madronich 1993) and other solar absorption features, particularly in the UV-visible broadband. In addition to the absorption lines, the UV band deviates considerably from the blackbody curve as a result of the non-isothermal behaviour of the solar atmosphere (Qiang 2003). The infrared and visible regions of the solar spectrum account for about 50% and 40% of the sun's emission respectively, while the UVA, UVB and UVC represent only about 6.3%, 1.5% and 0.5% of the total irradiance, respectively (Frederick et al. 1989). The extra-terrestrial spectrum is strongly affected by absorption and scattering when passing through the earth's atmosphere; these reduce the radiation intensity and modify the spectral shape, particularly in the UV region.

2.3.2 Global solar UV irradiance

In contrast with the extra-terrestrial UV irradiance which describes the radiation that comes directly from the sun, the measured UV irradiance at the earth's surface is a combination of direct and diffused UV radiation. Direct UV radiation is the radiation that is received at an object's surface directly from the sun. Diffuse UV radiation is the part of UV radiation that has been modified by scattering before reaching the object's surface. This combination is known as the global UV irradiance. Other common names are terrestrial, ambient, surface and total solar UV irradiance.

Global UV irradiance is proportional to the extra-terrestrial irradiance that enters the atmosphere and is affected by atmospheric geophysical variables. These variables include the absorption and scattering by atmospheric constituents and scattering by irregularities at the earth's surface. Other factors that lead to large seasonal and geographical variations in the global irradiance are geometric variables such as the sun-earth distance and the solar zenith angle, which depends on latitude, date of the year and time of the day (Kerr 2005).

2.3.3 Absorption and scattering of UV radiation

Absorption and scattering processes may cause the extinction of a beam of direct radiation passing through the atmosphere. Absorption, in general, occurs when the energy of the incident radiation is high enough to take off an electron from an atom (ionization) or break a molecular bond (dissociation). In scattering, the affected atom is excited to a higher energy and immediately drops down to its original level, emitting radiation at the same wavelength as the absorbed one, but in a random direction. If, however, the excited atom collides with another atom before reemitting the radiation, the absorbed energy will be converted into kinetic energy of the colliding atom and the process will be considered as absorption. The general formula that describes the decrease in intensity of the beam of radiation passing through an incremental path in the atmosphere is (Huffman 1992):

$$dI(\lambda) = -k(\lambda)I(\lambda)dl \qquad (2.9)$$

where $I(\lambda)$ is the radiation intensity, $k(\lambda)$ is the extinction coefficient, and dl is the path length.

2.3.3.1 Absorption

Taking into account the absorption process only, the decrease in intensity of the incident radiation at altitude h from the earth's surface is given by (Huffman 1992):

$$dI(\lambda) = I_0(\lambda)\sum_i \exp\left(-\sigma_i(\lambda)\int_h^\infty n_i(h)\sec\chi \quad dh\right)d\lambda \qquad (2.10)$$

where $I_0(\lambda)$ is the initial intensity, $\sigma_i(\lambda)$ is the absorption cross section of the atmospheric constituent i, $n_i(h)$ is the number density of the constituent i at altitude h, and χ is the solar zenith angle.

2.3.3.2 Scattering

The scattering process results in a change of direction of the radiation without a change in its wavelength, leading to a decrease in the direct radiation and a possible increase in the diffuse component of the local irradiance. Scattering in the

atmosphere can be caused either by molecules (Rayleigh scattering) or from larger solid or liquid aerosols (Mie scattering) (Sliney & Chaney 2006).

Rayleigh scattering

Rayleigh scattering is the scattering from atmospheric particles or molecules whose dimensions are much less than the wavelength of the incident radiation (Hansen & Travis 1974). The scattering cross section is a function of the reciprocal of the fourth power of the wavelength and, therefore, short wavelengths are scattered more effectively by atmospheric gases than are longer wavelengths (Heisler & Grant 2000a). However, the strong absorption of ozone and molecular oxygen and nitrogen reduces the effect of Rayleigh scattering in the atmosphere at wavelengths shorter than 250 nm (Huffman 1992).

Mie scattering

Mie scattering occurs when the dimensions of the particles in the atmosphere are comparable to the wavelength of the incident radiation (Hansen & Travis 1974). This scattering is wavelength independent (Platt et al. 2007), and is more important at lower altitudes where the clouds, aerosols and pollutants exist.

2.3.4 Atmospheric absorption

During its travel through the atmosphere, UV radiation is affected by various absorption and scattering processes before reaching the earth's surface. The absorption of solar radiation depends on the concentrations and absorption cross sections of the absorbing constituents of the atmosphere. The predominant absorbing atmospheric gases in the UV region are atomic oxygen (O), molecular oxygen and nitrogen (O_2, N_2) and ozone (O_3).

Most of the UV radiation of wavelengths shorter than 100 nm is absorbed at altitudes between 100 and 200 km by O, O_2 and N_2, resulting in ionizing products (Haigh 2007). UV radiation with wavelengths between 100 nm and 130 nm are absorbed in an irregular way at an altitude of about 100 km (Andrews 2000), making a significant contribution to heating rates and water vapour photolysis (Haigh 2007). The absorption of UV radiation in the range 130–175 nm occurs by molecular oxygen (O_2) at altitudes of between 80 and 120 km and leads to the photo-dissociation of O_2 into ground-state and excited oxygen atoms (Andrews 2000). Wavelengths between 175 and 200 nm are absorbed at altitudes of between 40 and 95 km and are associated with electronic and vibration transitions of the absorbing oxygen molecule O_2. Molecular oxygen is also responsible for absorption within the waveband of 200–242 nm. Part of this absorption dissociates the molecular oxygen into ground-state oxygen atoms required for the formation of stratospheric ozone at about 18–50 km height (Andrews 2000). The latter absorption process is overlapped by the absorption of the 200–350 nm waveband by the stratospheric ozone during ozone photo-dissociation at altitudes below 50 km (Haigh 2007).

The atmospheric ozone is the main absorber at wavelengths longer than about 250 nm. The absorption cross section of the ozone varies with wavelength and thereby the ozone absorption is 100% at 280 nm and decreases to 1% at 320 nm (Heisler & Grant 2000a), and the absorption is negligible at wavelengths longer than 340 nm (Parisi et al. 2004). As a result, atmospheric ozone completely filters out any UVC radiation infiltrating from high layers and no UVC is measured at sea level and middle altitudes. In addition, atmospheric ozone modifies the UVB radiation on the earth's surface, controlling not only its intensity, but also the cut-off wavelength of the global UV irradiance. Reduction in the atmospheric ozone reduces the cut-off wavelength and increases the irradiance in the UVB waveband. For instance, a 10% decrease in ozone with all other factors constant will lead to a doubling of the irradiance at 300 nm (Frederick et al. 1989). Variations in atmospheric ozone with season or altitude will influence global irradiance levels.

The total atmospheric absorption could be altered by the absorption of tropospheric ozone, aerosols and air pollutants, especially above industrialized regions where the tropospheric absorption could more than offset the predicted enhancement in UV radiation because of the decrease in the atmospheric ozone (Frederick et al. 1989). Tropospheric ozone is produced naturally or when emissions of nitrogen oxides and hydrocarbon compounds react in the atmosphere in the presence of UV radiation (WHO 1994). Although tropospheric ozone makes up less than 10% of the total atmospheric ozone, its higher density enhances the ozone absorption by 3% to 15% (Barnard & Wenny 2009). In addition, tropospheric ozone is a more effective UV absorber than the stratospheric ozone for high solar zenith angle (SZA) (the angle between the zenith, directly overhead direction, and the sun) because of the increase in the path length of the scattered radiation in the lower atmosphere

2.3.5 Cloud cover

Cloud cover is the predominant atmospheric variable that affects local solar UV irradiance at a given time and leads to short-term variations (Bais & Lubin 2006). The complexity of cloud effects on UV radiation restricts the accurate prediction of UV trends when other atmospheric conditions are constant. While clouds can decrease the direct radiation mainly by reflecting some radiation back to space (Diffey 2002a; Qiang 2003), they can also increase the amount of diffuse radiation reaching the earth's surface by scattering (Estupiñán et al. 1996). The overall instantaneous effect, therefore, could be either an attenuation or increase in the local irradiance, depending on a combination of factors such as cloud type, cloud altitude, fraction cover, cloud composition and geometry (Bais & Lubin 2006; Estupiñán et al. 1996; Weihs et al. 2000). However, attenuation seems to be the dominant process.

The effect of cloud cover on local UV irradiance is often described by the Cloud Modification Factor (CMF) defined by the relation:

$$CMF = \frac{UV_m}{UV_{cl}} \qquad (2.11)$$

where UV_m is the measured UV irradiance in the cloudy sky and UV_{cl} is the calculated UV irradiance for a cloudless sky for the same conditions as the actual measurements. CMF values less than one correspond to attenuations in the global irradiance and values more than one reflect irradiance enhancements.

A wide range of attenuations of UV radiation by clouds (CMF <1) has been reported in the literature. The annual CMF was reported to be 0.66 and 0.75 in temperate latitudes and tropics respectively (Diffey 2002a). A four-month average CMF of UV irradiance of 0.36 was recorded for cloudy weather (Aun et al. 2011), indicating that, in this study, a 64% decrease of the UV radiation could have resulted from the presence of clouds. Under heavy cloud conditions, reports indicate that UV irradiance can be reduced by more than 90% (WHO 1994), while Estupiñán et al. (1996) found that 99% of UVB irradiance can be attenuated by cumulus-type clouds during overcast conditions. Ilyas (1987) has established an empirical relationship for the attenuation of UV radiation measured on a horizontal surface as a function of cloud cover in the form:

$$F = 1 - (0.056 \times C) \qquad (2.12)$$

where F is the attenuation factor and C is the covered part of the sky expressed in numbers between 0 for clear sky and 10 for totally covered sky. However, the predicted change is only an attenuation which is not always the case. According to Equation 2.12, complete cloud cover will reduce the irradiance by 56% of its value if

the sky is clear. Many other formulae with different uncertainties in predicting cloud effect on UV irradiance have also been reported in the literature (Calbó et al. 2005).

A localized increase in the amount of the UV irradiance was observed under broken cloud conditions when direct solar radiation is unobstructed. The UV enhancement by a wide range of fractional cloud coverage is reported. It has been shown that in some partially covered skies the measured surface irradiances exceed those of clear skies by as much as 11% (Schafer et al. 1996). In addition, an increase in UVB irradiance by about 27% above irradiances of the corresponding clear sky cases was observed for 80–90% cloud cover (Estupiñán et al. 1996). Clouds can also increase local UV irradiance by reflecting back downward the reflected UV radiation from the earth's surface, especially for high albedo surfaces. An enhancement by tens of percent in local UV irradiance is possible by multiple reflections between clouds and snow-covered surfaces (Weatherhead et al. 2005).

The wavelength dependence of the cloud effect has been investigated by several studies. The effect of clouds on UV radiation is less than that for total solar radiation (Foyo-Moreno et al. 2003). The attenuation in the infrared part of the spectrum is greater than that in the UV waveband (Diffey 2002a), increasing the risk of overexposure to UV radiation as the warning sensation of heat is reduced. Although the cloud effect was assumed to be independent of wavelength over the UV region (Diffey 2002a; Frederick et al. 1989), some recent findings contradict this assumption (Kerr 2005; Sabburg & Parisi 2006; Weatherhead et al. 2005).

2.3.6 Surface albedo

The albedo of the surface is the ratio of the irradiances reflected from the surface to the irradiances falling on the surface (Melnikova 2005). The surface albedo is a function of the surface type and the waveband of radiation, and it ranges between 0.005 for grass and 0.8 for snow (Parisi et al. 2004). The enhancement of global irradiance measured on a horizontal surface by high albedo snow can be as high as 28% for clear sky conditions and increasing significantly under partly cloudy conditions (Parisi et al. 2004)

2.3.7 Solar zenith angle

Solar zenith angle (SZA) is the angle between the zenith, directly overhead direction, and the sun; it is a function of the latitude, time of day and day of year. Global UV irradiance is inversely proportional to the SZA. This can be explained as follows: the increase of SZA from its value at local solar noon to an angle θ will increase the area struck by the beam of direct radiation by $Sec\theta$ and, as a result, the irradiance will be reduced by a factor of $\cos\theta$ (Parisi et al. 2004). In addition, UV radiation has its shortest path length to the surface at local solar noon and thus, the greatest irradiance. As the SZA increases, the radiation takes a longer path through the atmosphere and, as a result, more absorption and scattering of the UV radiation will occur before reaching the earth's surface.

2.4 Effects of exposure to solar UV radiation on humans

Exposure to sunlight has always been part of humans' daily lives. People usually spend long times outdoors, either for work or recreational activities, and therefore almost everyone has some exposure to solar UV radiation on a daily basis. Solar UV radiation is known to have dual effects on human health. Small amounts of UV radiation are beneficial, while excessive exposure is a risk factor for several diseases. Fortunately, the penetration of UV radiation in human tissues is very weak (Diffey 1991) and therefore the harmful effects are limited primarily to the skin and eyes.

2.4.1 Positive effects: vitamin D production

One of the confirmed beneficial consequences of exposure to UV radiation is the production of vitamin D. Moderate exposures to UV radiation are essential for cutaneous synthesis of vitamin D (Holick 2008; Juzeniene et al. 2011). This vitamin is important for calcium homeostasis (Nordin, cited in Webb & Holick 1988) and skeletal maintenance in the human body (Powers & Gilchrest 2012; Webb & Holick 1988); there are also contradictory research findings regarding the role of vitamin D in reducing the incidence of some diseases and cancers (Powers & Gilchrest 2012; Schwartz & Hanchette 2006). Although vitamin D can also be taken in via diet and supplements, exposure to UV radiation is the primary source for vitamin D for most people (Grant & Holick 2005).

The daily exposure time required for an exposure dose that produces sufficient vitamin D levels, defined as a blood level of 25-hydroxyvitamin D of at least 20 ng/ml (50 nmol/litre) (Rhodes et al. 2010; Ross et al. 2011), varies mainly depending on the environmental conditions and individual genetic factors (Webb & Engelsen 2006). Generally, dark skinned people need about six times more sun exposure than people with white skin to give enough vitamin D (Juzeniene et al. 2011). Grant and Holick (2005) suggest that exposing 40% of the body surface to midday solar radiation in mid-latitude summer for 4–10 minutes for fair skinned people and 1–1.3 hours for dark skinned people provides an optimal amount of vitamin D for human health.

The effectiveness of UV radiation in producing vitamin D varies with wavelength and UVB is the responsible band for this action (Bouillon et al. 2006) (Figure 2.4), so that the best time for exposure to solar radiation is near solar noon when the UVB reaches its maximum (Grant & Holick 2005).

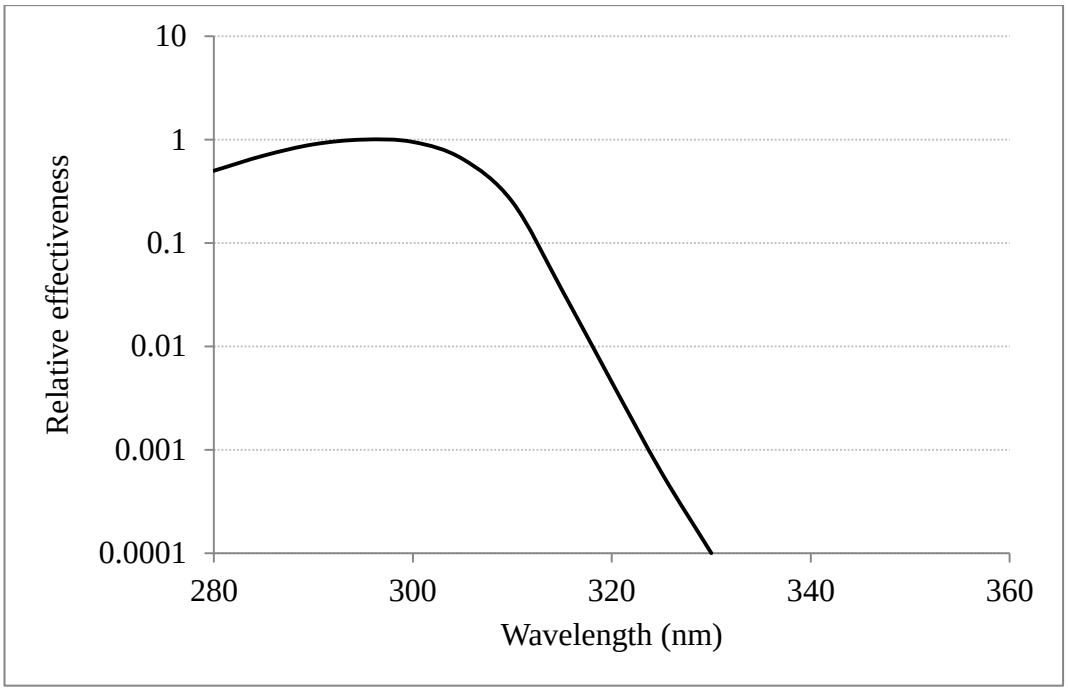

Figure 2.4: The action spectrum of vitamin D production by UV radiation (Bouillon et al. 2006).

2.4.2 Detrimental effects of exposure to UV radiation

The adverse effects of exposure to UV radiation can be classified into two general types of effects, acute and chronic. An acute effect, whose symptoms are severe, develops rapidly and leads quickly to damage that lasts for a relatively short time, is usually reversible. In contrast, a chronic effect develops gradually and its final result is often irreversible.

2.4.2.1 Acute effects on the skin

Sunburn (Erythema)

Sunburn is an acute skin injury following excessive exposure to solar UV radiation. It results in redness and sometimes blistering within 8–24 hours after exposure (ASCC 2008). In severe cases, in addition to blistering, sunburn may result in swelling, and later, peeling of the skin (WHO 1994). The susceptibility of individuals to sunburn depends mainly on the pigment in their skin (skin colour) and therefore, the time course of sunburn varies from 15–30 minutes to 1–2 hours of midday exposure to solar UV radiation in mid-latitude summer for moderately pigmented skin while some people with dark skin will not sunburn even after a full day of exposure (Vecchia et al. 2007). Sunburn is usually followed in 3–6 days by tanning in individuals capable of producing melanin. This mechanism is a protective device of the skin against further damage by the UV radiation. The actual amount of energy required to induce sunburn varies with wavelength, since some regions of the spectrum are more effective than others. The relative effectiveness of UV

wavelengths in inducing sunburn is represented by the erythema action spectrum (CIE 1998) shown in Figure 2.2.

It can be noticed from this figure that the UVB waveband is more erythmogenic than UVA by a factor of about 1000. The efficiency decreases rapidly with wavelength even within the UVB; the effectiveness of the 320 nm wavelength is only 1% of that at 300 nm. The radiant exposure, therefore, is weighted by the action spectrum to calculate the erythemal dose (eq. 2.8). The major problem of sunburn is that there is an increasing risk of skin cancer, as some cancers are believed to be related to episodes of sunburn (Heisler & Grant 2000b).

2.4.2.2 Chronic effects on the skin

Photo-aging

Photo-aging is the premature aging of the skin caused by repeated exposure to solar radiation (Yan et al. 2013). The resulting changes in the skin include dryness, wrinkling, dark spots, loss of elasticity and a leathery appearance (WHO 1979). These cutaneous changes are due to collagen degeneration in the dermis caused by cumulative injury from solar UV, which in turn depends on the degree and frequency of exposure to solar UV over the years (WHO 1979). The changes are irreversible and may cause major cosmetic and psychological problems, particularly for women. The spectral dependence for the cumulative damage in the skin (photo-aging) is different from the erythemal action spectrum (Lavker et al. 1995). UVA is the band responsible for photo-aging changes (Bens 2008) and the action spectrum of the photo-aging mechanism lies mainly in the UVA1 band.

Skin cancer

Skin cancer was identified as the cause of more than 2 thousands deaths of Australians in 2011 (ABS 2013). This is about 2.1% of all deaths registered in that year. Exposure to solar UV radiation is well established as the major cause of skin cancer in fair-skinned people (ASCC 2008). Prolonged exposure and/or intermittent episodes of sunburn can damage skin cells in a way that leads to the cancer. There are two main categories of skin cancer according to the skin cells that cancers can develop from. These are melanoma and non-melanoma skin cancers.

- ***Melanoma skin cancer:***

Cutaneous malignant melanoma (CMM) is the type of skin cancer that occurs in cutaneous cells called melanocytes. These cells are located between the epidermis and dermis skin layers, and produce melanin that gives human skin, hair and eyes their colour. Although the melanin produced by melanocytes cells and transferred to the outer skin layer provides some protection against skin damage from solar radiation, it has been proven that melanocytes cells themselves, especially in fair-skinned people, may become cancerous due to overexposure to solar UV radiation (Alexandrescu et al. 2013). CMM accounts for about 5% of skin cancer cases worldwide. However, the fatality rates are the highest of the types of skin

cancer (Diaz 2013) and may exceed 40% of diagnosed cases (WHO 1979). The major risk factor of CMM is believed to be intermittent overexposures and blistering sunburns in childhood and throughout adulthood (Alexandrescu et al. 2013; Diaz 2013; Norval et al. 2011). Three blistering sunburns or more before the age of 18 years is classified as one of the greatest risk factors for CMM (Diaz 2013).

- Non-melanoma skin cancers (NMSCs):

Non-melanoma skin cancers are the cancers that develop from cutaneous cells other than melanocytes. Although NMSCs are the most commonly occurring malignancies among fair-skinned people worldwide (Diaz 2013), they are much less dangerous than CMM with an associated mortality of about 1% of diagnosed cases (WHO 1979). The most common types of non-melanoma skin cancers are basal cell carcinoma (BCC) and squamous cell carcinoma (SCC).

- **Basal cell carcinoma (BCC):**

BCC is the most common non-melanoma skin cancer and represents about 75% of diagnosed non-melanoma skin cancers. This cancer develops from basal cells that are found at the bottom of the epidermis and are responsible for the production of all the normal skin cells found above the basal cells. The positive side is that this cancer rarely spreads to another part of the body. The risk of BCC is more related to the number of reported sunburns rather than to cumulative exposure (Norval et al. 2011).

- **Squamous cell carcinoma (SCC)**

SCC refers to the type of skin cancer that develops from cutaneous cells called keratinocytes which make keratin. SCC can spread to the deeper layer of the skin and nearby lymph nodes and other organs, causing secondary cancers. Therefore the risk of SCC is 10 times greater than BCC (Diaz 2013). The risk of SCC is believed to be more related to cumulative life-time exposure to solar UV radiation (Norval et al. 2011).

2.4.2.3 Acute effects on the eyes

In a similar way to the sunburn of the skin, excessive exposure to UV radiation may burn the eyes (O'Shea 1996), leading to what is known as photokeratitis and photoconjunctivitis. These are inflammations of the cornea and conjunctiva accompanied with eye pain, sensation of foreign body in the eyes, swelling and difficulties looking at unshielded lights (ASCC 2008). The latency of these symptoms varies inversely with the severity of exposure; they usually appear within 6–12 hours following the exposure (WHO 1979) and typically disappear after about 72 hours.

2.4.2.4 Chronic effects on the eyes

Prolonged exposure to UV radiation has also been linked to some eye disorders such as cataracts and the development of pterygium (Yam & Kwok 2014).

Cataracts:

Cataracts are the leading cause of blindness in the world (Long et al. 1996). The condition involves cloudiness or opacity in the transparent crystalline lens of the eye, leading to a decrease in vision that may progress to blindness. The eye lens is made up mainly of proteins and water. Degenerative changes in the proteins occur as people age and hence cataracts are common in the elderly and believed to be a normal part of the aging process. However, there is considerable evidence that prolonged exposure to UV radiation is a risk factor for the development of some types of cataracts (Roberts 2011; Yam & Kwok 2014) and about 20% of cataracts are believed to be associated with cumulative exposure to UV radiation (WHO 1994).

Pterygium:

A pterygium is simply an overgrowth of the conjunctiva on to the cornea of the eye (Sekelj et al. 2007) that may eventually interfere with vision. Exposure to UV radiation appears to be the most significant factor in the development of pterygium (Moran & Hollows 1984; Sekelj et al. 2007; Yam & Kwok 2014). It has been estimated that about half of the cases of pterygium treated in Australia are caused by exposure to solar UV radiation (Wlodarczyk et al. 2001).

2.5 Measuring personal exposure to UV radiation

One of the main goals of UV research is to optimise exposure levels to UV radiation in order to reduce the risks and gain the maximum benefits. In this regard, monitoring UV levels is fundamental.

The most measured UV quantities worldwide are the global UV irradiance (the incident irradiance on a horizontal plane), ambient irradiance (global irradiance weighted with the erythemal spectrum) and the ambient exposure (integrated ambient irradiance over the time the surface was exposed). These quantities can be obtained by spectroradiometers that measure the spectral irradiance in particular wavelength increments and give the entire spectral shape and power, or by narrow-band and broad-band radiometers that measure the irradiance in a desired spectral band and can be weighted to approximate a chosen action spectrum (Diffey 2002a). Although these instruments are necessary for the continuous measurements that provide information to the public on UV levels, they are too bulky, stationary and can be of limited value for monitoring personal UV exposure which is related to the moving body with differently oriented sites. Alternatively, personal UV dosimeters have been intensively used in human exposure studies. Three main categories of personal dosimeters are used to quantify personal UV exposure. These are physical, biological, and chemical UV dosimeters.

2.5.1 Physical UV dosimeters (Electronic dosimeters)

Physical dosimeters are miniature electronic devices that can be attached to clothing or worn on the wrist to record the incident UV radiation. In principle, the incident UV radiation induces a measurable physical property such as the thermoluminescent phenomenon in specific crystals (Wulf & Gniadecka 1996a), or initiates a photoelectric current in a photodiode that is proportional to the incident UV radiation (Wulf & Gniadecka 1996b). Physical dosimeters can either accumulate the exposure over any time or record the time varying irradiance with a resolution of a few seconds (Seckmeyer et al. 2012). They may measure the absolute irradiance or radiant exposure (Wulf & Gniadecka 1996b), or may have specific built in filters that adjust the spectral response of the detector to approximate a certain biological effect (McKenzie et al. 2013). The main advantages of physical UV dosimeters are the ability to deliver data with a high resolution in time and amplitude (Naggar et al. 1995), the re-usability (Allen & McKenzie 2010), ease-of-use and simple readout process. These advantages and the continuous development of the dosimeters have made physical dosimeters one of the optimum methods of measuring personal exposure to UV radiation. They have been effectively used to quantify personal exposure of some population groups such as skiers, fieldworkers and school students (Allen & McKenzie 2005; 2010; Cockell et al. 2001; Rigel et al. 2003a; Rigel et al. 2003b; Schmalwieser et al. 2010a; Weihs et al. 2013), to study the variation of anatomical exposure with day time (Hu et al. 2010) and to investigate some UV protection strategies (McMichael et al. 2013). Although electronic UV dosimeters are suitable for long term measurements, the cost and availability may restrict their use for simultaneous large scale anatomical measurements and reduce their advantage compared to biological and chemical UV dosimeters. Another disadvantage of physical dosimeters is the gradual loss in sensitivity due to frequent use (Izewska & Rajan 2005).

2.5.2 Biological UV dosimeters (Biosensors)

Biological UV dosimetry is a technique that employs biological organisms as targets of UV radiation. The biologically effective UV dose is quantified by measuring the UV-induced effect within the exposed simple biological target (Rontó et al. 2004). The dosimeter automatically weights the incident UV wavelengths according to their biological effectiveness and provides an integrated biologically weighted dose (Bérces et al. 1999; Gróf et al. 1996). Several biological targets of varying degrees of complexity have been developed and employed in personal UV measurements. For instance, *Bacillus subtilise* spores have been used in spore dosimeter and DLR-biofilm as UV detectors; the UV effect is evaluated by measuring the colony-forming survival after exposure to UV radiation (Munakata et al. 2000; Munakata et al. 1996; Rettberg & Cockell 2004). Another type of the biological targets is phage T7 where the UV-induced effect is quantified by the inactivation of phage particles as a result of DNA damage (Bérces et al. 1999; Rontó et al. 1992). Polycrystalline uracil thin layers also employed as targets in UV measurements. The layers undergo change in the optical density upon exposure to

UV radiation due to photodimerization of uracil monomers (Gróf et al. 1996; Horváth et al. 2001). In addition, vitamin D photoisomers produced under UV exposure has been used in D-dosimeters as a means of determining UV dose (Terenetskaya 2000; 2003).

Biological UV dosimeters have been successfully employed in personal exposure measurements during various activities in different environments (Cañada et al. 2014; Moehrle et al. 2000; Munakata 1999; Serrano et al. 2010; 2011). The DLR-biofilm was reported to be able to measure up to two months of continuous exposure to solar UV radiation (Rettberg & Cockell 2004). However, the preparation of the biological dosimeter and the analysis required to determine the degree of UV-induced effect of the dosimeter material involves, in many cases, specific laboratory techniques and is often time consuming, which hinder their wide use in comparison with chemical UV dosimeters.

2.5.3 Chemical UV dosimeters (UV actinometers)

Chemical dosimetry is the technique that employs thin films of synthetic polymers which undergo photochemical changes upon exposure to UV radiation. The measurement principle of chemical dosimeters is based on the UV-induced change that occurs in one of the physical properties of the film, usually the optical density, upon exposure to UV radiation. The change is then compared to the calibration curve (dose response curve) of the dosimeter to obtain the integrated exposure dose. A passive integrating personal UV dosimeter is, therefore, obtained as a cheap, small, handy UV monitor that requires no power (Kimlin 2003). The most common chemical UV dosimeters that have been proposed and used in UV measurements are polysulphone (Diffey & Davis 1978), polyphenylene oxide (Davis et al. 1976), phenothiazine (Diffey et al. 1977a; Parisi & Wong 2000), allyl diglycol carbonate (Wong et al. 1992) and nalidixic acid (Tate et al. 1980). Among these dosimeters, polysulphone have been widely employed in personal exposure research, followed by the recently characterised polyphenylene oxide.

The polysulphone polymer in a form of 40 µm thin film is the most widely used chemical UV dosimeter in research of personal exposure to solar UV radiation. Diffey and Davis (1978) reported the increasing fragility of polysulphone due to complex photo-degradation of the film when exposed to UV radiation. This degradation resulted in a change in the UV absorption spectrum of the film which can be determined to provide a measurement of the absorbed UV exposure (Casale et al. 2009). The highest relative UV-induced increase in the polysulphone film absorbance was found to be at 330 nm and thereby the film can be used as a UV dosimeter by relating the incident radiant exposure or exposure dose to the increase in the absorbance measured at 330 nm (Diffey & Davis 1978). The polysulphone dosimeter responds mainly to the UVB band of radiation and its spectral response approximates the CIE erythemal action spectrum (CIE 1993) (Figure 2.5); and, as a result, the dosimeter is often calibrated to measure personal erythemal UV doses.

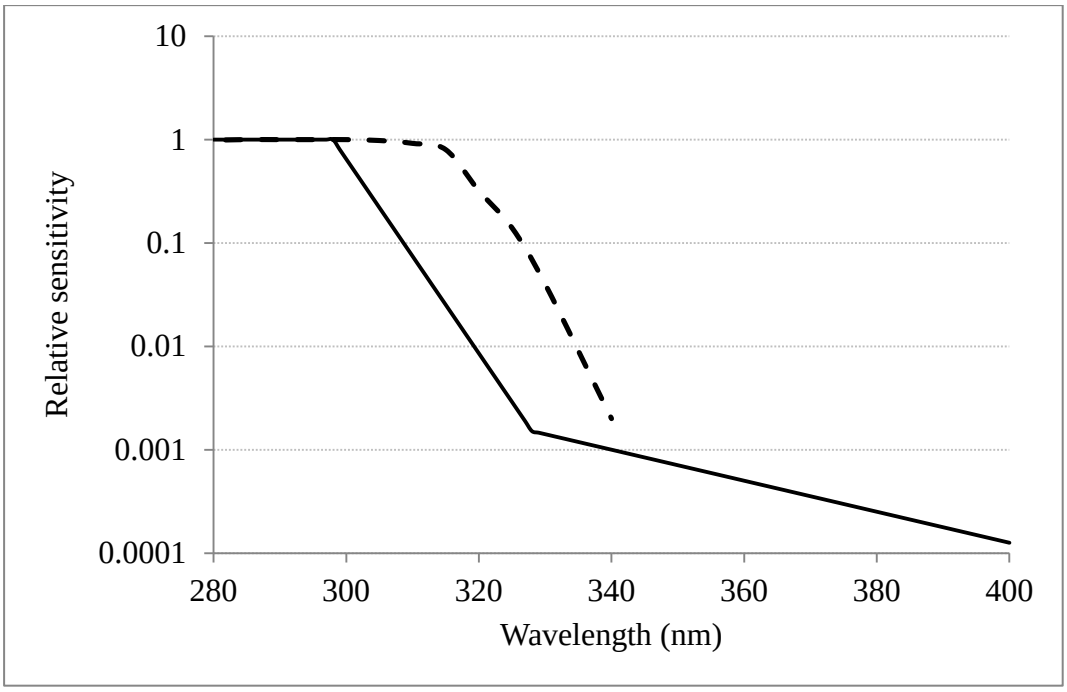

Figure 2.5: Polysulphone spectral response (CIE 1993) (dashed line) compared to erythemal action spectrum (CIE 1998).

In addition to the similarity between the PS dosimeter response and the erythemal response, the PS dosimeter is characterised by its independency of temperature (Diffey & Davis 1978), acceptable cosine response (Krins et al. 2000), ability to be miniaturised (Downs & Parisi 2009), low cost and light weight. The PS dosimeter has been extensively employed to: investigate the proportions of ambient UV radiation received at several anatomical sites in different occupations and various recreational activities (Allen & McKenzie 2005; Downs & Parisi 2008; Herlihy et al. 1994; Holman et al. 1983; Kimlin et al. 1998; O'Riordan et al. 2000; Siani et al. 2008; Siani et al. 2009; Siani et al. 2011); estimate the fluctuations of the stratospheric ozone layer (Kollias et al. 2003); evaluate different strategies of protection against solar UV radiation (Diffey & Cheeseman 1992; Gies et al. 2007; Gies et al. 2006; Gies & Mackay 2004); and correlate 25-hydroxycalciferol levels in blood with personal UV exposure dose (Beadle et al. 1980; Webb et al. 1990). The main disadvantage of the PS dosimeter is the fast saturation. The dosimeter is saturated after 3–6 hours of exposure to solar radiation (Parisi & Kimlin 2003), limiting its ability to continuously measure over long exposure periods. Therefore, the dosimeter has to be replaced regularly before it is saturated, increasing not only the cost and effort, but also the margin of error. Parisi and Kimlin (2003) have extended the polysulphone dynamic range to 3–6 days of exposure by incorporating an UV-attenuating filter with the dosimeter. Although this methodology was successfully applied in few-days-long measurements (Parisi & Kimlin 2004), in addition to the cost and time of preparing the dosimeter, it may increase the error margin due to changes in the transmission spectrum of the filter as a result of UV exposure (Parisi & Kimlin 2003).

Another polymer, besides polysulphone, that was recently reported as a reliable chemical UV dosimeter is polyphenyline oxide (PPO). Although the potential of PPO as a monitor for UV radiation was realised early by Davis et al. (1976), the full characterization of the dosimeter has been carried out later than PS (Berre & Lala 1989; Lester et al. 2003). The PPO quantification principle and dosimetric properties are similar to the PS, yet the dynamic range of the dosimeter is about five times longer than that of the PS (Lester et al. 2003). The PPO dosimeter has been employed to measure UV exposure in various environments such as evaluating UV radiation in air (Schouten et al. 2010) and aquatic locations (Schouten & Parisi 2012; Schouten et al. 2008; 2009), and measuring the incident UV on plant leaves (Parisi et al. 2010a; Turner et al. 2009). Specific filters have also been incorporated with the dosimeter to either extend its dynamic range (Schouten et al. 2010) or measure only the UVA exposure (Turnbull & Schouten 2007; Turnbull & Schouten 2008).

Chemical UV dosimeters as a measurement technique are much cheaper than electronic devices, and more simple and feasible than the biological dosimeters. The improvement of existing dosimeters for measuring longer periods, or the introduction of new polymers capable of measuring long-term exposures, will be of great benefit for studies of latent outcomes of exposure to UV radiation that are related to cumulative exposure throughout a lifetime.

2.5.4 Determination of UV-induced changes within chemical UV dosimeters

There is a wide spread of techniques used to determine the structure of compounds and detect possible changes over time. Examples of these techniques are: Mass spectroscopy (MS), Nuclear Magnetic Resonance spectroscopy (NMR), UV spectroscopy (UV) and Infrared spectroscopy (IR).

The quantification of UV-induced changes in chemical dosimeters is traditionally done using UV spectroscopy because of its low cost, ease of usage and simplicity of interpreting data (Field 1995) and its availability in basic physics laboratories. However, Fourier Transform Infrared (FTIR) spectrophotometers, which have long been used to identify unknown compounds and determine molecular structures (Sun 2004) and to investigate mechanical, thermal and photo-degradation of polymers, can also offer a promising simple technique for this purpose.

Regardless of the difference in the way that UV and IR interact with matter, Beer's law is the basis of both UV and IR spectroscopy. Beer's law states that the radiation absorbed by a sample at any particular wavelength is proportional to the concentration of the absorbing species in this sample (Smith 1996), i.e.

$$A = \varepsilon l c \qquad (2.13)$$

where A is the optical absorbance of the material, ε is the molar absorptivity of the material, l is the path length through the material and c is the concentration of the absorbing species.

The optical absorbance can also be written in terms of the incident radiation in the form:

$$A = \frac{1}{T} = \log \frac{I_0}{I} \qquad (2.14)$$

where T is the optical transmission of the material, I_0 is the radiation intensity before absorption and I is the radiation intensity after absorption. The absorbance of the material before and after exposure can be measured using an appropriate spectrophotometer and, therefore, any changes that may occur through the absorbing species can be recognised and quantified.

In the field of UV dosimetry, a UV spectrophotometer provides a graph of the absorption of a dosimeter in the UV region of the electromagnetic radiation as a plot of wavelength $\lambda(nm)$ against the absorbance (A). This is called the UV absorption spectrum. In many cases, the UV absorption spectra of a dosimeter before and after exposure to UV radiation can indicate if there are any UV-induced changes in the dosimeter material. Figure 2.6 illustrates the changes in the UV absorption spectrum of 40 µm polysulphone film as a result of the exposure to UV radiation.

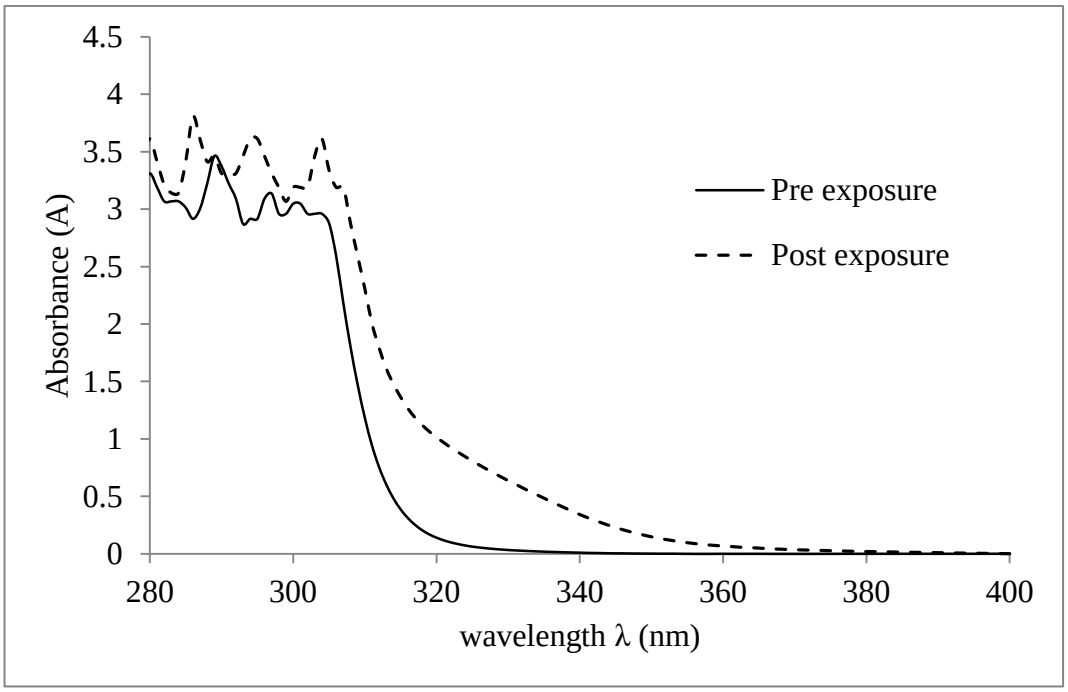

Figure 2.6: Changes in UV absorption spectrum of 40 µm polysulphone film as a result of the exposure to UV radiation.

The IR absorption spectrum provided by the IR spectrophotometer represents the absorbance (or transmission) of a sample in the IR region as a function of its wave number $(\bar{\nu})$, where $\bar{\nu} = \frac{1}{\lambda}$. This spectrum contains information about the sample structure and, as in the case of polymer degradation, can also be used to detect the formation or disappearance of some components in the sample (Schnabel 1981). Figure 2.7 shows the IR absorption spectrum of 40 µm polysulphone film.

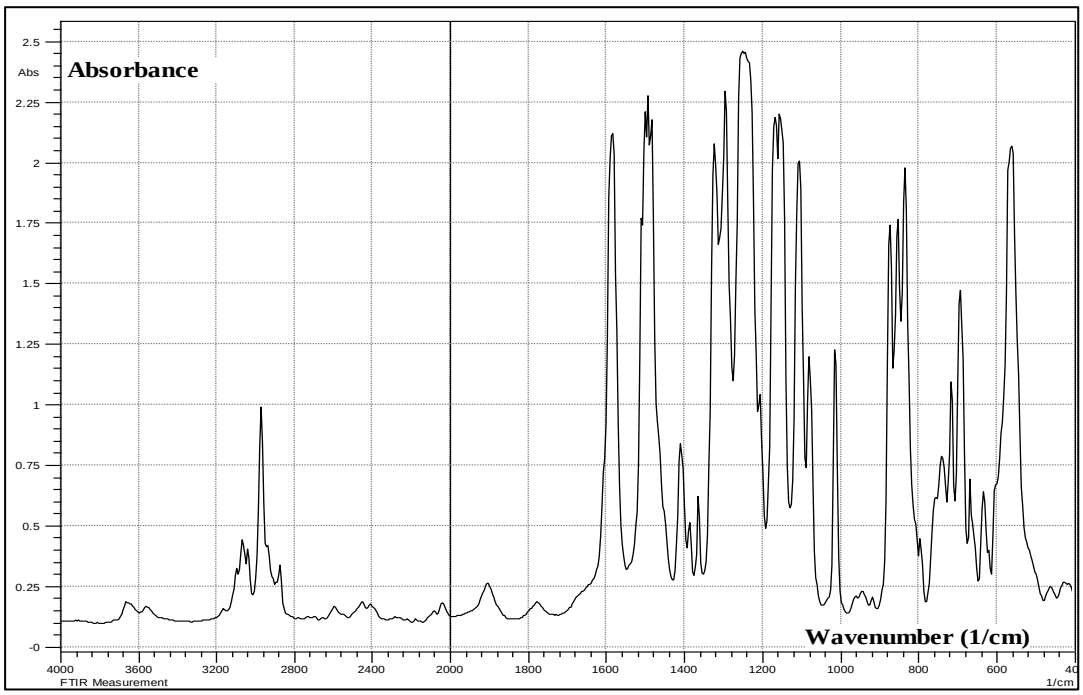

Figure 2.7: IR absorption spectrum of 40 µm polysulphone film.

The main advantage of using IR spectroscopy over UV spectroscopy is that IR absorption spectra contain far more bands (characteristics) than UV absorption spectra and therefore have a larger information content (Field 1995).

2.6 Chemical UV dosimeter requirements

2.6.1 Dosimetric properties

To function as a reliable UV dosimeter, the material used must satisfy the basic dosimetric properties of UV dosimeters. In this context, the following properties have to be investigated:

2.6.1.1 Monotonicity of dose response curves

The underlying principle of monitoring UV radiation using chemical UV dosimeters is to measure the absorbance change induced by UV radiation in the dosimeter material and then compare the change with a dose response curve (calibration curve) to obtain the UV exposure. In general, it is desirable for all measuring systems to have a linear response over the entire range of exposures which they may be expected to measure (Webb 1995). Therefore, the ideal dosimeter should show a doubled response whenever the incident radiation is doubled. However, non-linearity of a dose response curve can be accepted and the curve does not need to be a straight line as long as the response is a monotonic function of the exposure dose.

2.6.1.2 Reproducibility

The ability of the dosimeter to monitor UV radiation depends on its reproducibility. Equal radiant exposures from the same source should induce the same measured response. The dosimeters used to establish the calibration curve cannot be used again in the measurements; instead, other dosimeters from the same batch are used. The ideal dosimeter then should respond to the radiation in a reproducible manner as the calibration dosimeters do, and any errors related to the film reproducibility have to be assessed and taken into account during the measurement process.

2.6.1.3 Spectral response (Spectral sensitivity, Spectral dependence)

The response of UV-sensitive materials to UV radiation is usually wavelength dependent, i.e., equal exposures with different wavelengths will induce different responses. This property is referred to as a spectral response, and it is one of the most important characteristics of radiation dosimeters. The spectral response of a UV dosimeter shows how the dosimeter response changes as a function of the wavelength of the incident UV radiation. The overall responsivity (S) of a dosimeter to a UV source of radiation with constant irradiance spectrum is given by: (CIE 1984)

$$S = \frac{\Delta A}{H} \qquad (2.15)$$

where ΔA is the absorbance change (dosimeter response) and H is the radiant exposure received by the dosimeter during the exposure period t and given by

$$H = \left(\int_{280}^{400} E(\lambda) d\lambda \right) t \qquad (2.16)$$

where $E(\lambda)$ is the spectral irradiance. The response of the dosimeter to monochromatic radiation of wavelength λ (spectral response) is then:

$$S(\lambda) = \frac{\Delta A(\lambda)}{H(\lambda)} \qquad (2.17)$$

The relative spectral response $S(\lambda)_r$ is the ratio of the spectral response $S(\lambda)$ of the dosimeter at wavelength λ to a given reference value. The reference value is often taken as the spectral response at wavelength λ_m that maximises the response

$$S(\lambda)_r = \frac{S(\lambda)}{S(\lambda_m)} = \frac{\Delta A(\lambda)}{\Delta A(\lambda_m)} \qquad (2.18)$$

The spectral response should be defined in order to identify which UV wavebands the dosimeter can detect and whether the polymer response approximates any of the biological action spectra.

2.6.1.4 Dose-rate independency (Receprocity law)

Chemical UV dosimeters measure the integrated radiant exposure (dose), i.e., the product of the irradiance and the exposure time:

$$H = \int_0^t \int_{280}^{400} E(\lambda) d\lambda dt = \left[\int_{280}^{400} E(\lambda) d\lambda \right] t \qquad (2.19)$$

where H is the radiant exposure, $E(\lambda)$ is the spectral irradiance and t is the total exposure time. Therefore, the UV induced response within the dosimeter should be independent of the rate of the received dose (irradiance), i.e., equal doses are supposed to induce the same response regardless of the dose-rate and duration of exposure. In other words, the response should obey the reciprocity law. The law which was first investigated by Bunsen and Roscoe and states that all photochemical reactions depend only on the total absorbed energy and are independent of the radiant intensity (irradiance) I and exposure time t (Martin et al. 2003). The reciprocity law has the form

$$It = const. \qquad (2.20)$$

The validity of the reciprocity law means that the same response is observed when dosimeters receive the same integrated total exposure regardless to whether the exposures are performed at high irradiance for a short time or at low irradiance for a long time.

2.6.1.5 Temperature independency

Chemical dosimeters employed in solar UV radiation measurements experience different ambient temperatures. Different findings for the temperature effect on chemical UV dosimeters have been reported in the literature. Polysulphone and polyphenylene oxide dosimeters, for instance, have been classified as temperature independent dosimeters (Casale et al. 2009; Davis et al. 1976; Lester et al. 2003) while the measurements obtained by a chemical dosimeter based on nitrate and nitrite solution are strongly dependent on ambient temperature (Jankowski et al. 2000). Therefore, the thermal stability of the dosimeter has to be ensured and the temperature range of the dosimeter validity should be identified.

2.6.1.6 Angular dependence

The angular dependence of the dosimeter is the variation in its response with the angle of incidence of incoming radiation. The direct component of solar irradiance strikes the dosimeter surface with an angle that varies according to the solar zenith angle (SZA). In addition, the diffuse part of the irradiance strikes the dosimeter at random angles. The dosimeter area (a) irradiated by a beam of radiation increases in proportion to the increase of the angle of incidence of the beam (θ)

$$a \propto \frac{a_0}{\cos\theta} \qquad (2.21)$$

where a_0 is the area corresponding to $\theta = 0^0$. The result is that the number of incident photons that strike a fixed area decreases with the increasing θ, i.e. the irradiance E is reduced according to the relation (Parisi et al. 2004)

$$E = E_0 \cos\theta \qquad (2.22)$$

where E_0 is the irradiance at $\theta = 0^0$. The relative change in irradiance $(\frac{E}{E_0})$ is then a cosine function. Therefore, for an ideal UV dosimeter, the response to the change in the angle of incidence of the beam (cosine response) should be a cosine function.

2.6.1.7 Dark reaction

Previous research has reported changes in the responses of some chemical UV dosimeters after the UV exposure has been terminated (Davis et al. 1976; Diffey 1989; Lester et al. 2003; Parisi & Kimlin 2003). This behaviour is commonly known as the dark reaction. The dark reaction induced change in the dosimeter response (ΔA_D) after a period t of terminating the exposure can be calculated by

$$(\Delta A_D) = A_t - A_{t=0} \qquad (2.23)$$

where $A_{t=0}$ is the dosimeter absorbance as measured immediately after exposure and A_t is the absorbance after a period t of terminating the exposure.

For dosimeters that are designated for long term use, the measurement intervals may include nocturnal periods. In addition, the readout process is not always available immediately after exposure and the dosimeters may have to be stored for a while. In both cases, the dark reaction may take place during exposure or after exposure and may invalidate the results of the dosimeter. However, the change that occurs between exposures can be overcome as it is included in the calibration curve, since the calibration dosimeters will experience the same change. Any changes after exposure can be eliminated by adopting a standardization of read-out time after exposure (Diffey 1989). Ideally, a dosimeter with no dark reaction will allow it to be used in remote and inhospitable areas, leaving the read out process to a more convenient time and conditions (Webb 1995).

2.6.2 Practical requirements

In addition to the aforementioned dosimetric properties that the material must exibit to function as a UV dosimeter, practical conditions impose some requirements for personal UV dosimetry. A reasonable personal UV dosimeter would have the following characteristics:

2.6.2.1 Ease of preperation

Chemical dosimeters are preferable to biological and electronic dosimeters, in part, because of their low cost per dosimeter which permit large scale monitoring (Vecchia et al. 2007). The dosimeter material, therefore, should be commercially available at low cost and easy to synthesise (Kuhn et al. 2004) using simple techniques that require no specific experience or sophisticated equipment.

2.6.2.2 Convenience of use

The ease with which the dosimeter can be exposed should be one of its advantages. The dosimeter has to be small and light so that it does not restrict the activities of the wearers. In addition, the dosimeter has to be sufficiently physically sturdy and environmentally stable to withstand weather conditions during outdoor applications.

2.6.2.3 Readout convenience

In contrast to physical dosimeters which give direct measurements, chemical dosimeters as passive dosimeters do not provide immediate readings. Additional measurements, analysis and calculations are required to determine the dose. The ease and reliability of the technique used to determine the exposure are considered when the overall applicability of a dosimeter is evaluated (Webb 1995). In this regard, the direct spectrophotometric technique is preferred (Kuhn et al. 2004).

2.7 Suitability of polyvinyl chloride (PVC) for long-term UV dosimetry

The polymer polyvinyl chloride (PVC), with the chemical formula $[C_2H_3Cl]_n$, is one of the most widely produced and used plastics worldwide (Kaczmarek et al. 2005) because of its particular properties and low production cost. PVC is a light-weight and non-flammable thermoplastic with a strong and durable structure (Gupta et al. 2012). The use of PVC is widespread and diverse; and PVC products are included in almost all industrial activities including the manufacture of agricultural and household goods. The main disadvantage of using PVC is that PVC materials undergo serious deterioration when they are exposed for a long time to natural weathering, especially solar UV radiation (Zhang et al. 2012).

PVC is produced by free-radical polymerization of monomer vinyl chloride (MVC) according to the equation (Patrick 2005):

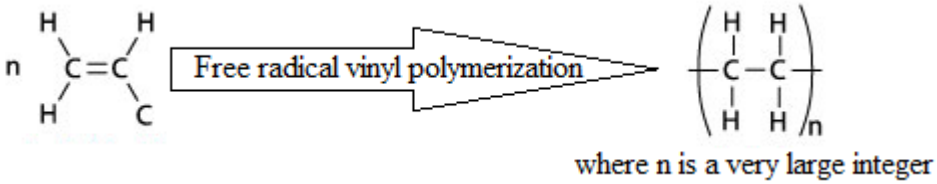

Figure 2.8: Polymerization of monomer vinyl chloride (MVC) to polyvinyl chloride (PVC).

The most common commercial techniques involved in PVC production are suspension polymerization, emulsion polymerization and bulk polymerization (Braun 2004). At the research level, PVC films can be produced by either casting from solution or pressing PVC powder under high pressure at high temperature.

Figure 2.8 shows that the PVC polymer contains only the saturated bonds $C-C$, $C-H$ and $C-Cl$. These bonds absorb only radiation of wavelength less than 200 nm (Wirth & Andreas 1977). According to the first law of photochemistry, the Grotthuss-Draper law, which states that light must be absorbed by a compound in order for a photochemical reaction to take place, pure PVC is expected to be transparent to terrestrial sunlight and should not show any UV exposure related changes. Nevertheless, the susceptibility of PVC to photodegradation during outdoor applications due to UV exposure has long been confirmed and extensively reported in the literature (Baum 1967; Hirt & Searle 1967; Martin & Tilley 1971; Rasheed et al. 2009; Reinisch et al. 1966; Ye et al. 2010). This degradation has been attributed mainly to the chromophoric impurities (Wiles & Carlsson 1980) introduced during syntheses, processing or storage.

Polymer photo-degradation is a very complex process (Kaczmarek et al. 2002) that is governed by a large number of factors such as the number and nature of absorbing chromophores in the polymer system, polymer morphology, crystallinity, photo-physics and chemical chain reactions (Wiles & Carlsson 1980). In general, the

detailed process is out of the scope of this project; however, the main photochemical reactions in PVC are cleavage of main chain, photo-dehydrochloration, photo-oxidation, branching, crosslinking and side group abstraction (Kaczmarek et al. 2005; Sabaa et al. 2005; Yi et al. 2011). As a result of these reactions, the appearance of the PVC material, and its mechanical and physical properties, would be deteriorated (Yi et al. 2011). The degradation mechanisms and effects are analysed and followed using several modern experimental techniques such as FTIR, UV-Vis, and NMR spectroscopy (Sabaa et al. 2005). These techniques are used also to determine the effectiveness of UV wavelengths in inducing PVC photo-degradation.

Since pure PVC is transparent to ambient UV radiation (280–400 nm) and any absorption in this region is dependent upon the processing conditions or added ingredients, the spectral response of PVC varies according to the type of photo-degradation process, which in turn depends on the nature and concentration of existing impurities, and the criterion employed to evaluate this degradation.

Change in the carbonyl absorbance at 1730 cm^{-1} of melt-pressed 160 µm PVC films as a function of the wavelength of irradiation has been reported (Martin & Tilley 1971) and the wavelength region 355–385 nm was identified as the most active region in inducing photo-oxidation within the polymer. Different findings were reported by Hirt and Searle (1967) who found that 320 nm was the wavelength with the greatest effect on photodegradation of PVC as detected by means of the change in UV absorbance spectra, but neither the film preparation method nor its thickness were given. Reinisch et al. (1966) irradiated PVC films in a vacuum to investigate the potential of PVC for use in extra-terrestrial space. The UV absorbance spectra were used to measure the UV induced changes in solvent-cast PVC films of thickness 14–30 µm. The resulting response was to wavelengths between 238 and 332 nm with a maximum response at 254 nm. Andrady and Searle (1989) used the yellowness index (YI) as a measure of photo-degradation of UV irradiated PVC thin films and found that the maximum change in YI for extruded rigid 1 mm thick PVC films is due to wavelengths between 300 and 320 nm while, under similar exposure conditions, the solvent-cast 5 µm thick films did not show any change in YI.

Although the main topic of PVC research is the stabilization of PVC products against UV radiation by the use of UV absorbing additives or opaque pigments and polymer blends, some research has focussed on the positive side of PVC degradation. The enhancement of PVC photo-degradation has been studied in order to produce degradable polymers with the aim of decreasing waste plastics (Torikai & Hasegawa 1999). PVC has also been investigated as a monitor for measuring high energy particles and radiation (Ilic-Popovic 1966; Kattan et al. 2011; Mai et al. 2004; Miller & Liqing 1985).

In UV dosimetry, PVC has usually been used as a matrix for UV sensitive chemicals employed as dosimeters. The reason for using PVC as a matrix is that the UV absorption spectrum of PVC can be affected by doses much greater than those measured by the incorporated chemicals (Diffey et al. 1977a). Several photoactive

chemicals have been incorporated into thin PVC films to form UV dosimeters. Such chemicals include phenothiazine (Diffey et al. 1977a) that was introduced to measure about 0.3 MJ/m^2 of UVA radiation, 8-methoxypsoralen (Diffey & Davis 1978), and nalidixic acid (Tate et al. 1980) that was found to be suitable as a short term dosimeter within the range 280–350 nm.

The suitability of pure PVC for use as a UV dosimeter was reported by Martin (1973) who tested the unstabilised PVC to use as a simple UV monitor. Martin has reported that the infrared absorbance at 1730 cm^{-1} of PVC film linearly increases with the incident total solar radiation up to about 14 MJ/m^2. The films were used to compare the ratio of UV to global radiation in different cities. However, to the best of our knowledge, a full characterization of the investigated dosimeter or any other UV dosimeter based on PVC has not been undertaken.

2.8 Conclusion

Ultraviolet (UV) radiation is one component of solar radiation that reaches the earth's surface and, therefore, almost everyone has some exposure to solar UV radiation in a daily basis. Ambient solar UV levels are affected by some geophysical factors including absorption and scattering by atmospheric constituents, and geometric factors such as the sun-earth distance and the solar zenith angle. Moderate exposures to solar UV radiation are beneficial, especially for cutaneous production of vitamin D. Exceeding safe exposure levels increases the risk factor of some diseases including sunburn, photo-aging, skin cancer and UV-related eye diseases. The assessment of personal UV exposure is therefore required for UV dose-response relationship studies. Chemical UV dosimetry is an effective tool for this purpose and is preferred over biological and physical methodologies, but is limited to short-term measurements. In addition to possessing adequate dosimetric properties for UV quantification, chemical dosimeters are characterised by their low cost and high versatility. Quantification of long-term UV exposure, which is responsible for UV-related effects with a cumulative nature, can be achieved by replacement of short-term exposure dosimeters, increasing the cost, effort and measurement error. Development of long-term exposure chemical UV dosimeter capable of monitoring large UV doses with single dosimeters would be of great value. There is sufficient evidence in the literature for the deterioration of unstabilised PVC on prolonged exposure to UV radiation. Whether this deterioration can be used to quantify UV exposure is a question that has previously not been investigated.

Chapter 3

Materials and Methods

3.1 Introduction.

3.2 Equipment and instrumentation.

3.3 Optimal parameters and construction specifications of the PVC based dosimeter.

3.4 Determination of dosimetric properties.

3.1 Introduction

The review of research on PVC materials (Section 2.7) demonstrated the high susceptibility of PVC to photo-degradation when exposed to long-term solar UV radiation, leading to detectable changes in its physical properties. In addition, the results of the pilot study (Appendix A) showed that the UV-induced changes within solvent cast PVC thin film can be described in terms of the absorbance change in the 1064 cm^{-1} peak intensity. This change was found to be proportional to the incident UV radiation and, therefore, the PVC satisfies the fundamental requirement for any chemical UV dosimeter (Davis et al. 1976; Webb 1995). The pilot study results also showed that PVC can be calibrated against a suitable instrument to provide a measure of solar UV radiation for periods of at least three weeks of exposure at subtropical sites. Therefore, a full characterization of the dosimetric properties of the PVC film was required before acknowledging PVC as a suitable long-term UV dosimeter.

The investigation of the dosimetric properties of the proposed dosimeter listed in Section 2.6.1 requires first the determination of the optimal parameters for the fabrication of PVC thin films and the development of standardized specifications of the dosimeter.

The following sections describe in detail a variety of indoor and outdoor experiments that were performed at the University of Southern Queensland (USQ), Toowoomba, Queensland (27° 33' S 151° 55' E, elevation of 691 m) using a wide range of available research instruments to test the optimal parameters, specifications and the dosimetric properties of the PVC based UV dosimeter.

3.2 Equipment and instrumentation

3.2.1 Polymer film casting table

PVC sheets of A4 paper size in differing thickness were produced using a polymer film casting table (Figure 3.1).

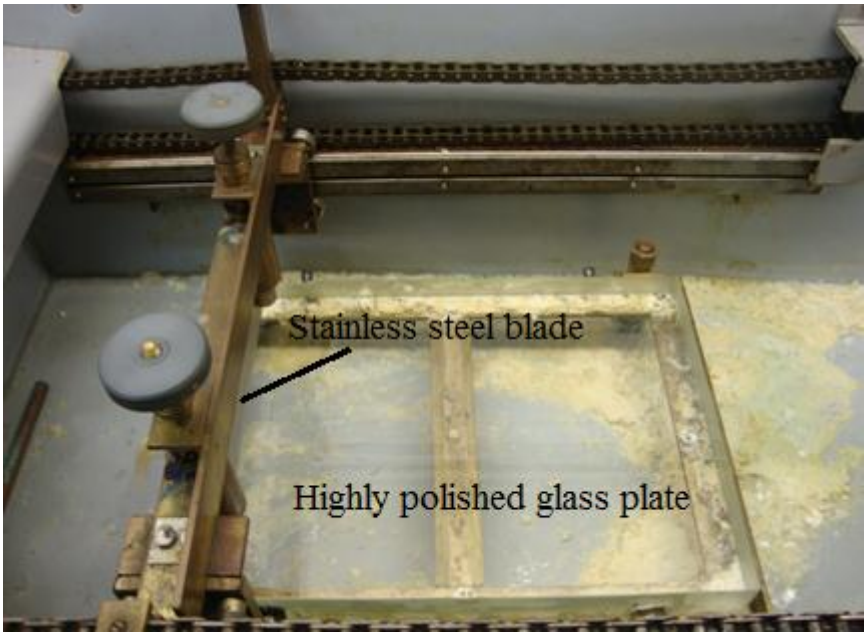

Figure 3.1: The polymer film casting table

The casting table consists of a stainless steel blade and a highly polished glass plate to one micron of flatness. The latter is installed on a metallic base that is mounted on four adjustable screws to level the plate horizontally. The stainless steel blade is installed above the glass plate so that it can be driven along the glass plate by an electric motor. The blade can be adjusted in height using side screws to achieve the desired film thickness.

3.2.2 Film thickness measurements

The thickness of the prepared PVC sheets was measured using a dial thickness gauge (Logitech, UK) mounted on a metal base (Figure 3.2).

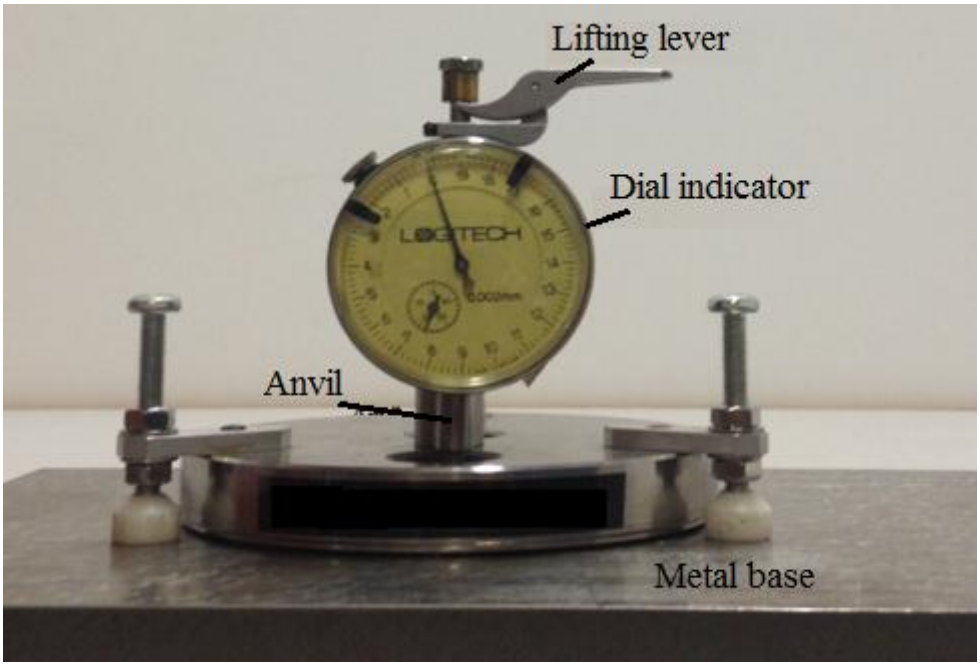

Figure 3.2: Dial thickness gauge employed in determining the PVC thin sheets.

The metal base provides a smooth flat ground surface upon which the PVC sheet is placed. The dial gauge consists of a dial indicator attached to a circular metal table and connected to a flat-end steel anvil. The dial indicator has a thumb-operator lifting lever at the top in order to raise the anvil through a spring-loaded spindle. The entire assembly is supported upon a tripod of three equidistant legs. The measuring range of the gauge is 0–10 mm with 2 μm resolution.

Before taking the measurements, the metal base and the anvil were cleaned with alcohol. A clean piece of paper was then put between the anvil and the base and pulled out slowly in order to polish and further clean the surfaces. After removing the paper, the gauge was allowed to close. The bezel was adjusted until the indicator lined up exactly with the zero. The anvil was lifted several times by pressing the lifting lever to ensure that the indicator coincided with zero. In order to avoid the localised compression of the PVC film by the anvil of the measuring gauge, the measured PVC film was placed between two feeler gauge leaves of known thickness and the combined thickness of the sheet and the leaves was measured. From this value the thickness of the film was determined by difference.

The accuracy of the manual thickness gauge was investigated using feeler gauge leaves of different thickness. Each leaf was measured five times and the standard deviation and percentage error were calculated (Table 3.1).

Table 3.1: Deviation of the thickness gauge measurements from the thickness of standard feeler gauge leaves.

Sample	Leaf thickness (µm)									
	60	**100**	**150**	**200**	**250**	**300**	**350**	**400**	**450**	**500**
1	60	101	158	207	258	304	362	400	454	512
2	60	101	158	207	259	306	360	402	454	508
3	61	102	158	207	259	305	364	402	454	512
4	60	102	158	207	258	304	364	402	454	512
5	60	101	158	208	258	304	364	402	454	512
Average	60.2	101.4	158.0	207.2	258.4	304.6	362.8	401.6	454.0	511.2
SD	0.40	0.49	0.00	0.40	0.49	0.80	1.60	0.80	0.00	1.60
Error (%)	0.3	1.4	5.3	3.6	3.4	1.5	3.7	0.4	0.9	2.2

The maximum error encountered for an averaged five measurements was 5.3%. The average error for all measurements was 2.1%. However, the error for thicknesses up to 100 µm (thin film dimensions) was less than 1.5%. The accuracy of the measured thicknesses, therefore, will be considered to be within ±2% of the measured thickness.

3.2.3 Irradiation facilities

3.2.3.1 Fluorescent UV lamp

A 40-watt fluorescent UV lamp (model TL 40/12, Philips, Lawrence and Hanson, Toowoomba, Australia) was employed as an artificial UV source to irradiate a large number of dosimeters simultaneously. Figure 3.3 shows the relative spectral irradiance of the fluorescent lamp as measured using a spectroradiometer (model USB4000, Ocean Optics). The UV band represents about 80% of the total radiation intensity of the lamp with predominant UVB output (63%).

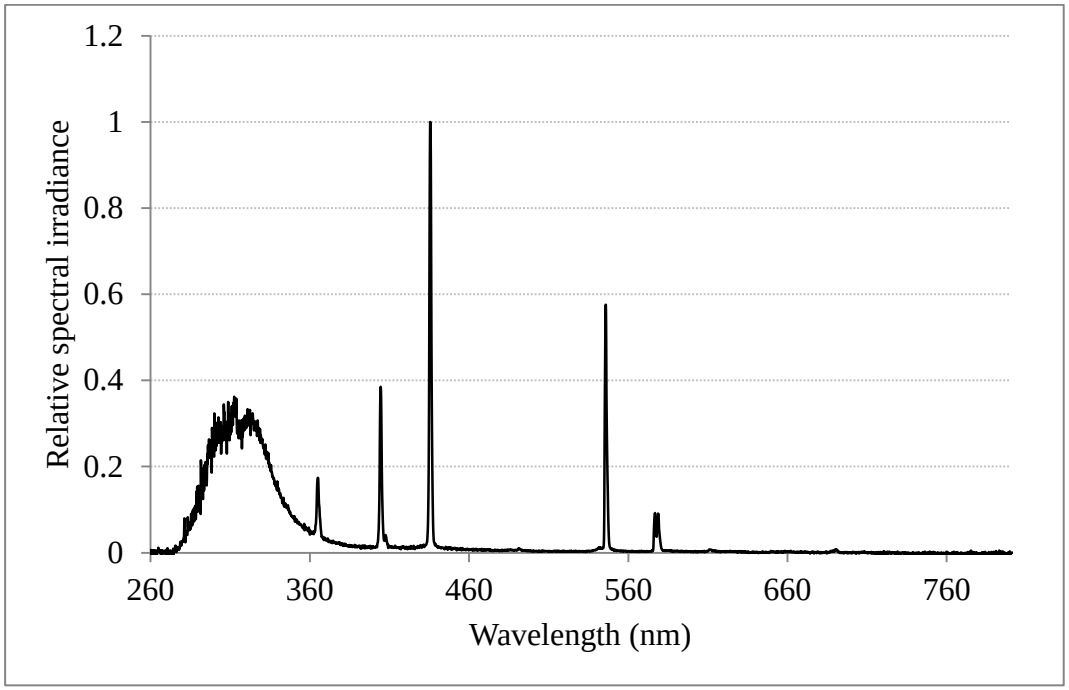

Figure 3.3: The relative spectral irradiance of the fluorescent lamp as measured at the exposure site.

Since fluorescent lamps usually require warm-up time before reaching their full output, the warm-up time of the lamp was investigated and was found to be about 10 minutes. Furthermore, as the lamp is employed without an exposure controller and the output of the lamp is expected to fluctuate with time, the UV irradiance of the lamp was measured using a spectroradiometer (model DMc150, Bentham Instruments Ltd, Reading UK) at a distance of 7 cm at various intervals over about 900 hours and the average deviation from the measured irradiance was about 3.5%. In addition, the UV irradiance was measured at different distances from the lamp. The measured UV irradiances between 280 nm and 400 nm as a function of the distance are shown in Figure 3.4. The error bars represent an uncertainty of 3.5% of the measured irradiance related to the instability of the lamp output.

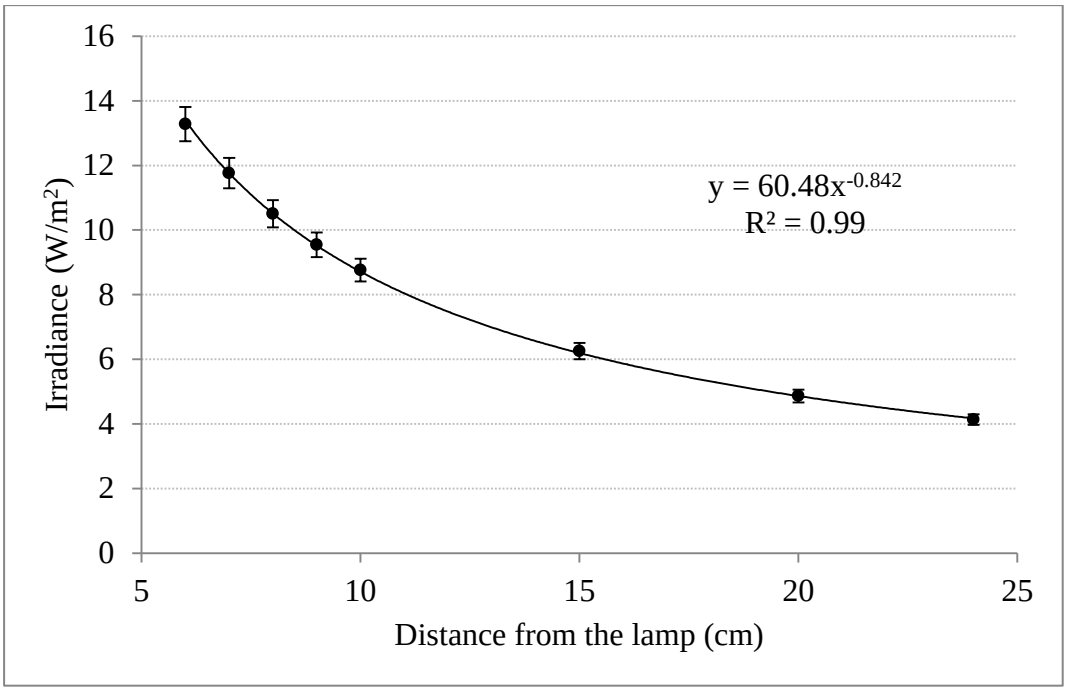

Figure 3.4: The UV irradiance between 280 nm and 400 nm at the exposure site as a function of the height of the lamp.

A UV irradiation mini chamber (Figure 3.5) was constructed to facilitate the measurements using the fluorescent lamp and provide the maximum protection to the researcher from UV radiation.

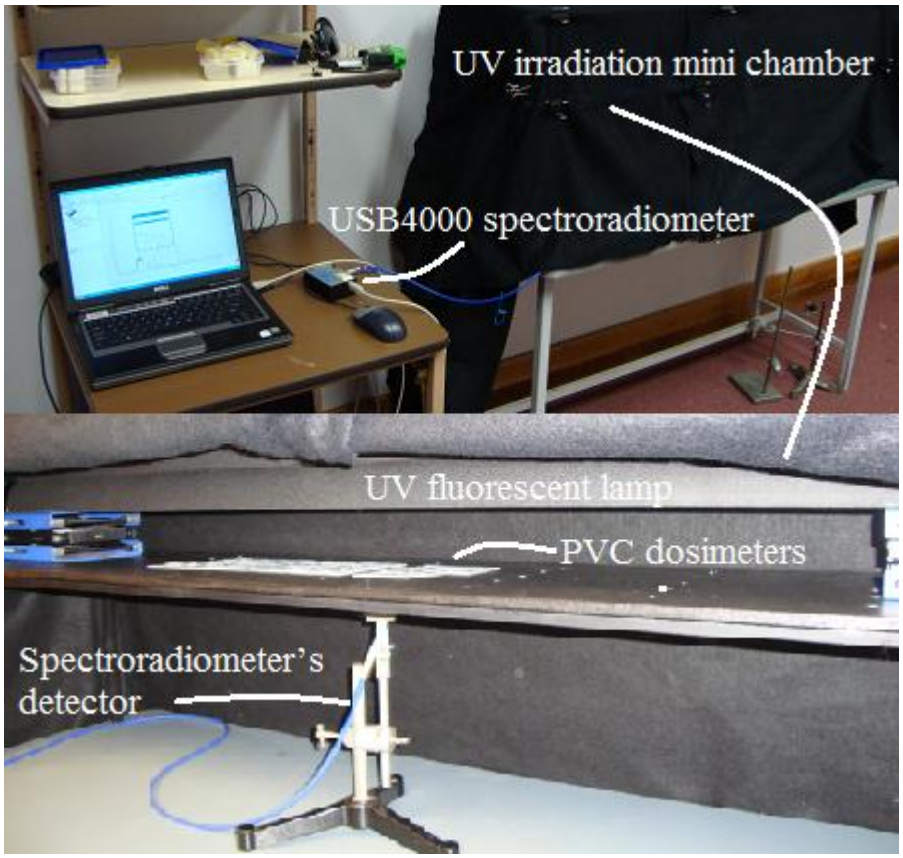

Figure 3.5: UV irradiation mini chamber employed in exposing a number of PVC dosimeters to the same UV radiant exposure.

The chamber is a 130 cm × 50 cm × 30 cm frame covered by black cloth and contains a horizontal 128 cm × 28 cm black board that was installed across the middle of the frame. The lamp was mounted on the board using adjustable stands to control the height of the lamp and hence the irradiance at the dosimeters site. The board was designed with a specific arrangement of 3 mm diameter holes (to suit the spectroradiometer's detector) through which the distribution of UV radiation over the board can be mapped. The irradiance at an area of 10 cm × 60 cm was measured along the lines parallel and perpendicular to the longitudinal axis of the lamp.

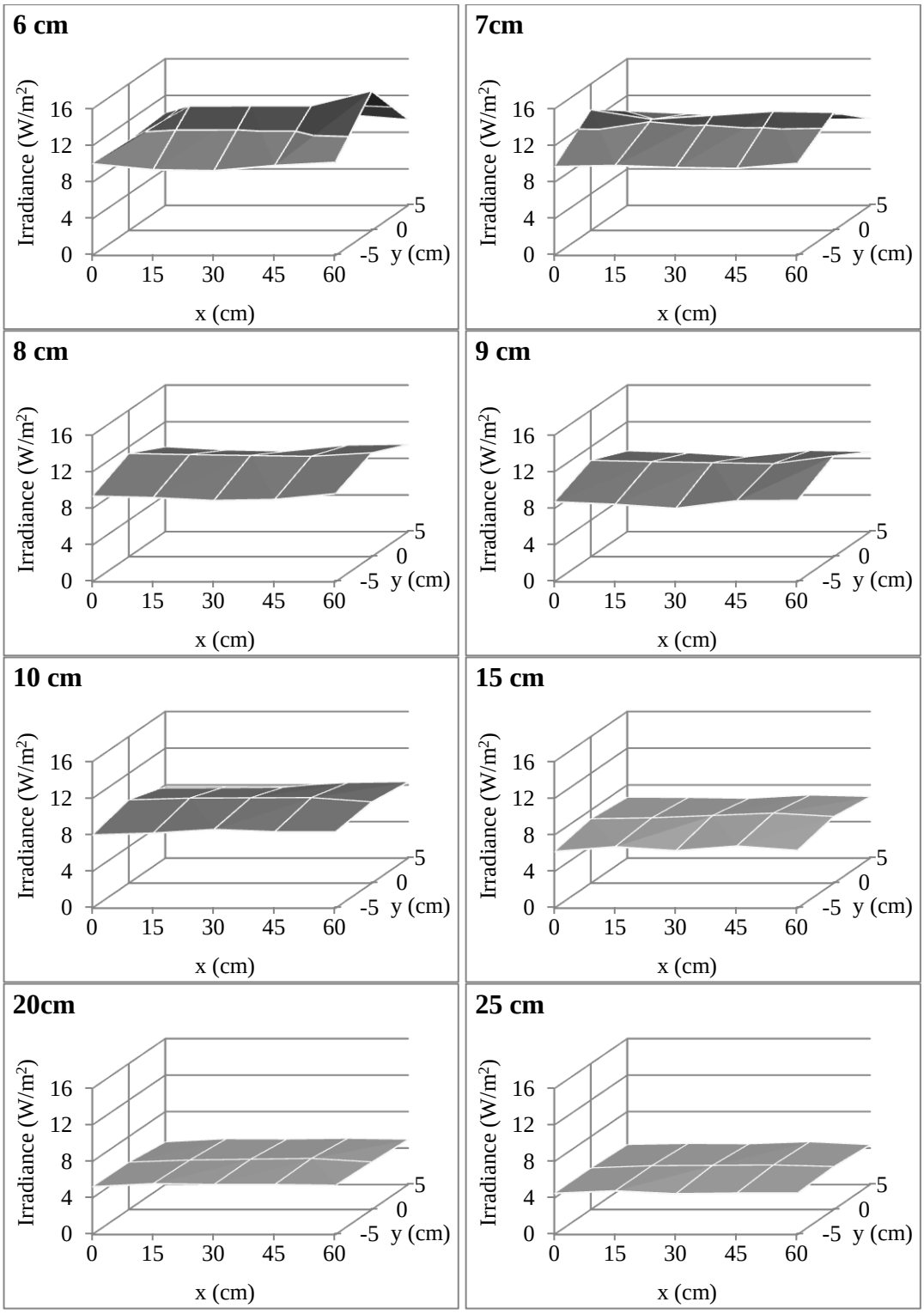

Figure 3.6: The irradiance distribution as measured at the exposure site for different distances between the lamp and the exposure site. The x and y axes represent the length and the width of the board, respectively.

The uniformity of the irradiance over the studied area was calculated at distances between 6 cm and 25 cm from the lamp (Figure 3.6) using the following IEC (International Electro-technical Commission) standard formula (IEC 2007):

$$Uniformity = \pm 100 \times \left(\frac{E_{max} - E_{min}}{E_{max} + E_{min}} \right) \qquad (3.1)$$

where E_{max} and E_{min} are the maximum and minimum irradiances measured at the investigated area respectively.

An area of 10 cm × 30 cm was determined to be suitable to ensure that the dosimeters were uniformly irradiated (within 3%) along the parallel lines for all distances from the lamp. However, the uniformity along the perpendicular lines varies, as expected, from about 15% to about 3.5% for distances between 6 cm and 25 cm from the lamp. Therefore, the dosimeters were exposed in parallel lines across the test area so that they received irradiance with a uniformity of about 4%.

3.2.3.2 Solar UV simulator

For laboratory experiments that require a stable spectrum and a collimated beam of UV radiation, a 300 W UV solar simulator (19160–1000, Newport Co., California, USA) combined with a digital exposure controller (model 68945, Newport Co., California, USA) (Figure 3.7) was used to simulate the UV portion of solar radiation. The simulator is powered by a highly regulated power supply (model 6991, Newport Co., California, USA) that provides constant power required for stable output and includes a multi-function LED display to monitor the power supply functions.

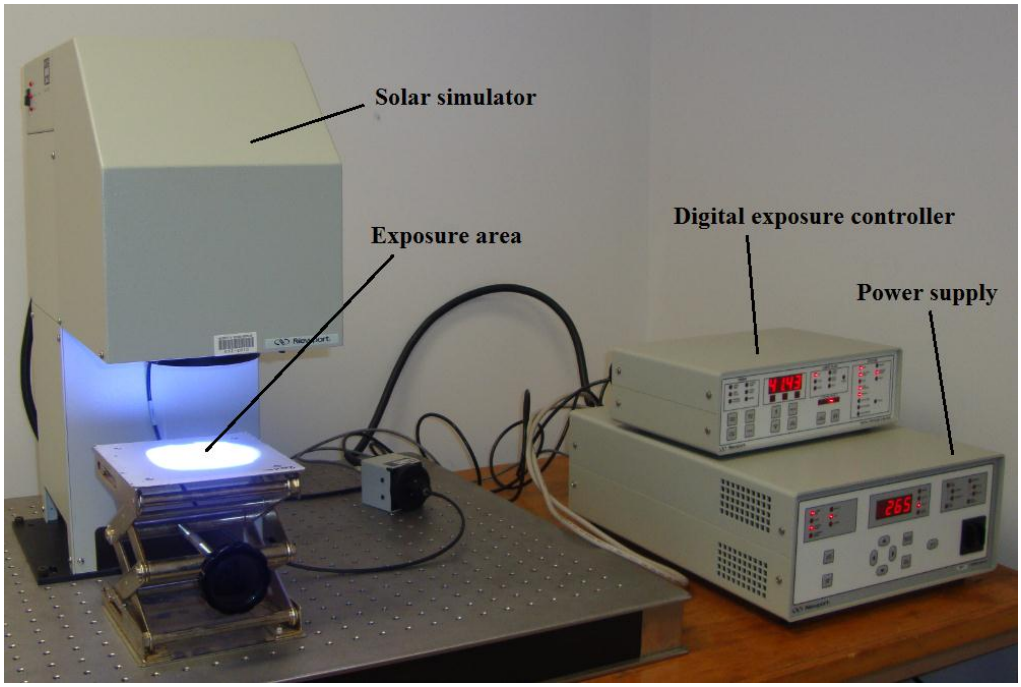

Figure 3.7: Set up of exposures using the solar simulator.

The optical components of the simulator are shown in Figure 3.8.

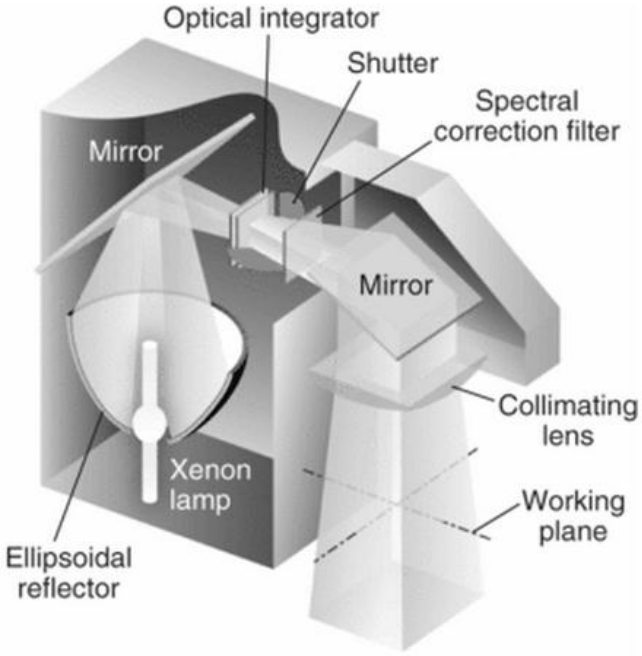

Figure 3.8: Optical configuration of the 19160–1000 solar simulator (Jeong 2007).

The radiation source is a 300 W xenon arc lamp that emits a 5800 K blackbody-like spectrum positioned at one focus of an ellipsoidal reflector. The small dimensions of the arc allow efficient beam collimation. A combination system of reflecting mirrors, optical integrator, spectral correction filter (atmospheric attenuation filter No. 81017), UVA/UVB dichronic mirror, Vis-IR attenuating filter and collimating lens modify the irradiance geometry to obtain a continuous collimated beam with a solar-like spectrum (Figure 3.9) of ± 5% uniformity over a 5.1 cm × 5.1 cm working plane.

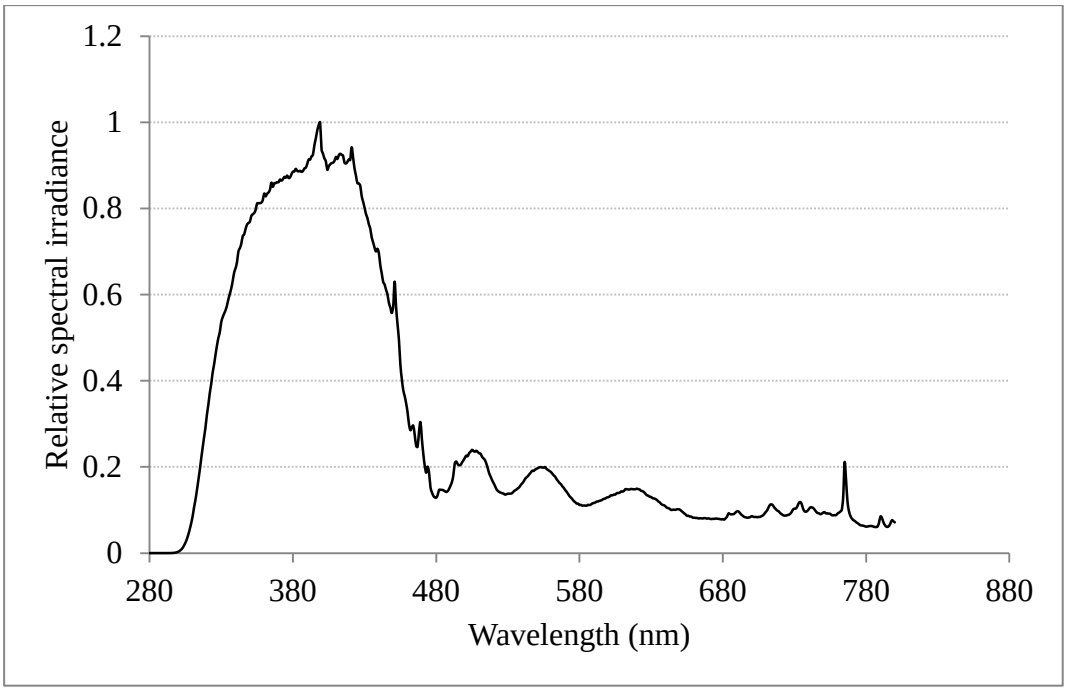

Figure 3.9: The relative spectral irradiance of the solar simulator as measured at the exposure site.

A digital exposure controller was employed with the solar simulator to maintain the irradiance relatively constant, regardless of lamp aging or changes in ambient temperature; it also allowed predefined timed exposures to be preset.

3.2.3.3 Irradiation monochromator

The investigation of the effectiveness of different wavelengths for producing change in the examined polymer has been undertaken using a Cornerstone™ 260 ¼ m motorized monochromator (Oriel Instruments, USA). The radiation source was a 1600 W xenon mercury arc lamp held in a sophisticated housing (model 66870, Oriel Instruments, USA). The lamp was powered by a digital arc lamp power supply (model 69922, Oriel Instruments, USA) with an exposure controller (model 68945, Newport Co., California, USA) (Figure 3.10) to stabilize the lamp output.

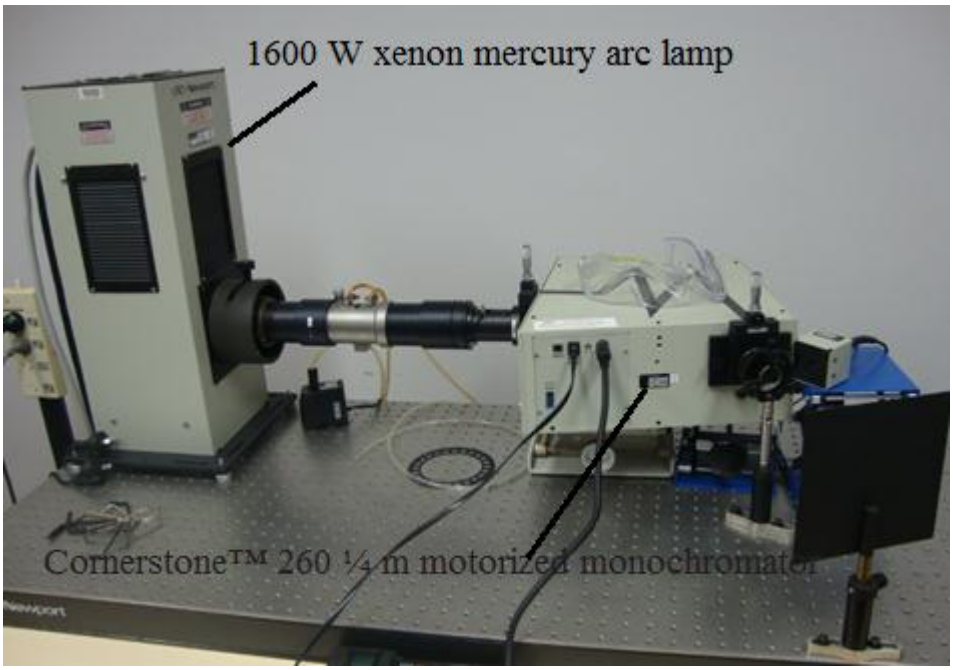

Figure 3.10: The system of the monochromator and the xenon mercury housing lamp.

The monochromator is characterised by a double grating, 0.35 nm wavelength accuracy and 0.08 nm wavelength precision (Newport n.d.). The width of the input and output slits of the monochromator can be adjusted to control the full width at half maxima (FWHM) of the output beam. The slits were set to produce a beam with a FWHM of approximately 5 nm.

The relative spectral distribution of different wavebands produced by the monochromator is shown in Figure 3.11.

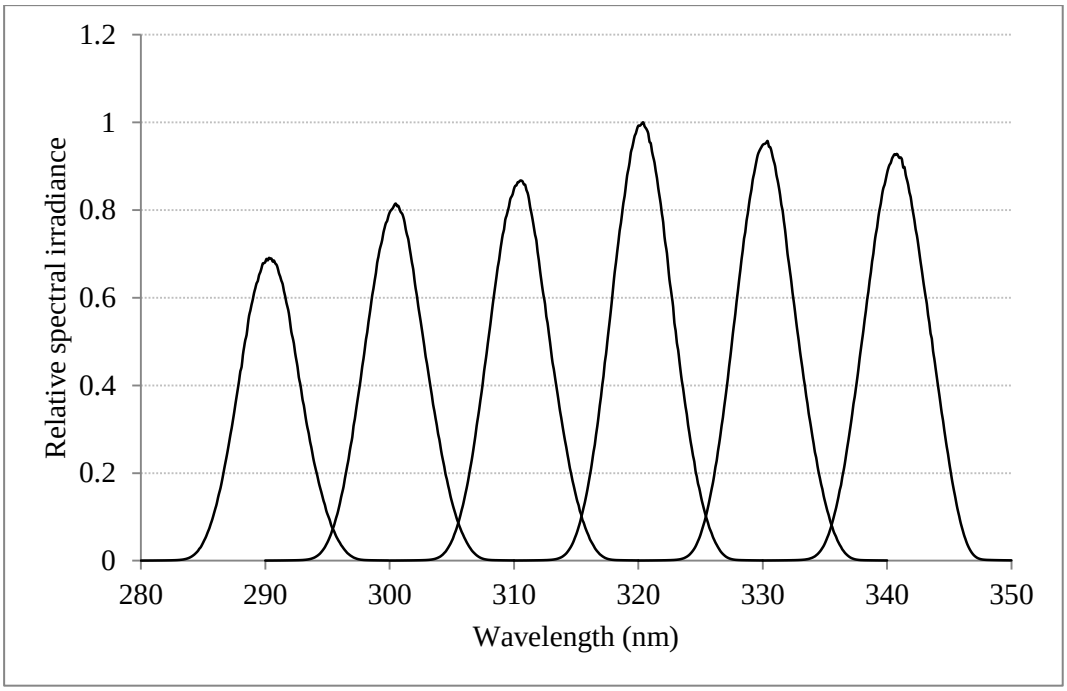

Figure 3.11: The relative spectral distribution of the irradiation monochromator at different UV wavebands.

3.2.3.4 Solar UV radiation

Solar UV radiation was used to establish the seasonal calibration curves and in anatomical exposure measurements conducted outdoors. Figure 3.12 shows the solar UV spectrum as measured in a partially cloudy day at Toowoomba, Australia (27º33´ S), for solar zenith angle of 64.72º.

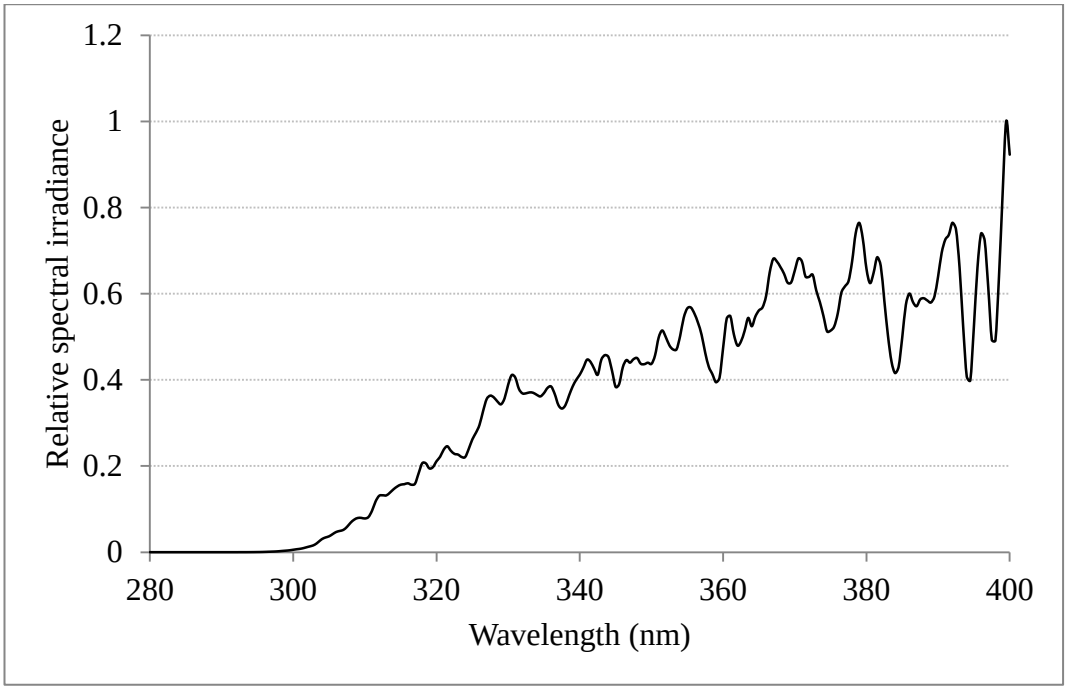

Figure 3.12: Global solar UV irradiance.

3.2.4 Irradiance measurements

3.2.4.1 The Bentham spectroradiometer

The primary instrument used for spectral irradiance measurements of artificial sources of UV radiation was a scanning spectroradiometer (model DMc150, Bentham Instruments Ltd., Reading UK) (Figure 3.13).

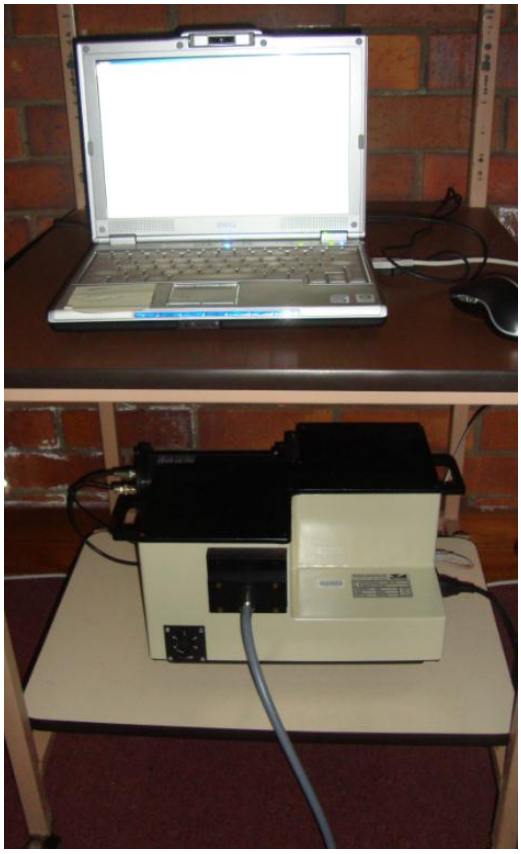

Figure 3.13: The DMc150 Bentham spectroradiometer.

The Bentham instrument is a double monochromator spectroradiometer with gratings of 1200 lines/mm. The incident radiation on the diffuser is transferred through a quartz fibre optic cable to the monochromator where the radiation is directed by a particular arrangement of mirrors to the first diffraction grating that separates the radiation into its specific wavebands. Further dispersion takes place through the second grating and the radiation is then directed, wavelength by wavelength, through the movements of the grating to measure a complete spectrum (Bentham 1997). A calibration was applied to provide a spectrum in units of $mW/m^2/nm$. The spectroradiometer was calibrated for wavelength against the 365.0 nm mercury emission line of a mercury electric discharge lamp to within ± 0.1 nm, and against an air-cooled secondary standard quartz-tungsten halogen lamp for spectral irradiance.

3.2.4.2 The Ocean Optics Spectrometer

A portable spectrometer (model USB4000, Ocean Optics, USA) was used in monitoring the irradiance uniformity of the fluorescent UV lamp (Figure 3.14).

Figure 3.14: Ocean Optics USB4000 Fiber Optic Spectrometer.

The spectrometer is characterised by a resolution of less than 1 nm. Wavelength and irradiance calibration of the USB4000 was undertaken by employing the 365 nm mercury spectral line and a 150 W quartz halogen lamp with calibration traceable to the National Physical Laboratory, UK standard. The USB4000 measured the spectral irradiance from 178 nm to 888 nm in approximately 0.2 nm steps with an integration time of 20 ms and averaged over 10 scans. The main advantage of the USB4000 is that it draws power from the host computer, eliminating the need for an external power supply. Other advantages are the light weight, ease of usage and the small size of the detector.

3.2.4.3 The Erythemally weighted Biometer

Outdoor exposure measurements for erythemally weighted UVB were made using a permanently installed outdoor UVB Biometer (model 501 Biometer, Solar Light Co. PA. USA) mounted on the roof of one of the university buildings with no significant obstructions to the hemispheric field of view of the sky (Figure 3.15).

Figure 3.15: The outdoor UVB Biometer mounted on the roof of a USQ building.

The Biometer is a Robertson-Berger type meter with a sensor that comprises a gallium-arsenide diode positioned under a phosphor-coated glass detector. The sensor is protected from weather conditions by a quartz dome. The angular response of the Biometer detector is within ±5% from ideal cosine for incident zenith angles less than 60º (Morys & Berger 1993). The output signals, which are proportional to the measured solar UV irradiance and ambient temperature, are directed from the Biometer to the data logger by a shielded cable. The Biometer has a controlled internal temperature to ensure a high level of accuracy within an ambient temperature range of -40 to +50 ºC. The measured spectrum range is 280–320 nm with spectral response close to the erythema action spectrum defined by the International Commission on Illumination (CIE) (CIE 1998); and the measured dose range of 0–10 MED/hr. The instrument is regularly calibrated against the Bentham spectroradiometer and set to record the cumulative erythemal UV exposures each 5 minutes. The accuracy of the Biometer is ±10% of the daily total (Lester et al. 2003).

3.2.5 Optical absorbance measurements

3.2.5.1 Fourier Transform Infrared (FTIR) spectroscopy

FTIR spectrophotometer (model IRPrestige-21 FTIR-8400S, Shimadzu Co., Kyoto) combined with IRsolution software version 3.1 was used to record and compare the IR absorption of the dosimeters (Figure 3.16). The spectra were obtained at a resolution of 4 cm^{-1} with the absorption mode and corrected baseline within the range 400–4000 cm^{-1}.

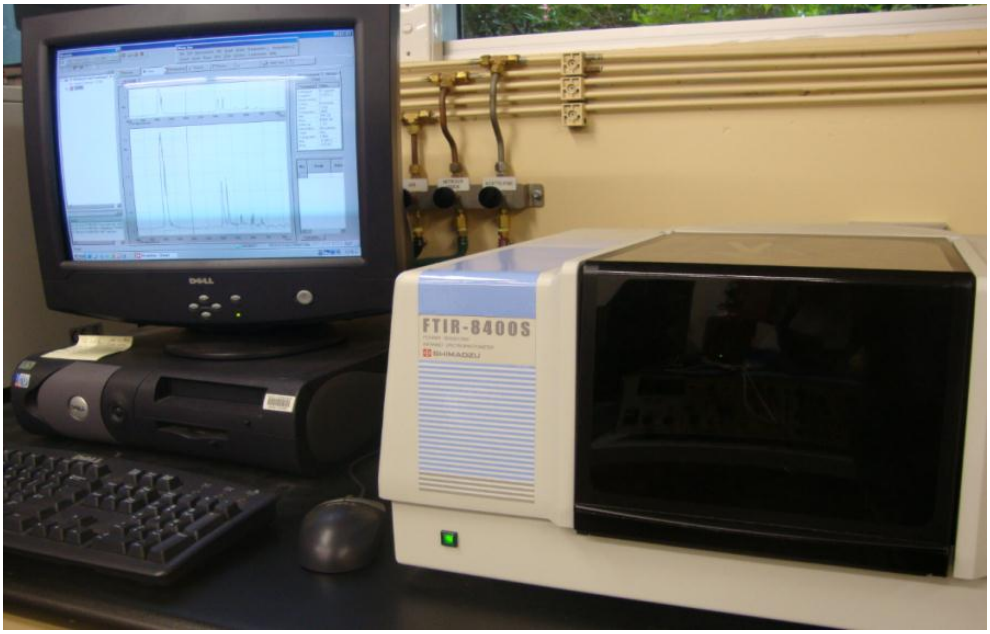

Figure 3.16: The FTIR spectrophotometer employed in measuring the IR absorption of the dosimeters.

The uncertainty of the measured absorbance related to the reproducibility of both the instrument and the dosimeter placement was investigated by measuring the absorbance of five dosimeters ten times in a random order. The measured absorbance was found to be within ± 1% of the mean and, therefore, the absorbance uncertainty will be considered within ± 1%.

3.2.5.1 UV spectroscopy

A UV-Vis double beam spectrophotometer (model UV-1601, Shimadzu Co., Kyoto, Japan) combined with UV Probe software (Figure 3.17) was used to monitor changes in the UV absorbance spectra of the investigated polymers due to exposure to UV radiation.

Figure 3.17: UV-Vis Spectrophotometer

The radiation sources of the instrument are halogen and deuterium lamps with an on-board automatic light source positioning mechanism. The spectrophotometer is characterised by a photometric range of -0.5 to 3.99 ABS for the absorbance mode and 0.0 to 300% for the transmittance mode. The manufacturer specifies the wavelength accuracy to be ± 0.5 nm and the photometric accuracy to be ± 0.4% at 1.0 ABS (Shimadzu 1994).

3.3 Optimal parameters and construction specifications of the PVC based dosimeter

3.3.1 Mixing ratio

In order to determine the best mixing ratio (mass concentration), defined as the ratio of the mass of dry PVC powder in grams to the volume in millilitres of the tetrahydrofuran (THF) solvent used in the PVC solution for casting multiplied by 100 (W/V%); for the preparation of solvent cast PVC thin films, different concentrations of PVC solution were prepared by dissolving between 2 and 15 grams of PVC powder (Aldrich Chemical Company, Inc., catalogue number 34675-6) in 100 ml of THF solvent under vigorous stirring at 25 ± 2 °C. The dissolving time was recorded for each concentration and then each solution was cast in a thin layer using the polymer casting table and adjusting the stainless steel casting blade to be 100 μm above the plate. The solvent was allowed to evaporate at 25 ± 2 °C for at least two hours and the dry thin film was then removed. The thickness was measured at five different sites on the film using a dial thickness gauge (Logitech, UK) which was previously calibrated against feeler gauge leaves; its accuracy was found to be within ± 2% of the measured thickness. Five PVC dosimeters were then fabricated from each film by cutting the PVC film into 2 cm × 2 cm pieces, each attached with tape to cover the 1.8 cm × 1.2 cm aperture of a 3 cm × 3 cm plastic holder. The infrared (IR) absorption spectra of the dosimeters within the range 400–4000 cm^{-1} (IR region) were recorded using a Fourier Transform Infrared (FTIR) spectrophotometer (IRPrestige-21/FTIR-8400S, Shimadzu Co., Kyoto) at a resolution of 4 cm^{-1} in the absorption mode and corrected baseline.

3.3.2 Film thickness

The concentration of 10% of PVC/THF solution was determined as the best concentration for preparing PVC thin sheets for use in PVC based UV dosimeters (Section 4.4.1). This concentration was therefore employed for casting all subsequent PVC sheets that were used in this research.

In order to determine the thickness of PVC thin film appropriate for use for the UV dosimeters, PVC sheets of different thicknesses were prepared, as described in Section 3.3.1, using 10% PVC/THF solution and changing the distance between the casting blade and the glass plate from 60 μm to 480 μm in 30 μm steps. After measuring their thicknesses, the films were utilised to fabricate PVC dosimeters whose IR absorption spectra were measured using the FTIR spectrophotometer. The dosimeters' quality was evaluated and four thicknesses were selected to examine the relationship between the PVC's sensitivity to UV radiation and film thickness. Three dosimeters of each of the four thicknesses were irradiated (after measuring their pre exposure IR absorption spectra) at 28 ± 2 °C for about 650 hours (~ 20 MJ/m^2 of UV) using a UV fluorescent lamp (model Philips TL40/12, supplier Lawrence and Hansen, Toowoomba). The distance between the lamp and the dosimeters was

adjusted to be 7 cm and the spectral irradiance of the lamp was measured regularly with a calibrated scanning spectroradiometer (model DMc150, Bentham Instruments Ltd, Reading UK). The average integrated UV irradiance, average deviation of the lamp output and irradiance uniformity at the dosimeters' site were 9.1 W/m^2, 3% and 3% respectively. The dosimeters were removed from exposure for measurement of the IR absorption spectra at various exposure time intervals. The decrease in the absorption intensity of the dosimeters at the 1064 cm^{-1} peak after a period t of exposure $(\Delta A)_t$ was calculated by:

$$(\Delta A)_t = A^{initial} - A_t^{final} \tag{3.1}$$

where $A^{initial}$ is the initial absorbance of the dosimeters at 1064 cm^{-1} and A_t^{final} is the absorbance after a period t of exposure. The dose response curves were generated by relating the change in the absorbance to the corresponding unweighted UV radiant exposure (H) over 280–400 nm which was calculated from the relation:

$$H = \left(\sum_{\lambda=280}^{\lambda=400} E(\lambda) \times \Delta\lambda \right) \times t \tag{3.2}$$

where $E(\lambda)$ is the spectral irradiance, $\Delta\lambda$ is the wavelength increment and t is the exposure time. The dose response curves were then compared to determine the most suitable thickness for the PVC dosimeter.

3.3.3 Drying time determination

Pure PVC does not absorb any radiation above 220 nm (Zweifel et al. 2009) and thereby no changes should occur in PVC during its exposure to UV radiation. However, PVC is known to be degraded on exposure to UV radiation mainly because of impurities, arising from either thermal treatment during processing or added ingredients, which catalyse photodegradation processes or absorb UV radiation to form radicals that initiate further reactions (Wypych 2008). In this research, PVC thin films prepared by casting from tetrahydrofuran solution for use in UV dosimetry have not been treated thermally and contain no additives. Therefore, the UV-induced changes are assumed to be a result of the influence of residual tetrahydrofuran, which is a photosensitiser (Wypych 2008) and responsible for the 1064 cm^{-1} peak in the infrared (IR) absorption spectra of solvent cast PVC samples (Wypych 1985). Solvent residues remain even when the films are dried at high temperatures (up to 120 ºC) for extremely long times (Maláč et al. 1969). Maláč et al. (1969) dried solvent cast PVC samples at 50 ºC in air and found that the amount of residual tetrahydofuran in the samples decreases with time up to about 25 days and then remains nearly constant (Figure 3.18). The response of PVC dosimeters, that have been dried for various times, to UV radiation, therefore, has to be investigated to determine if it is necessary to dry the PVC thin films and for how long.

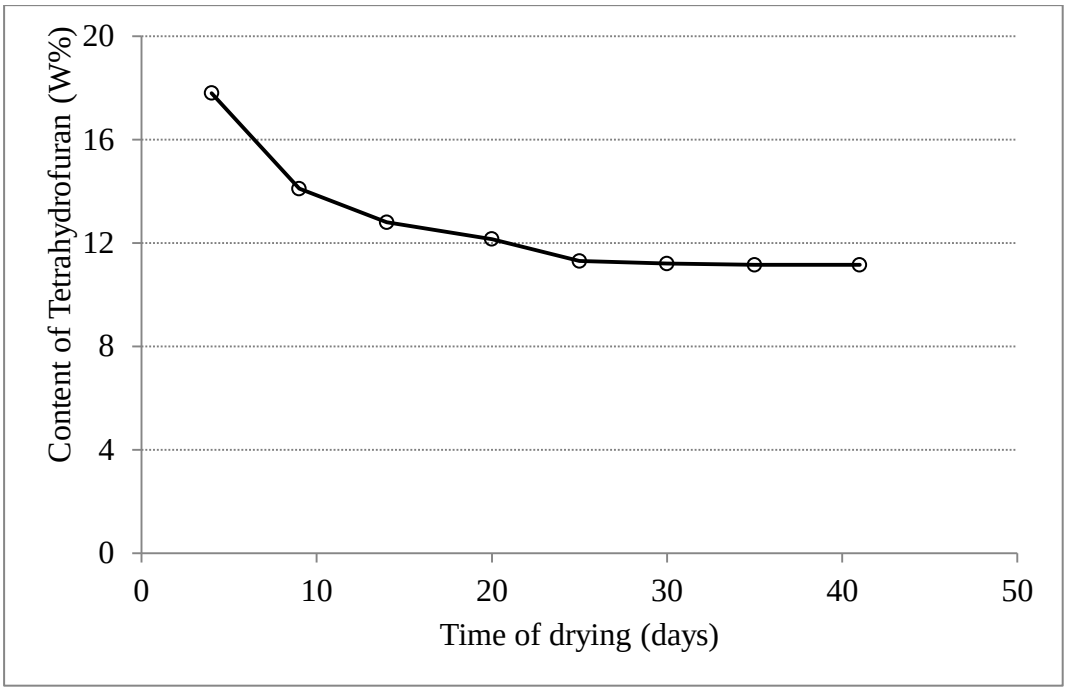

Figure 3.18: Quantitative dependence of residual tetrahydrofuran in solvent cast PVC samples on drying time at 50 ºC (Maláč et al. 1969).

Ninety solvent cast PVC dosimeters of thickness of about 16 µm were prepared as described in Section 3.3.1. The absolute absorbance of the dosimeters at 1064 cm^{-1} was measured immediately using the FTIR spectrophotometer and found to be 0.249 ± 0.012. The dosimeters were then dried at 50 °C in air for about four weeks and their absorbance was measured periodically. During the drying process, eight dosimeters were removed each five days and exposed to a broadband UV radiant exposure of 200 kJ/m^2 supplied by the UV fluorescent lamp that emits radiation primarily in the UVB region of the UV spectrum. Four of the dosimeters were exposed at 25 °C and four at 45 °C. The spectral irradiance at the dosimeters' site $E(\lambda)$ was measured with the calibrated Bentham spectroradiometer and the radiant exposure H received by the dosimeters was calculated by using Equation 3.2. The corresponding absorbance change (ΔA) was calculated with Equation 3.1. The average deviation of the lamp output during the exposure and the irradiance uniformity at the dosimeters' site were about 3% and 4%, respectively.

3.4 Dosimetric properties

3.4.1 Reproducibility

The reliability of any chemical UV dosimeter is determined, in part, by its reproducibility. Equal radiant exposures from the same source should induce the same measured response. Any errors related to the film response sensitivity have to be quantified and taken into account during the measurement process. To quantify the reproducibility of the measurements taken by the PVC based UV dosimeter, ten dosimeters were irradiated evenly by the fluorescent UV lamp for 20 days, receiving a total radiant exposure of 27 MJ/m^2 of broadband UV radiation.

The absorbance change of the ten dosimeters $(\Delta A\%)_i$, where $i = 1,2,...,10$ is the dosimeter number, was measured at various intervals during the exposure. The average absorbance change of the ten dosimeters was then calculated by:

$$(\Delta A\%) = \frac{\sum_i (\Delta A\%)_i}{10} \qquad (3.3)$$

and the absolute deviation from the mean for each dosimeter δ_i was obtained by

$$\delta_i = \frac{\left|(\Delta A\%) - (\Delta A\%)_i\right|}{(\Delta A\%)_i} \times 100 \qquad (3.4)$$

The average deviation then equals

$$\delta = \frac{\sum_i \delta_i}{10} \qquad (3.5)$$

The average deviation from the mean was obtained and plotted as a function of the radiant exposure.

3.4.2 Determination of the spectral response

The responsivity of chemical dosimeters to UV radiation is dependent on wavelength and therefore the dosimeter spectral response should be known. The spectral response of the PVC based UV dosimeter was investigated in this research using three different approaches and employing both poly and monochromatic radiation sources. This is because of the importance of the spectral response property of the proposed dosimeter, and to ensure the reliability of the obtained results.

In the first approach, which was used in an earlier study by Martin and Tilley (1971) to determine the relative wavelength sensitivity of unstabilised PVC to photo-oxidation, PVC dosimeters were irradiated behind a series of cut-off UV filters. Each filter transmitted UV radiation of wavelengths greater than a specific threshold wavelength. The wider transmitted wavebands are expected to induce higher responses. Comparing the difference between the waveband widths and the resulting responses will give a general evaluation about what wavebands are able to induce a change within the dosimeter and the relative effectiveness of these wavebands in inducing this change. The dosimeters in the second technique were irradiated by narrower UV wavebands using band-pass filters that are designed to transmit a portion of the UV spectrum, while rejecting all other wavelengths. The spectral response was also determined with a monochromatic source that provides very narrow wavebands with FWHM of 5 nm. The detailed procedures are presented in the following sections.

3.4.2.1 Cut-off filter technique

A set of nine glass cut-off filters (Schott AG, Mainz, Germany) with threshold wavelength range 285–377 nm (10% transmission) was used to investigate the relative ability of the UV sub-bands to induce changes in 16 μm thick PVC dosimeters. Figure 3.19 shows the transmittance spectra $T(\lambda)$ of the nine filters measured using a spectrophotometer (model UV-1601, Shimadzu Co., Kyoto, Japan).

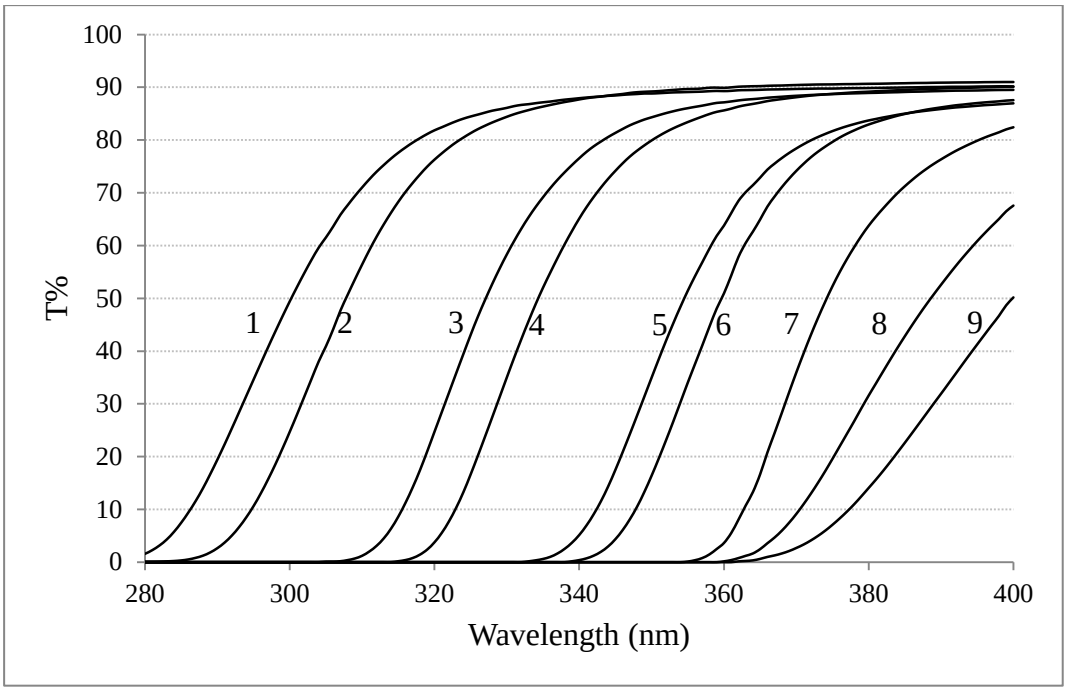

Figure 3.19: Transmittance spectra of the nine cut-off filters.

Nine pairs of PVC dosimeters were simultaneously exposed behind the filters to the Philips UV fluorescent lamp for 135 hours at 28 ± 2 °C along with an unfiltered pair, a pair covered with a UV cut-off filter (Llumar, Scotchline, Australia) to block wavelengths below 400 nm from reaching the dosimeters and a pair covered with an opaque cardboard that obscured the dosimeters from any radiation. The spectral irradiance of the source $E(\lambda)$ over the UV band (280–400 nm) at the dosimeters exposure plane was periodically measured with the Bentham spectroradiometer. The spectral irradiance behind each filter $E_n(\lambda)$ was then calculated by:

$$E_n(\lambda) = E(\lambda)T_n(\lambda) \qquad (3.6)$$

where $T_n(\lambda)$ is the spectral transmission of the nth filter. The IR absorbance of the dosimeters was measured before the exposure $A_n^{initial}$ and immediately after the exposure A_n^{final}; and then the absorbance change $(\Delta A)_n$ was calculated by:

$$(\Delta A)_n = A_n^{initial} - A_n^{final} \qquad (3.7)$$

The resulting absorbance change was compared with the corresponding waveband and radiant exposure.

3.4.2.2 Narrow band-pass filter technique

Four narrow band-pass filters (model 03 FIU, Melles Griot Optics) with wavelengths of maximum transmittance 300 nm, 324 nm, 343 nm and 361 nm as measured using the Shimadzu spectrophotometer were used in the irradiation of four PVC dosimeters using different narrow UV sub bands.

The irradiation source was a 300 W UV solar simulator (19160-1000, Newport Co., California, USA) combined with an exposure controller (model 68945, Newport Co., California, USA) to minimise variations in the lamp output. The dosimeters were positioned 1 cm behind the filters and continuously exposed at 32 ± 2 °C for 31 hours to the collimated UV beam. The UV spectral irradiance at the dosimeters' site $E(\lambda)$ was measured by the Bentham spectroradiometer and then utilised with the transmission spectra of the filters to calculate the spectral irradiance behind each filter using Equation 3.6 (Figure 3.20).

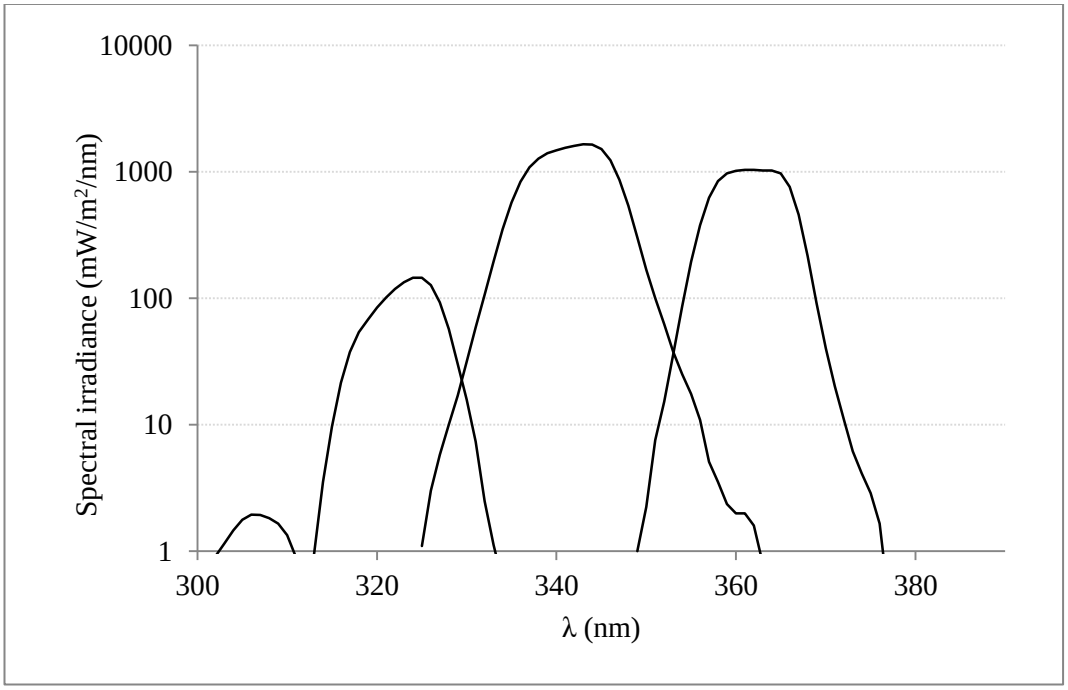

Figure 3.20: Spectral irradiance as calculated behind each of the four narrow band-pass filters.

Pre and post exposure FTIR absorbance was measured to compare the resulting change with the received exposure.

3.4.2.3 Monochromatic radiation

Six PVC dosimeters were sequentially exposed to a fixed dose of 0.5 MJ/m^2 at 25 ± 2 ºC using different UV wavelengths obtained by setting a 1600 W irradiation monochromator (model 66870, Oriel Instruments, USA) at the selected wavelength from 290 to 340 nm in 10 nm increments. For the maximum output irradiance, the monochromator input and output slits were set to a width of 4.5 mm and 4 mm, respectively, and the resulting irradiances at the dosimeters' surface (measured by the Bentham spectroradiometer) were very narrow wavebands of nearly the same FWHM (5.6 ± 0.1 nm) (Figure 3.21).

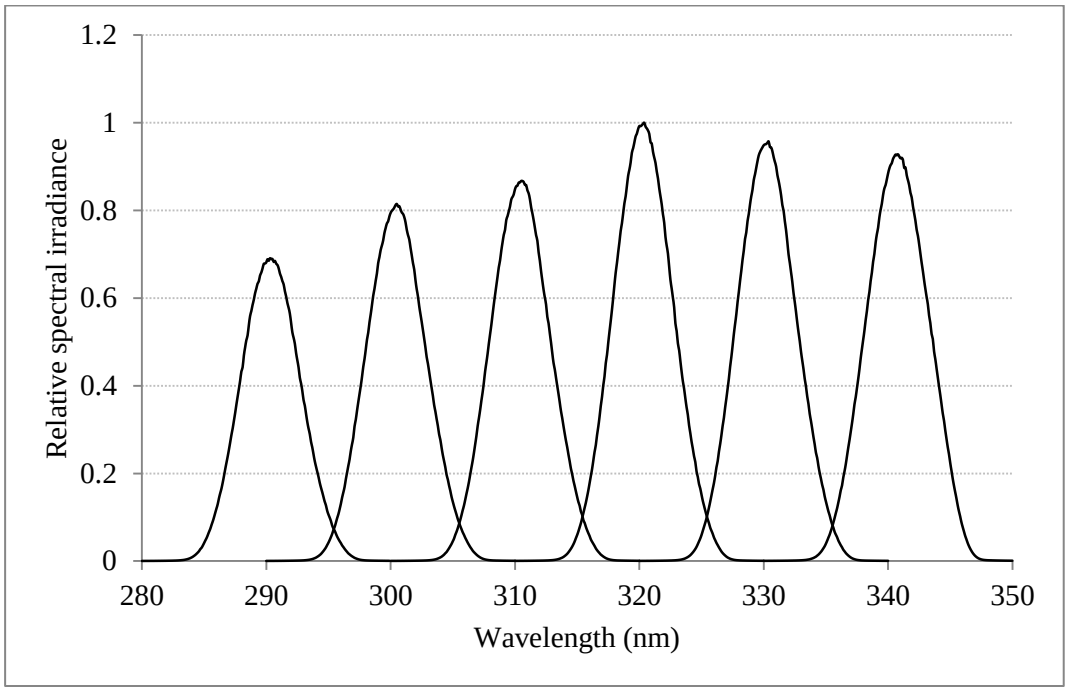

Figure 3.21: Relative spectral irradiance of the narrow bands supplied by the irradiation monochromator.

The integrated irradiance of the selected wavelengths was between 14.0 and 21.5 W/m^2 and the exposure time ranged between 6.5 and 9.9 hours. The exposure related IR absorbance change of the dosimeters was measured with wavelength and the wavelength responsible for the maximum change was determined (290 nm) and used to normalise the results to unity. The exposure was repeated for a dose of 0.1 MJ/m^2 at 25 ± 2 ºC and 40 ± 2 ºC to investigate the dependency of the spectral response on exposure dose and temperature. The exposure time in this case ranged from about 1.3 to 2 hours.

3.4.3 Temperature independency

Chemical dosimeters employed in solar UV radiation measurements experience different ambient temperatures. Therefore, the thermal stability of the dosimeter has to be ensured and the valid temperature region of the dosimeter should be identified.

The effect of ambient temperature on the PVC dosimeter response to UV radiation was investigated by irradiating PVC dosimeters using both the fluorescent lamp and the solar UV simulator at a temperature-controlled environment. Five batches of three PVC dosimeters, previously dried at 50 °C for four weeks, were sequentially exposed at 5 ºC, 12 ºC, 20 ºC, 30 ºC, 40 ºC, and 45 ºC to an equal broadband radiant exposure of 0.2 MJ/m^2 using the fluorescent lamp. In addition, five batches of four dosimeters were sequentially subjected to 0.5 MJ/m^2 from the solar simulator at the abovementioned temperatures. The exposure using the solar simulator was repeated with a total exposure dose of 1 MJ/m^2.

Irradiation at different temperatures was achieved by controlling the air flow temperature, except for 5 ºC in which a water bath containing a mixture of ice and water was used. The temperature error was estimated to be ± 2 ºC. The IR absorbance was measured before and after the exposure to allow comparison of the absorbance change of the dosimeters exposed to the same exposure dose at different temperatures.

3.4.4 Dose-rate independency

Chemical UV dosimeters measure the integrated radiant exposure (dose). Therefore, the UV-induced response within the dosimeter should be independent of the rate of the received dose (irradiance), the property which is known as the Bansen-Roscoe law of reciprocity. The law states that equal doses are supposed to induce the same response regardless of the dose-rate.

The validity of the reciprocity law for the PVC dosimeter was studied by exposing several groups of PVC dosimeters to the same exposure dose accumulated from different irradiances during different exposure times. The desired irradiances were obtained by either changing the distance between the fluorescent lamp and the dosimeters or incorporating neutral density filters with the solar UV simulator.

Seven batches of six PVC dosimeters were sequentially exposed to the fluorescent lamp at different distances from the lamp for different durations of exposure so that all batches received an equal broadband UV radiant exposure of 2 MJ/m^2. The distance between the dosimeters and the lamp ranged between 6 cm and 34 cm. The UV irradiance as measured by the Bentham spectroradiometer at the exposure site was between 2.9 W/m^2 and 12.9 W/m^2 and the required exposure time ranged between 43 and 193 hours. Figure 3.22 illustrates how the spectral irradiance at the exposure site changes with increasing distance between the fluorescent lamp and the dosimeters.

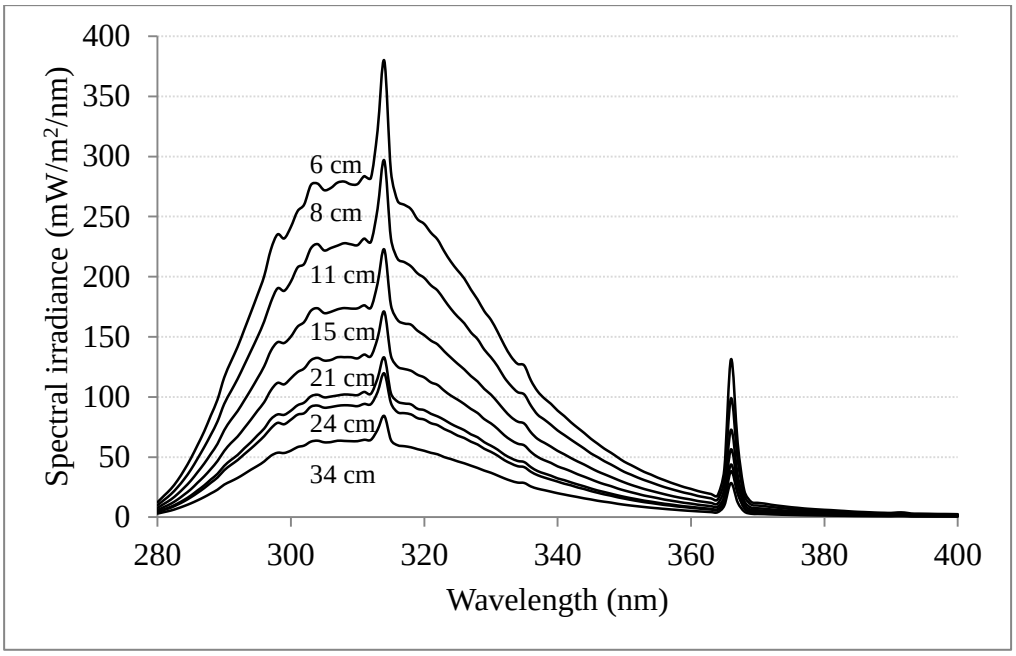

Figure 3.22: The change of the spectral irradiance measured at the exposure site as a function of the distance between the fluorescent lamp and the dosimeters.

It is important that the employed irradiances have similar distributions, i.e. the spectral irradiance decreases evenly for all wavelengths with increasing distance. For instance, the integrated irradiance may halve, but this should be due to a uniform halving in intensity of the whole irradiation spectrum. The percentage decrease of the spectral irradiance from its initial value (maximum value when the distance is 6 cm) with the increase of the distance was calculated and is provided in Figure 3.23.

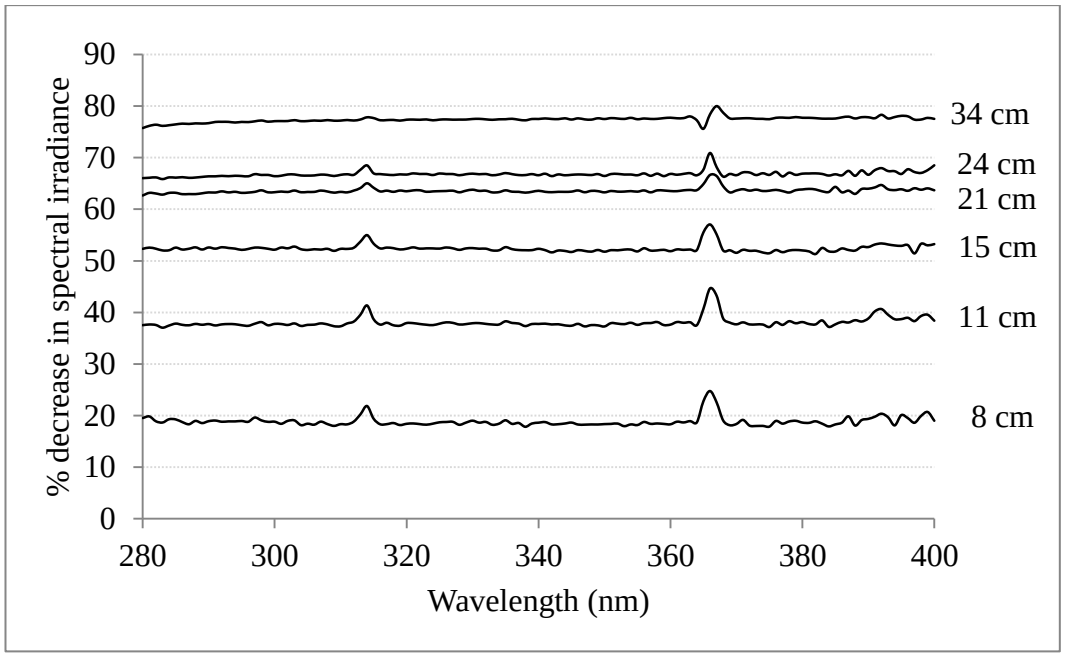

Figure 3.23: The percentage decrease of the spectral irradiance from its initial value (when the distance is 6 cm) as a function of the distance between the fluorescent lamp and the dosimeters.

The change in the spectral irradiance is almost equal for all wavelengths, with a noticeable deviation for the wavelengths 312–316 nm and 364–368 nm. The equality of the change improves with increasing distance. The average deviation from the mean of the percentage decrease was 2.99%, 1.50%, 0.81%, 0.50%, 0.48% and 0.44% for the distances 8 cm, 11 cm, 15 cm, 21 cm, 24 cm and 35 cm, respectively. The uncertainty related to the spectral uniformity of the employed irradiances can, therefore, be considered within 3%.

For each exposure, an additional three dosimeters covered with cardboard were employed as control dosimeters. The covered dosimeters were placed at the exposure site to ensure that they were at the same temperature as the exposed dosimeters. The 1064 cm^{-1} peak intensity of each dosimeter was measured before and after exposure by the FTIR spectrophotometer in order to relate the change to the subjected irradiance.

Further investigation of the reciprocity law has been undertaken employing the solar UV simulator as an irradiation source. The advantage of using the solar simulator, in addition to the high stability and uniformity of its irradiance, is the ability of attaining irradiances comparable with the solar UV irradiances which are higher than those that can be obtained from the fluorescent lamp. However, the small exposure area only allows the exposure of four dosimeters at the same time.

Due to the fact that the output of the solar simulator is collimated, increasing the distance between the simulator and the dosimeters does not change the irradiance. Alternatively, a number of neutral density filters (NDF) were employed with the solar simulator to obtain the required irradiances. The neutral filter is a polypropylene (PP) thin film that provides about 20% attenuation for the band 300–

400 nm with 5% spectral uniformity. The transmission of the filter was measured by the UV spectrophotometer and is shown in the Figure 3.24. The change in the transmission due to exposure was found to be within 3% of its initial value.

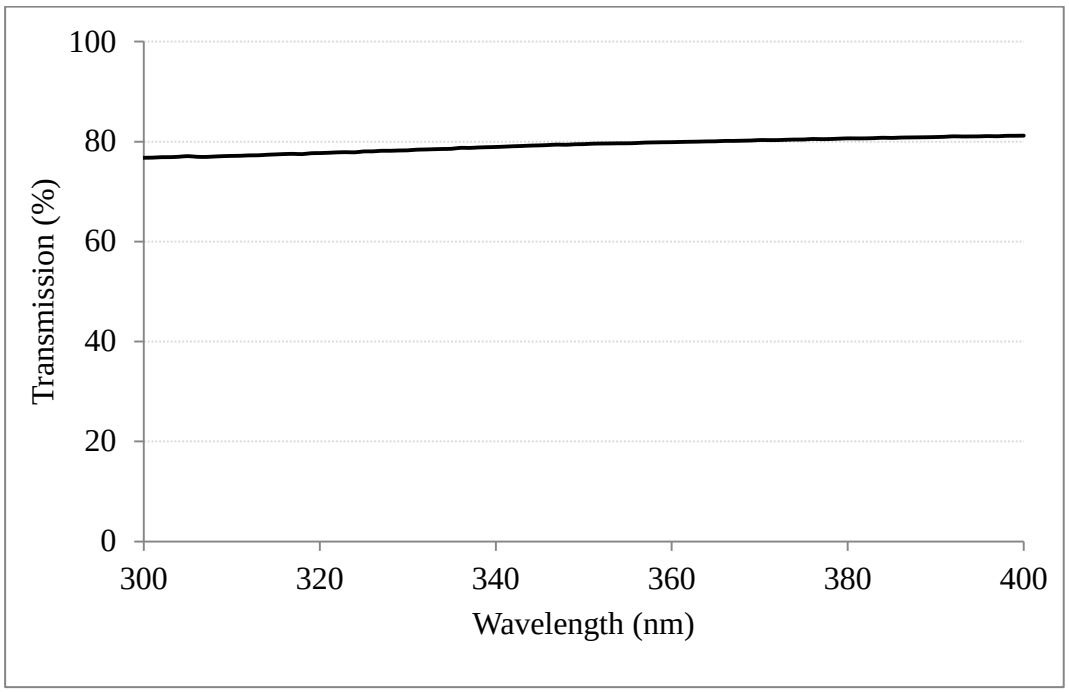

Figure 3.24: Transmission of the PP sheet employed to attenuate the irradiance of the solar UV simulator.

Six batches of four PVC dosimeters were sequentially irradiated behind an increasing number of NDF filters using the solar simulator so that each batch would be subjected to different levels of irradiance. The spectral irradiance was regularly measured during exposure using the Bentham spectroradiometer. The exposure time was calculated so that all batches received an equal UV exposure of 1 MJ/m^2. The UV irradiance as measured by the Bentham spectroradiometer at the exposure site was between 53.5 W/m^2 and 10.4 W/m^2; and the required exposure time ranged from 5.2 to 26.7 hours. Figure 3.25 shows the irradiance spectra employed in exposing the dosimeters to a total exposure of 1 MJ/m^2.

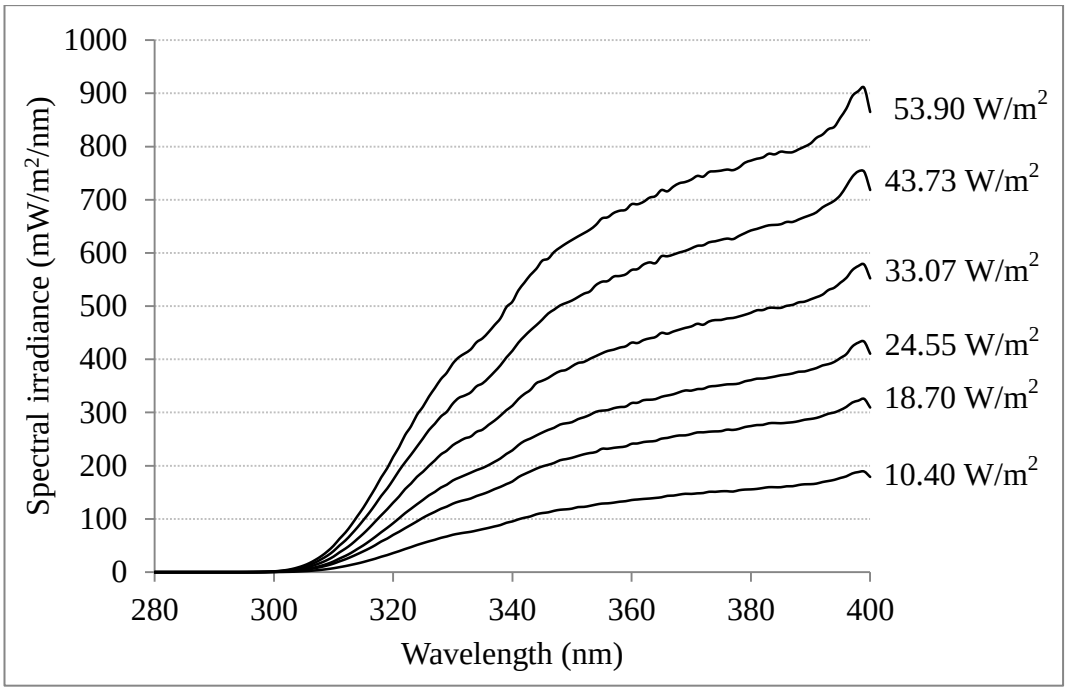

Figure 3.25: Irradiance spectra of the solar UV simulator employed in exposing the PVC dosimeters to 1 MJ/m^2 broadband UV.

The pre and post exposure 1064 cm^{-1} peak intensity of each dosimeter was measured by the FTIR spectrophotometer and the UV induced change was compared and analysed.

3.4.5 Angular dependence

The angular dependence of the dosimeter is the variation in its response with the angle of incidence of incoming radiation. The maximum irradiance of a stable beam of radiation corresponds to 0° angle of incidence (θ) and is reduced by a factor of $\cos(\theta)$ with increasing angle (Parisi et al. 2004). Therefore, for an ideal UV dosimeter, the response to the change in the angle of incidence of the beam should be a cosine function. To quantify any differences of the angular response of the PVC dosimeter from the cosine function, nine sets of PVC dosimeters were irradiated by a collimated UV beam at nine different angles of incidence. The irradiation source was a UV solar simulator (19160-1000, Newport Co., California, USA) combined with an exposure controller (model 68945, Newport Co., California, USA) to minimise variations in the lamp output. The simulator provides a stable collimated beam of 5 cm × 5 cm with measured irradiance uniformity across the entire exposure area of about 5%. Batches of four PVC dosimeters were irradiated sequentially at angles ranging from 0º to 80º at intervals of 10º. The exposure lasted for 24 hours at each angle. The average absorbance change of the dosimeters corresponding to each angle was measured and then normalised for the comparison with the cosine function. The deviation of the dosimeter angular response from the ideal cosine response was calculated for each angle.

3.4.6 Backscattering effect

Butson et al. (2000) have reported variation of up to 19% in the measurements of UV exposure obtained with a UV dosimeter based on a radiochromic film due to various background materials. This discrepancy is assumed to be associated with backscattered radiation reflected off backing material. Therefore, the effect of the background material and colour on the response of PVC dosimeters to UV radiation was examined. White, black and purple papers along with black polyethylene and glossy wood were employed as backgrounds for five batches of PVC dosimeters. The dosimeters were exposed evenly to the fluorescent UV lamp for 100 hours, providing 5 MJ/m^2 of broadband UV radiant exposure at each dosimeter site. The UV-induced absorbance change of the dosimeters was measured and normalised for the comparison.

3.4.7 Erythemal dose response curves

The erythemal dose response curves of the PVC dosimeter were determined at the University of Southern Queensland, Toowoomba, Australia (latitude 27.6 ºS) in Autumn (23rd April – 29th May 2012), Winter (23rd July – 28th August 2012), Spring (10th September – 8th October) and Summer (5th February – 22nd February 2013). For each season, five dosimeters were exposed on a horizontal unshaded plane near an erythemally weighted UV meter (model 501 Biometer, Solar Light Co. PA. USA), that records the cumulative erythemal exposure each five minutes. The Biometer was calibrated to the Bentham spectroradiometer each season. The angular response of the Biometer is assured by the manufacturer to be within 5% from ideal cosine for all incident angles. The dosimeters were removed only for the absorbance measurements (15 minutes) and were not brought indoors at night. The absorbance change of the dosimeters was measured at different intervals and related to the corresponding exposure dose to construct dose response curves. During the summer calibration, three covered dosimeters (control dosimeters) were placed at the exposure site as controls to investigate any effects of the ambient temperature on the UV-induced changes within the dosimeter.

3.4.8 Threshold dose

The threshold dose is the smallest dose that can induce a measureable response within the dosimeter. The erythemal dose response curves obtained for the PVC dosimeter indicate that the dose capacity of the dosimeter extends to more than 900 SED. However, the response to small doses does not exactly match the general trend of the data. Further investigation of the dosimeter response to small doses has been carried out using the solar simulator. A set of four PVC dosimeters was evenly irradiated to a total radiant exposure of 6 SED, during which the absorbance change was regularly measured.

3.4.9 Dark reaction

Previous research has reported changes in some chemical UV dosimeter responses after the UV exposure has been terminated (Davis et al. 1976; Diffey 1989; Lester et al. 2003; Parisi & Kimlin 2003). This behaviour is commonly known as the dark reaction. The proposed PVC dosimeter is designed to measure weeks of exposure to solar UV radiation and would therefore experience nocturnal periods during the measurement period. In addition, the readout process is not always conducted immediately after exposure and the dosimeters may have to be stored for a while. The post exposure behaviour of the PVC dosimeter was investigated by exposing 16 PVC dosimeters to a broadband radiant exposure of 3.5 MJ/m^2 supplied by the fluorescent UV lamp. After measuring the UV-induced absorbance change, the dosimeters were divided into four groups and maintained in a UV free environment at -15 ºC, 0 ºC, 15–20 ºC and 40 ºC respectively. The absorbance

change was measured at different times during the storage and plotted against time for each temperature.

In order to explore the dependency of the dark reaction, if in evidence, on the radiant exposure received by the dosimeters, the previous investigation was repeated for PVC dosimeters irradiated by 1.75 MJ/m^2 (half of the first exposure) and the abovementioned procedures were followed.

Chapter 4

Results

4.1 Optimal parameters and construction specifications of the PVC based UV dosimeter.

4.2 Dosimetric properties of the PVC dosimeter.

4.1 Optimal parameters and construction specifications of the PVC based UV dosimeter

4.1.1 Mixing ratio

Table 4.1 summarises the results obtained from the preparation of PVC thin sheets using different concentrations. The table compares the time required to dissolve the PVC powder (t), the physical properties of the produced sheet, the thicknesses (l) and initial absorbance (A_i) of sheets prepared from different concentrations of PVC/THF solution.

Table 4.1: A comparison of the preparation process and physical properties of PVC sheets prepared using different concentrations.

W/V%	t (hrs)	Film specifications	l (μm)	A_i
2	< 0.1	✓ Colourless transparent sheet. × Difficult to remove from the glass plate. × Very fragile. × Easy disruption. × Tends to wrinkle and tear. × Difficult to handle and attach to the holder.	4.2	0.016
3	~ 0.5	✓ Colourless transparent sheet. × Difficult to remove from the glass plate. × Very fragile. × Easy disruption. × Tends to wrinkle and tear. × Difficult to handle and attach to the holder.	5.8	0.056
4	~ 1.0	✓ Colourless transparent sheet. × Difficult to remove from the glass plate. × Fragile. × Easy disruption. × Tends to wrinkle and tear. × Difficult to handle and attach to the holder.	8.6	0.075
5	~ 1.5	✓ Colourless transparent sheet. × Difficult to remove from the glass plate. × Fragile. × Difficult to handle and attach to the holder.	6.8	0.044
6	1.5-2.0	✓ Colourless transparent sheet. ✓ Absence of surface blemishes and defects. × Fragile. × Difficult to handle and attach to the holder.	10.0	0.186
7	~ 2.0	✓ Colourless transparent sheet. ✓ Absence of surface blemishes and defects. ✓ Good quality.	12.2	0.182
8	~ 3.0	✓ Colourless transparent sheet. ✓ Absence of surface blemishes and defects. ✓ Good quality.	10.0	0.115

9	~ 4.0	✓ Colourless transparent sheet. ✓ Absence of surface blemishes and defects. ✓ Good quality.	14.2	0.211
10	~ 5.0	✓ Colourless transparent sheet. ✓ Absence of surface blemishes and defects. ✓ Good quality.	15.4	0.160
11	~ 6.0	✓ Colourless transparent sheet. ✓ Absence of surface blemishes and defects. ✓ Good quality.	18.0	0.276
12	~ 7.0	✓ Colourless transparent sheet. × Appearance of surface unevenness. × Start to be brittle.	18.8	0.331
13	~ 8.0	× High viscosity solution. ✓ Colourless transparent sheet. × Appearance of surface unevenness. × Brittle.	15.6	0.235
14	~ 10.0	× High viscosity solution. ✓ Colourless transparent sheet. × Appearance of surface unevenness. × Brittle.	15.6	0.275
15	~ 12.0	× High viscosity solution. ✓ Colourless transparent sheet. × Appearance of surface unevenness. × Brittle.	18.4	0.304
16	∞	× Very high viscosity solution.	-	-

It can be noticed from the table that PVC sheets prepared using solutions of concentrations less than 7% tended to wrinkle and tear; while solutions of concentrations greater than 12% were difficult to spread on the glass plate and resulted in brittle films that showed a pronounced surface unevenness. Smooth films with an acceptable quality could be cast using concentrations between 7% and 12% with a dissolution time up to 6 hours at 25 ± 2 °C. In addition, for concentrations less than 11%, the thickness of the film increased in proportion to the concentration used in preparing the sheet (Figure 4.1). Concentrations higher than 11% give almost the same thickness of about 17 μm. In other words, for a fixed height of the casting blade, the greater the concentration, the thicker the resulting film.

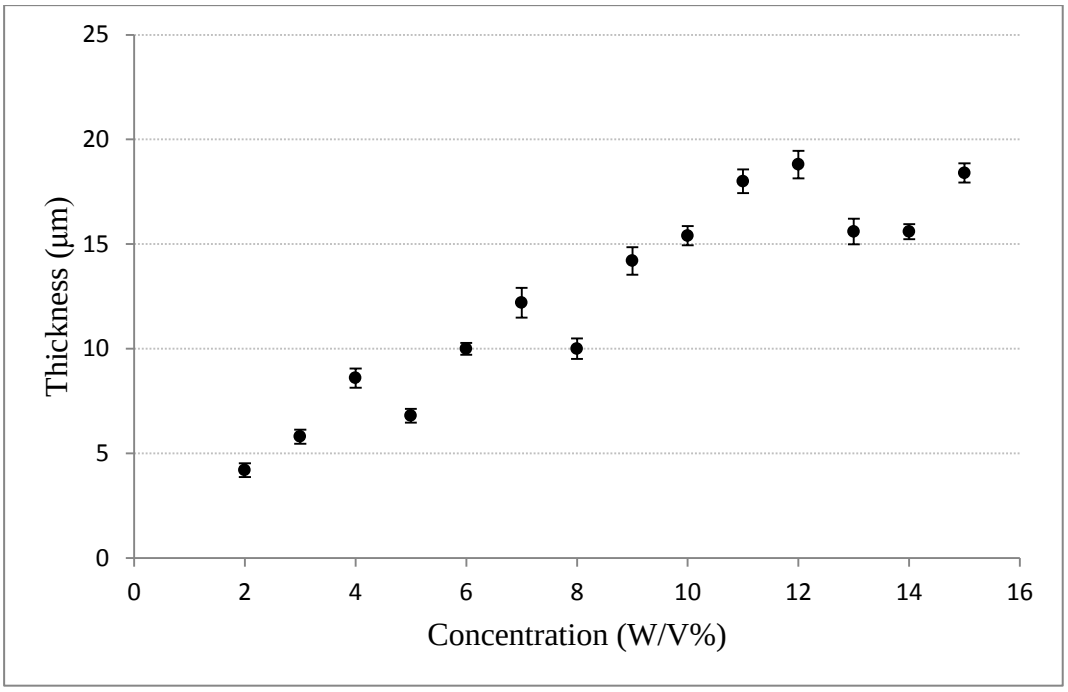

Figure 4.1: The measured thickness of PVC sheets prepared with a fixed height of the casting blade (100 µm) as a function of the employed concentration of PVC/THF solution. The error bars represent the standard error of the measured thickness.

Comparison of the PVC powder dissolving time and the physical properties of the films showed that a 10% concentration is the most suitable concentration for preparing PVC sheets for use in UV dosimetry.

4.1.2 Film thickness

Table 4.2 summarise the results obtained for different thickness PVC sheets cast from 10% PVC/THF solution. Sheets with different thicknesses were obtained by changing the distance (height) between the casting blade and the glass plate. The table compares the physical properties of the produced sheets, their thicknesses (l) and initial absorbance (A_i).

Table 4.2: A comparison of the physical properties of PVC sheets prepared from 10% PVC/THF solution using different heights of the casting blade.

Height of the blade (µm)	**Film properties**	***l* (µm)**	**A_i**
60	✓ Colourless transparent sheet. × Difficult to remove from the glass plate. × Very fragile. × Easy disruption. × Tends to wrinkle and tear. × Difficult to handle and attach to the holder.	4.0	0.020
90	✓ Colourless transparent sheet. × Fragile. × Easy disruption. × Tends to wrinkle and tear. × Difficult to handle and attach to the holder.	5.7	0.021
120	✓ Colourless transparent sheet. ✓ Absence of surface blemishes and defects. × Fragile. × Difficult to handle and attach to the holder.	6.8	0.089
150	✓ Colourless transparent sheet. ✓ Absence of surface blemishes and defects.	8.4	0.116
180	✓ Colourless transparent sheet. ✓ Absence of surface blemishes and defects. ✓ Good quality.	8.8	0.159
210	✓ Colourless transparent sheet. ✓ Absence of surface blemishes and defects. ✓ Good quality.	14.0	0.176
240	✓ Colourless transparent sheet. ✓ Absence of surface blemishes and defects. ✓ Good quality.	16.0	0.214
270	✓ Colourless transparent sheet. ✓ Absence of surface blemishes and defects. ✓ Good quality.	20.0	0.288
300	✓ Colourless transparent sheet. × Appearance of surface unevenness.	22.4	0.361
330	✓ Colourless transparent sheet. × Appearance of surface unevenness. × Signs of brittleness.	23.4	0.377
360	✓ Colourless transparent sheet.	25.8	0.474

	× Appearance of surface unevenness. × Signs of brittleness.		
390	✓ Colourless transparent sheet. × Appearance of surface unevenness. × Brittle.	37.8	0.629
420	✓ Colourless transparent sheet. × Appearance of tears and surface unevenness. × Brittle.	45.4	0.677
450	✓ Colourless transparent sheet. × Appearance of tears and surface unevenness. × Very thick. × Brittle.	55.0	0.857
480	✓ Colourless transparent sheet. × Appearance of tears and surface unevenness. × Very thick. × Brittle.	58	0.881

PVC sheets prepared from a 10% PVC/THF solution were of thicknesses between 4 μm and 58 μm. The relationship between the initial absorbance (A_i) at 1064 cm^{-1} and thickness (l) of dosimeters (Figure 4.2) was:

$$A_i = 0.0155 \times l \qquad (4.1)$$

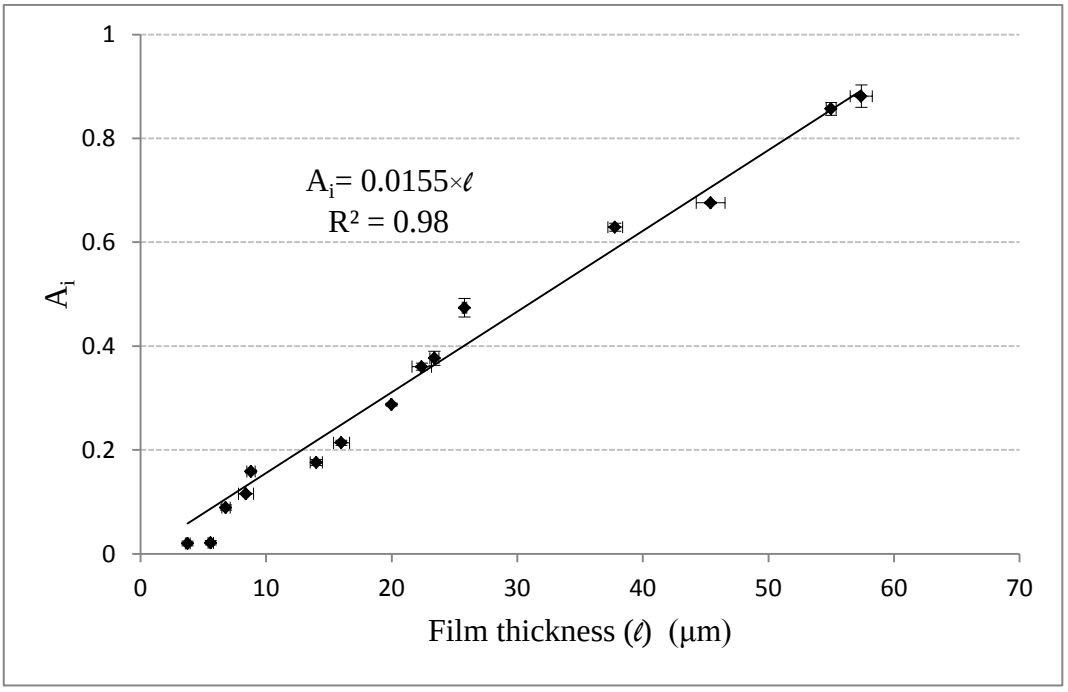

Figure 4.2: The absorbance of PVC thin films at 1064 cm^{-1} as a function of film thickness. The error bars are the standard error in the measured thickness and in the IR absorbance of five PVC dosimeters fabricated from each sheet.

This is in agreement with the Beer-Lambert law. Thicknesses between 8.4 µm and 20 µm were of a better quality in terms of the absence of surface blemishes and defects and hence they were employed to investigate the dose response of PVC as a function of film thickness.

Figure 4.3 shows the dose response curves of PVC dosimeters fabricated from films of thicknesses 8.4 µm, 14 µm, 16 µm and 20 µm.

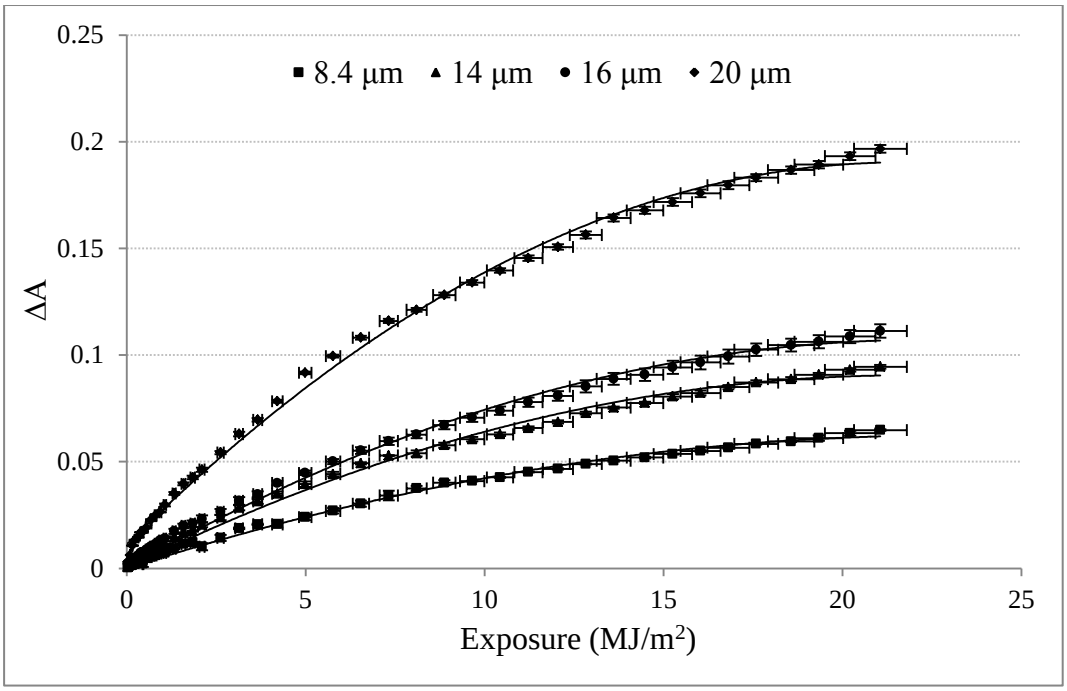

Figure 4.3: Dose-response curves of PVC thin films of different thicknesses. The y error bars represent the standard error in the measured absorbance of the three irradiated dosimeters of each thickness while the x error bars represent a variation of 3% in the lamp output.

It can be noticed that the curves for the thicker films, which have higher initial absorbance, have a higher change to the same exposure as well as a higher gradient. However, the curve linearity decreases with increasing thickness. The 16 µm thickness seems to be the best compromise between physical quality, sensitivity to UV and linearity of dose response curve. Consequently, the 16 µm thick PVC film cast using 10% (W/V%) concentration and obtained by altering the blade height to 240 µm was determined as the most suitable thickness for the PVC dosimeters. The short error bars reflect the high reproducibility of the dosimeters.

4.1.3 Drying time determination

Figure 4.4 shows the absorbance of the 16 µm PVC based UV dosimeters dried at 50 °C as a function of the drying time. There was a gradual absorbance reduction with a decreasing rate of change.

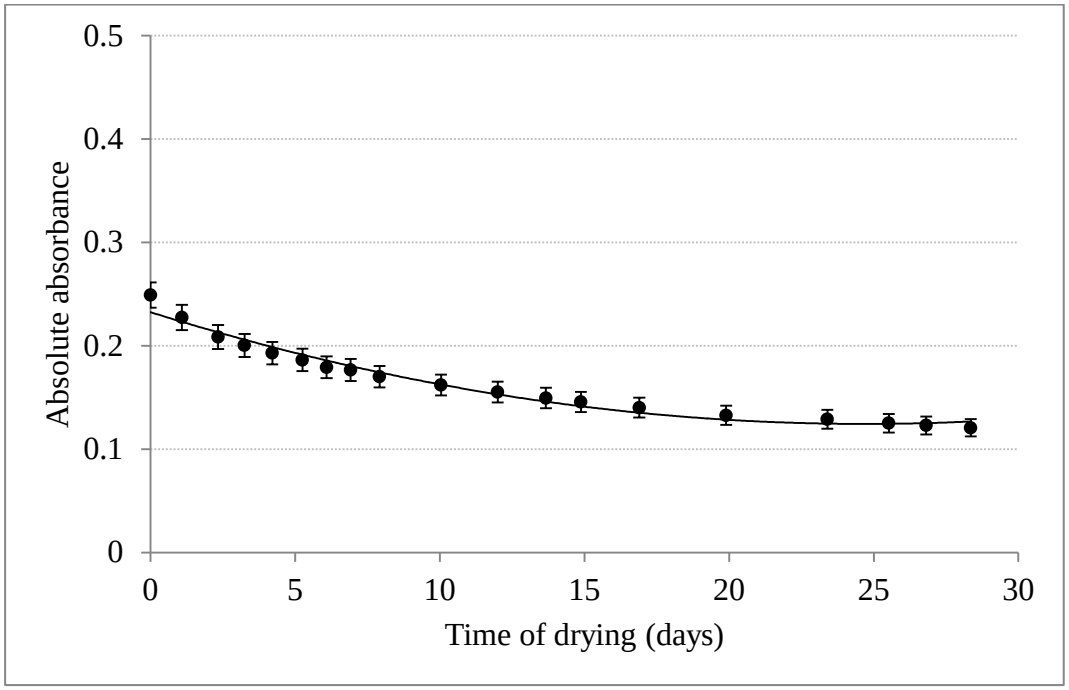

Figure 4.4: Change of absolute absorbance at 1064 cm^{-1} of PVC dosimeters as a function of drying time at 50 ° C. The error bars represent the standard error of the measured absorbance.

Although the absorbance curve has not eventually levelled as expected by Maláč et al. (1969), the rate of absorbance decrease reached its minimum after about 3 weeks of drying. The absorbance dropped to 50% of its initial value after four weeks of drying. The difference between the absorbance change of PVC dosimeters exposed to 200 kJ/m^2 at 25 ºC and 45 ºC decreased with the increase of drying time (Figure 4.5).

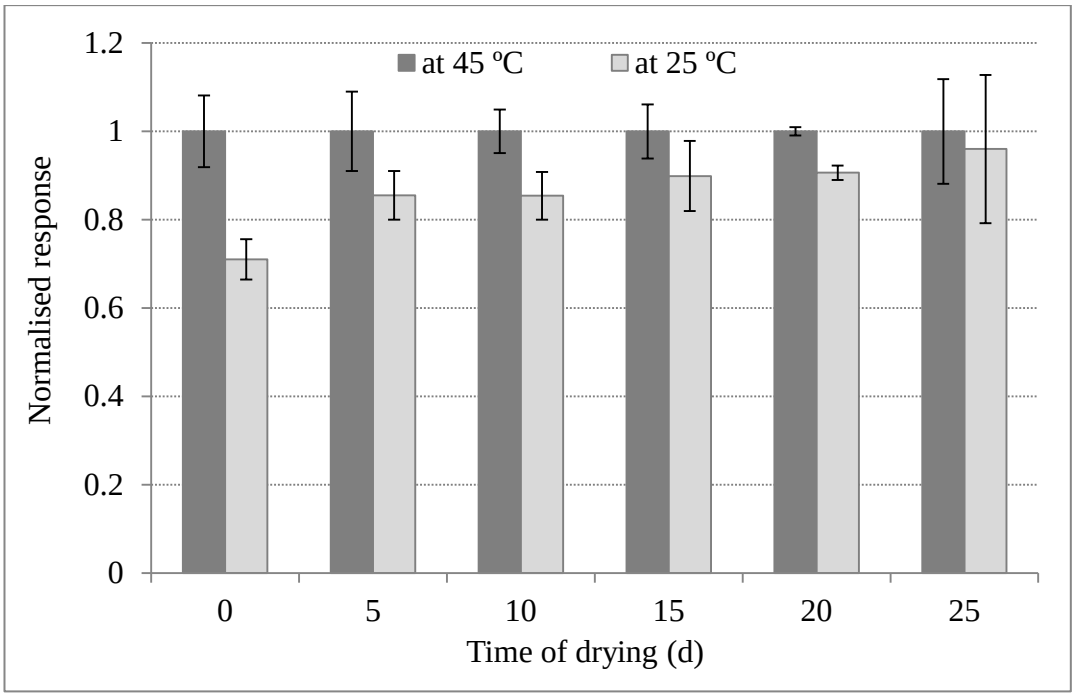

Figure 4.5: The normalised absorbance change of PVC dosimeters exposed to 200 kJ/m^2 at 25 °C and 45 °C after being dried for different periods at 50 ºC. The error bars represent the standard error of the normalised absorbance change as calculated by the error propagation formulae.

The absorbance change of the undried dosimeters exposed at 45 ºC was about 30% higher than those exposed at 25 ºC. This difference dropped to just about 5% for those dosimeters dried for 25 days, indicating that drying the dosimeters for about 25 days at 50 ºC will minimise the temperature dependence of the dosimeters.

4.1.4 Conclusion on the optimal parameters of the proposed dosimeter

Based on the results obtained in Section 4.1.1–4.1.3, the optimal parameters for a PVC based UV dosimeter are:

- The most suitable concentration of PVC/THF solution for preparing the PVC sheets is10% (W/V%).
- Dissolution time of five hours with vigorous stirring at 25 °C is adequate to dissolve all PVC powder in the THF solvent.
- The optimal film thickness for the dosimeter in terms of physical quality and UV sensitivity is 16 µm. This thickness can be obtained by adjusting the blade height to 240 µm.
- At least two hours of solvent evaporating time at 25 °C is required to dry the PVC sheets, followed by drying the sheets for four weeks in air at 50 °C.

4.2 Dosimetric properties of the PVC dosimeter

4.2.1 Reproducibility

The average deviation from the mean for the ten dosimeters exposed to the same UV exposure was 3–5% for UV exposures up to 2.5 MJ/m^2 and dropped to ≤ 2% for higher exposures (Figure 4.6). The average reproducibility is 2.5%.

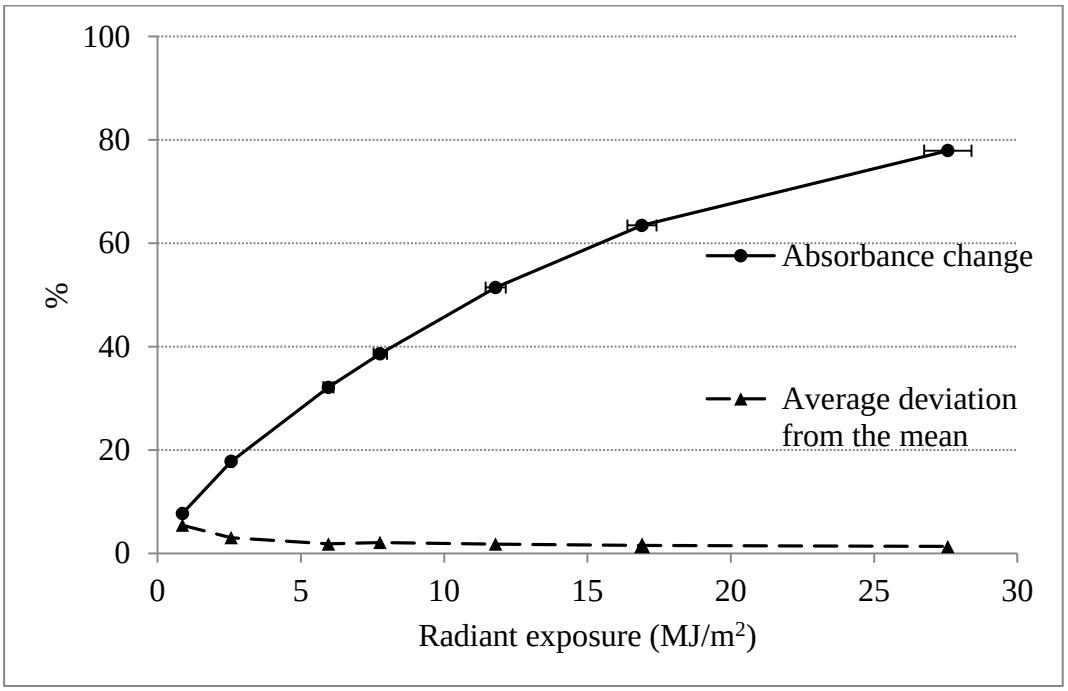

Figure 4.6: Dose response curve of ten PVC dosimeters subjected to a total broadband UV radiant exposure of 27 MJ/m^2 of radiation presented along with the average deviation from the mean of the dosimeters' absorbance change as a function of the radiant exposure. The y error bars represent the standard error of the measured absorbance change, they are shorter than the dimensions of the associated symbol and do not appear clearly on the graph, while the x bars represent 3% variation in the output of the lamp.

4.2.2 Determination of the spectral response

4.2.2.1 Cut-off filter technique

After 135 hours of exposure, the cumulative UV dose received by the dosimeters ranged between 4.9 MJ/m^2 for the unfiltered pair and 12.6 KJ/m^2 for the pair exposed behind filter number 9. All the dosimeters underwent a measureable change at the 1064 cm^{-1} peak. The largest change was for the unfiltered pair (16%), while those pairs exposed behind filters 5−9 experienced approximately the same change as the pairs covered with the cardboard and the UV cut-off filter (3.2%), indicating that this change may be due only to thermal degradation and that wavelengths longer than about 345 nm do not contribute to the photo-degradation process. Each pair (n) of dosimeters was subjected to an integrated irradiance of ΔE more than the next pair $(n+1)$, where:

$$\Delta E = \sum \left[E_n(\lambda) - E_{n+1}(\lambda) \right] \times \Delta\lambda$$

$$= \sum E(\lambda) \left[T_n(\lambda) - T_{n+1}(\lambda) \right] \times \Delta\lambda \qquad (4.2)$$

where $T_n(\lambda)$ is the spectral transmission of the nth filter. The difference in irradiance ΔE leads to a difference (δA) between the absorbance change of the two pairs, where:

$$\delta A = \left[(\Delta A)_n - (\Delta A)_{n+1} \right] \qquad (4.3)$$

The overlap between spectral bands encompasses the correlation between the spectral irradiance and the difference in the absorbance change. As a result, just three bands that had minimum overlap and covered the active part of the UV region were chosen for comparison (Figure 4.7).

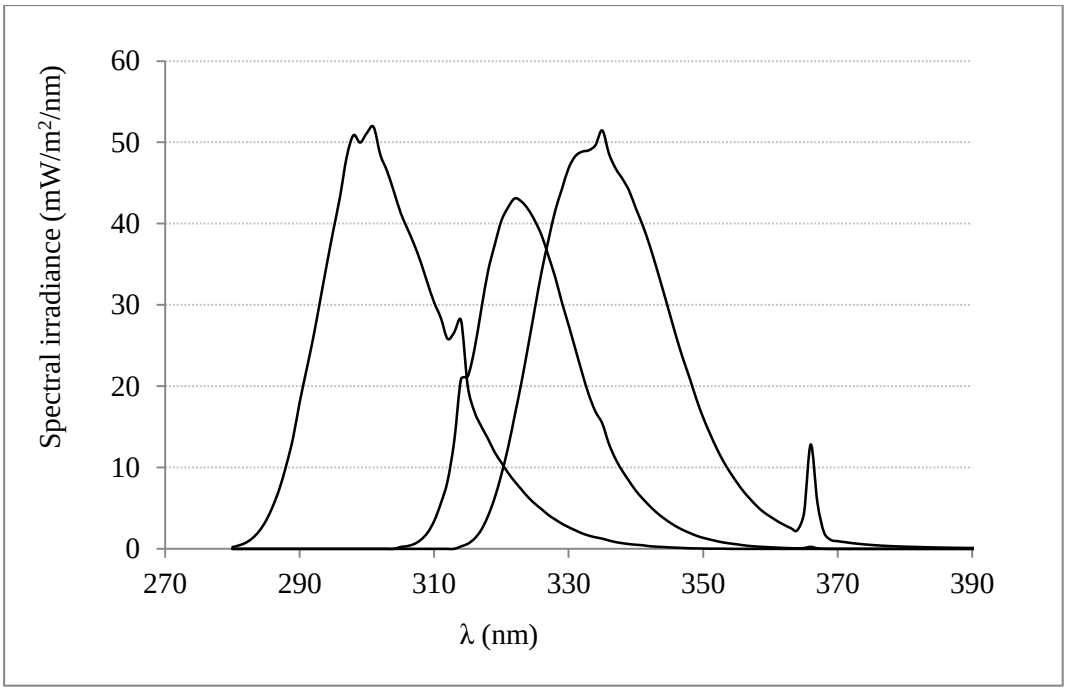

Figure 4.7: The irradiance difference received by the consecutive pairs irradiated behind the filters 1-2, 2-3, and 4-5.

Assuming the validity of the reciprocity law and the linearity between the exposure dose and absorbance change, the difference in the absorbance change per exposure dose unit $(\delta A)_u$ was calculated for the consecutive pairs by:

$$(\delta A)_u = \frac{\delta A}{\Delta E \times t} \qquad (4.4)$$

where t is the total exposure time.

$(\delta A)_u$ was then normalised to obtain the relative sensitivity of each of the spectral bands. Figure 4.8 presents the three bands, using the FWHM, and their relative ability in inducing change in the PVC dosimeter. The maximum sensitivity was for the shorter wavelengths investigated to approximately 312 nm.

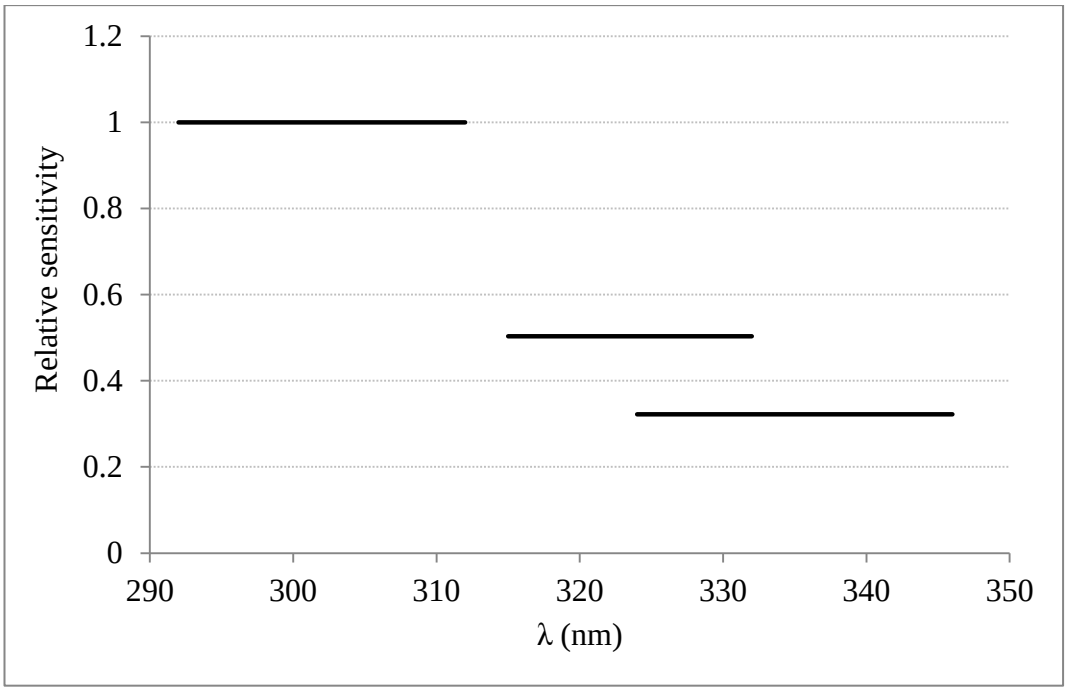

Figure 4.8: Spectral response of the PVC dosimeter as obtained using the cut-off filter technique.

4.2.2.2 Narrow band-pass filter technique

After 31 hours of exposure, the four dosimeters exposed behind the filters with wavelengths of maximum transmittance 300 nm, 324 nm, 343 nm and 361 nm received about 2.1 KJ/m^2, 138.2 KJ/m^2, 2.1 MJ/m^2 and 1.2 MJ/m^2, respectively. The absorbance change per exposure dose unit for each dosimeter was calculated using Equation 4.4, and then normalised and presented in Figure 4.9 which shows that the maximum effectiveness in inducing change within the PVC dosimeter was again at the shorter wavelengths.

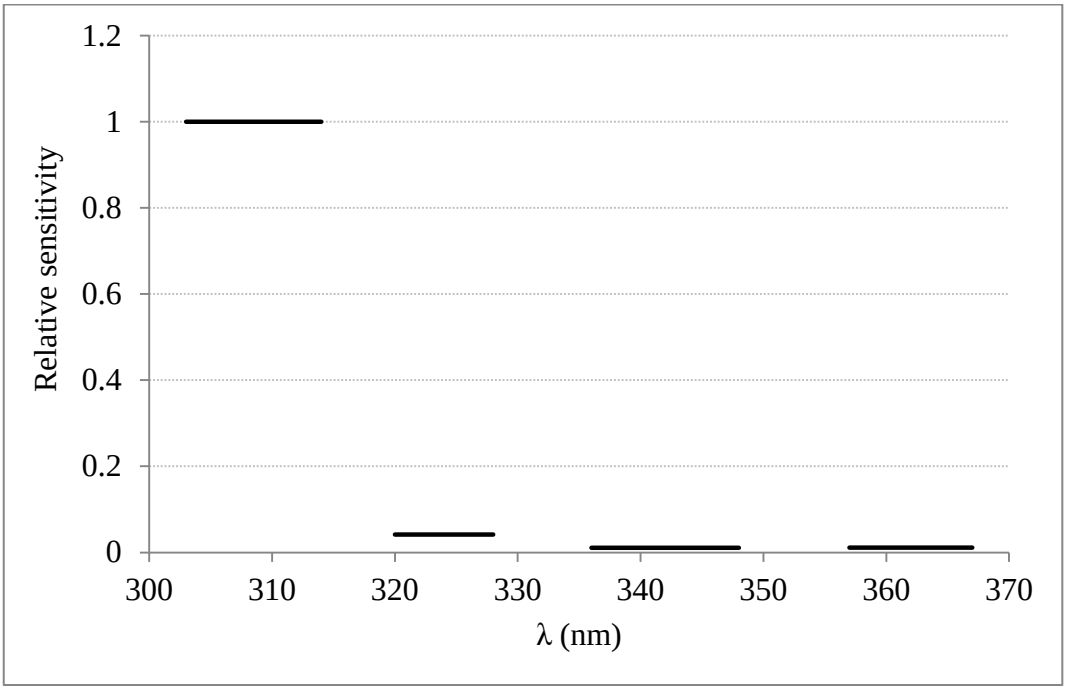

Figure 4.9: Spectral response of the PVC dosimeter as obtained using the narrow band-pass filter technique.

4.2.2.3 Monochromatic radiation

The PVC spectral response as measured using the irradiation monochromator by exposing the dosimeters to 0.5 MJ/m^2 at 25 ± 2 ºC, 0.1 MJ/m^2 at 25 ± 2 ºC and 0.1 MJ/m^2 at 40 ± 2 ºC is presented in Figure 4.10. The maximum response of the dosimeter occurred at 290 nm and decreased with increasing wavelength up to 340 nm independently of temperature and exposure dose. The averaged spectral response measured by the irradiation monochromator is shown in Figure 4.11

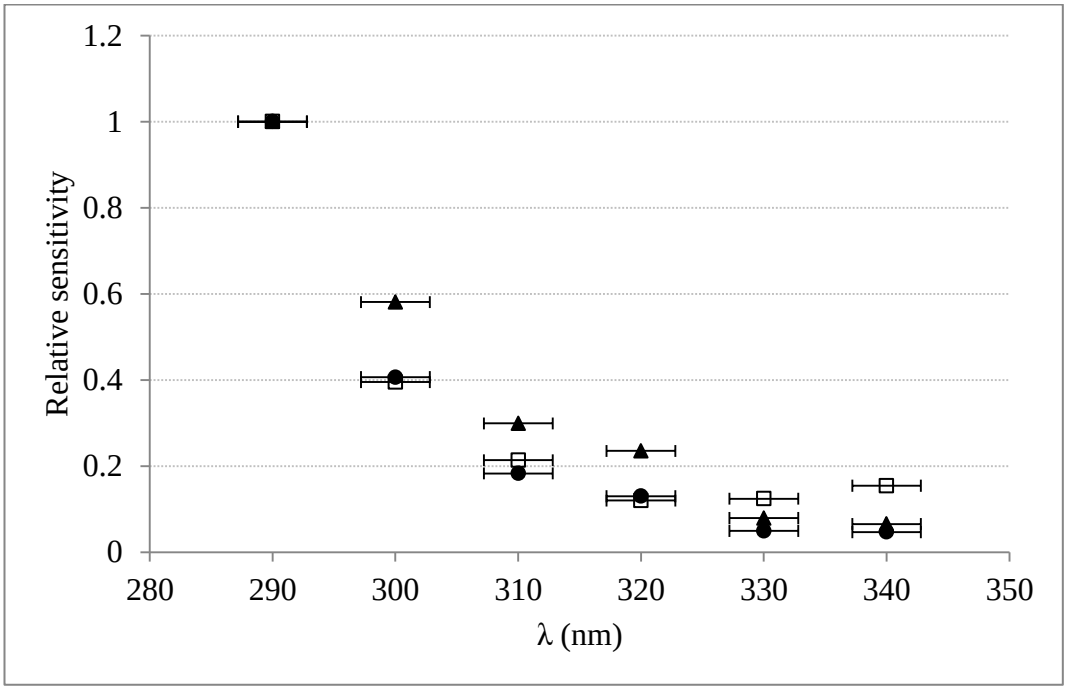

Figure 4.10: Spectral response of the PVC dosimeter obtained using an irradiation monochromator where the dosimeters were exposed to 0.5 MJ/m^2 at 25±2 ºC (circle), 0.1 MJ/m^2 at 25±2 ºC (square) and 0.1 MJ/m^2 at 40±2 ºC (triangle). The error bars indicate the 5.6 nm FWHM of each exposure waveband.

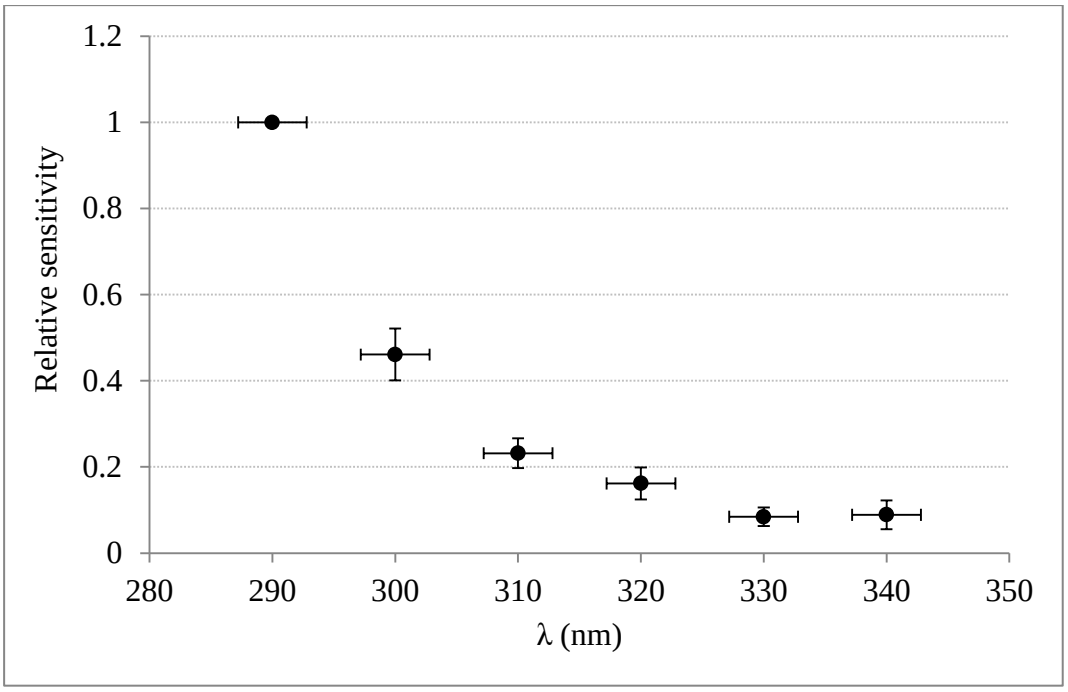

Figure 4.11: Averaged spectral response of the PVC dosimeter as obtained using the irradiation monochromator with different radiant exposures at different temperatures.

4.2.3 Temperature independency

The normalised response of PVC dosimeters subjected to a total broadband UV exposure of 0.2, 0.5 and 1 MJ/m^2 as a function of the exposure temperature is shown in Figure 4.12, 4.13 and 4.14.

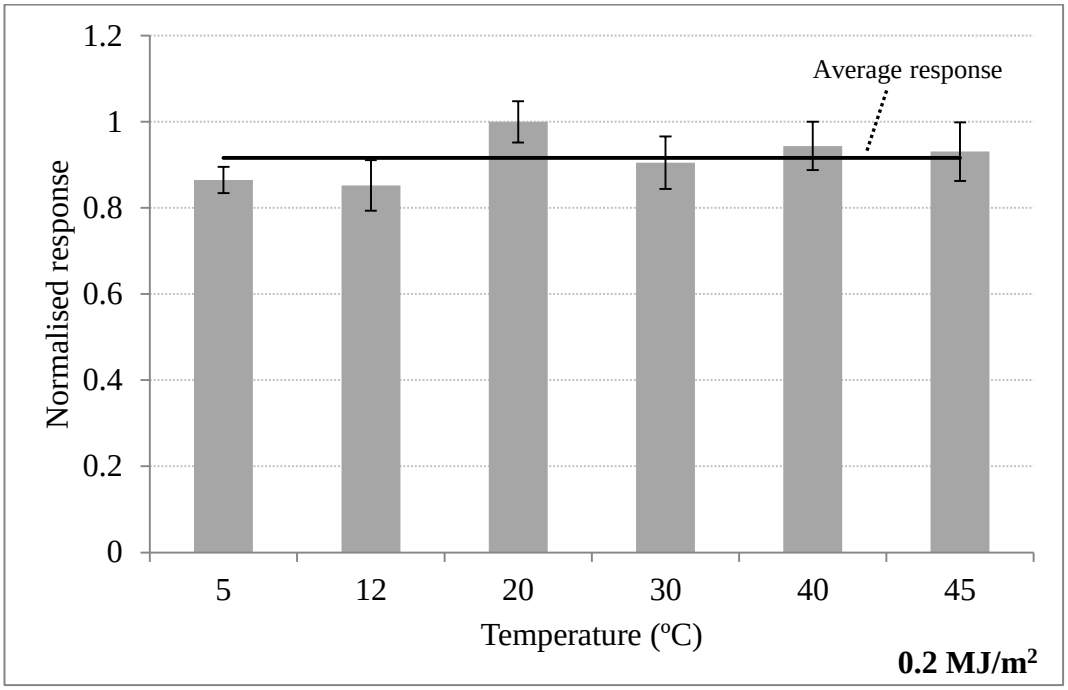

Figure 4.12: The response of PVC dosimeters subjected to 0.2 MJ/m^2 of broad band UV as a function of the exposure temperature.

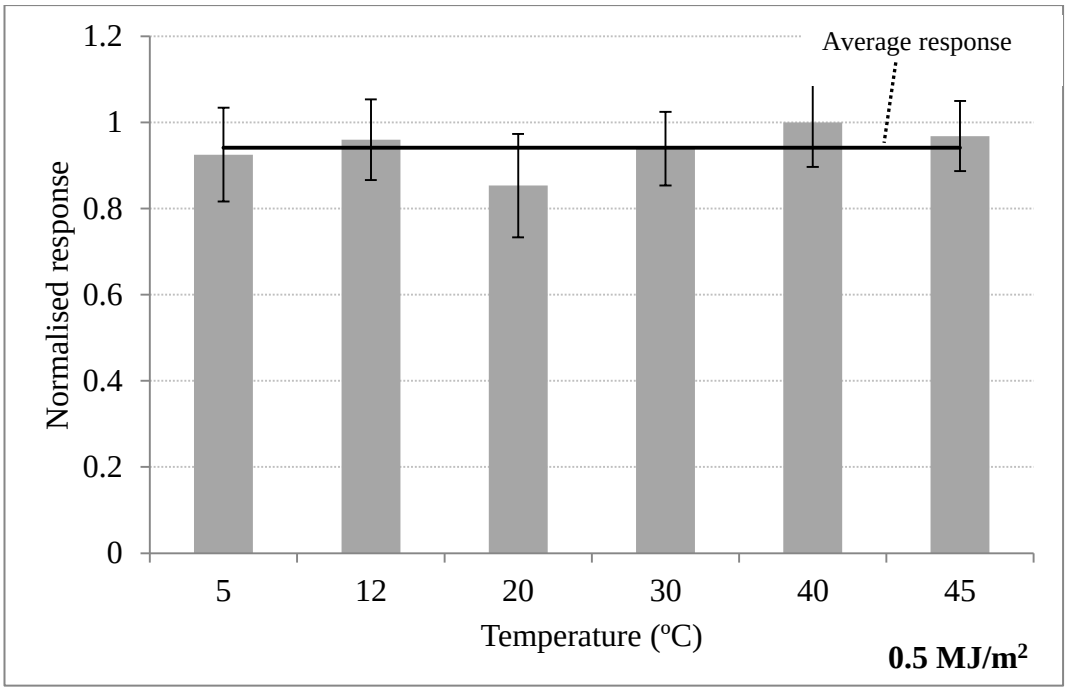

Figure 4.13: The response of PVC dosimeters subjected to 0.5 MJ/m^2 of broad band UV as a function of the exposure temperature.

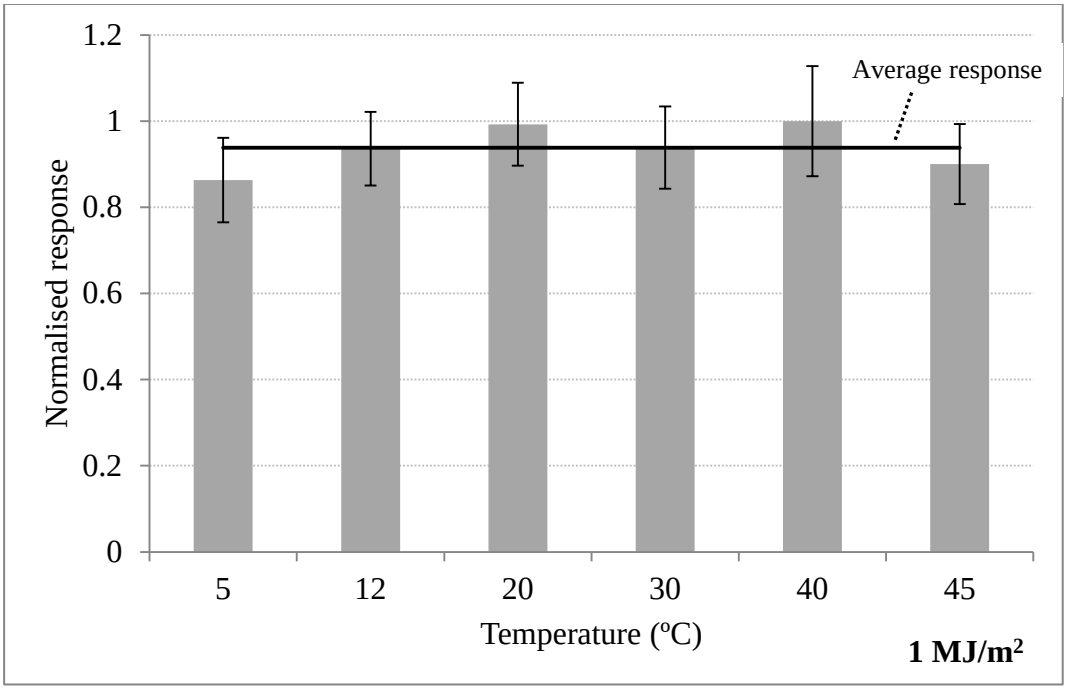

Figure 4.14: The response of PVC dosimeters subjected to 1 MJ/m^2 of broad band UV as a function of the exposure temperature.

The dosimeters showed no significant difference in their behaviour and the response seems to be independent of temperature over the range 5–45 ºC. The average deviation from the mean response was 4.6%, 3.7%, and 4.1% for the exposures 0.2, 0.5, and 1 MJ/m^2 respectively, indicating that the response is independent of temperature regardless of the received exposure.

4.2.4 Dose-rate independency

The normalised response of PVC dosimeters exposed to 2 MJ/m^2 of broadband UV radiation accumulated from different irradiances obtained from the fluorescent lamp is given in Figure 4.15.

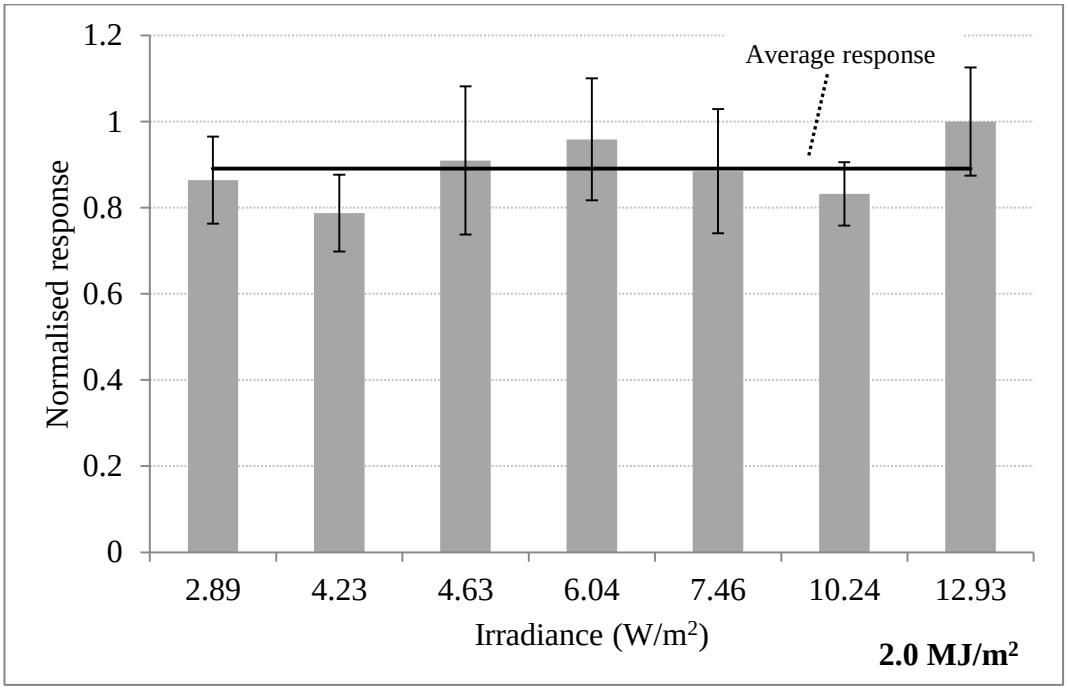

Figure 4.15: The response of PVC dosimeters exposed to 2 MJ/m^2 of broadband UV exposure as a function of the irradiance supplied by the fluorescent lamp. The error bars are the standard error of the normalised absorbance change as calculated by the error propagation formulae.

The average deviation from the mean response was about 6%. This deviation can be considered within the experimental error, taking into account an uncertainty of 3.5% in the stability of the lamp output, 4% uncertainty in the irradiance uniformity over the exposure area and 3% uncertainty in the spectral uniformity.

The control dosimeters showed no response, indicating that the response of the exposed dosimeters was due only to the subjected UV radiation.

For the dosimeters irradiated by 1 MJ/m^2 using the solar UV simulator, the response of the dosimeters was within 3% of the average response (Figure 4.16).

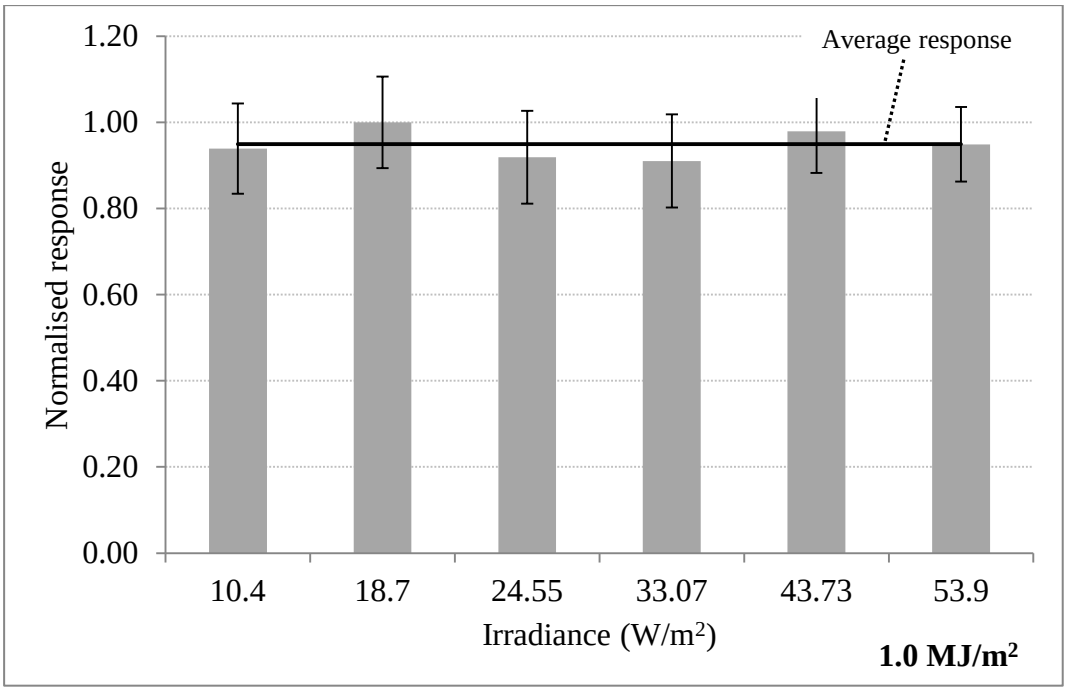

Figure 4.16: The response of PVC dosimeters exposed to 1 MJ/m^2 of broadband UV exposure as a function of the irradiance supplied by the solar UV simulator. The error bars are the standard error of the normalised absorbance change as calculated by the error propagation formulae.

4.2.5 Angular dependence

The response of the PVC dosimeter as a function of the angle of incidence of the UV radiation is shown in Figure 4.17 together with the cosine function and the corresponding cosine error. The average cosine error in the range 0-80º was 18%. The measured cosine error was less than 6.5% for angles up to 40º, increasing to 16% at 50º and reaching its maximum of about 40% at higher angles.

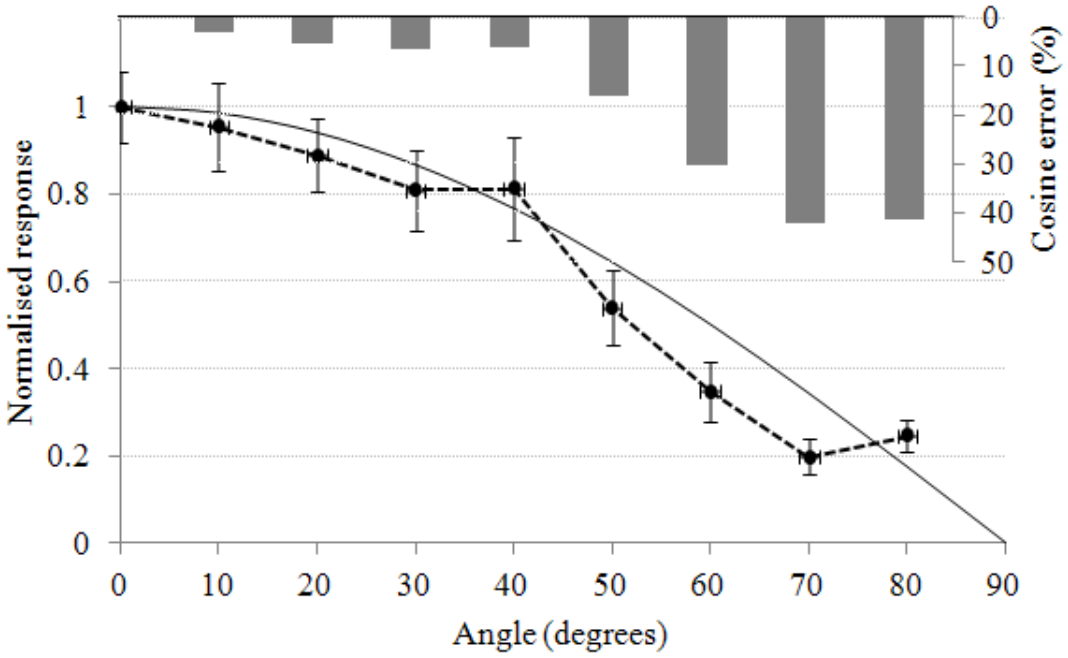

Figure 4.17: The response of PVC dosimeters as a function of the angle of the incident beam (dashed line) compared with the ideal cosine function (thin line). The bar chart shows the deviation of the PVC angular response from the cosine function. The y error bars represent the standard error of the normalised response as calculated by error propagation formulae, while the x error bars represent an estimated angular alignment error of ± 1º.

4.2.6 Backscattering effect

The response of PVC dosimeters evenly irradiated using different backgrounds is shown in Figure 4.18.

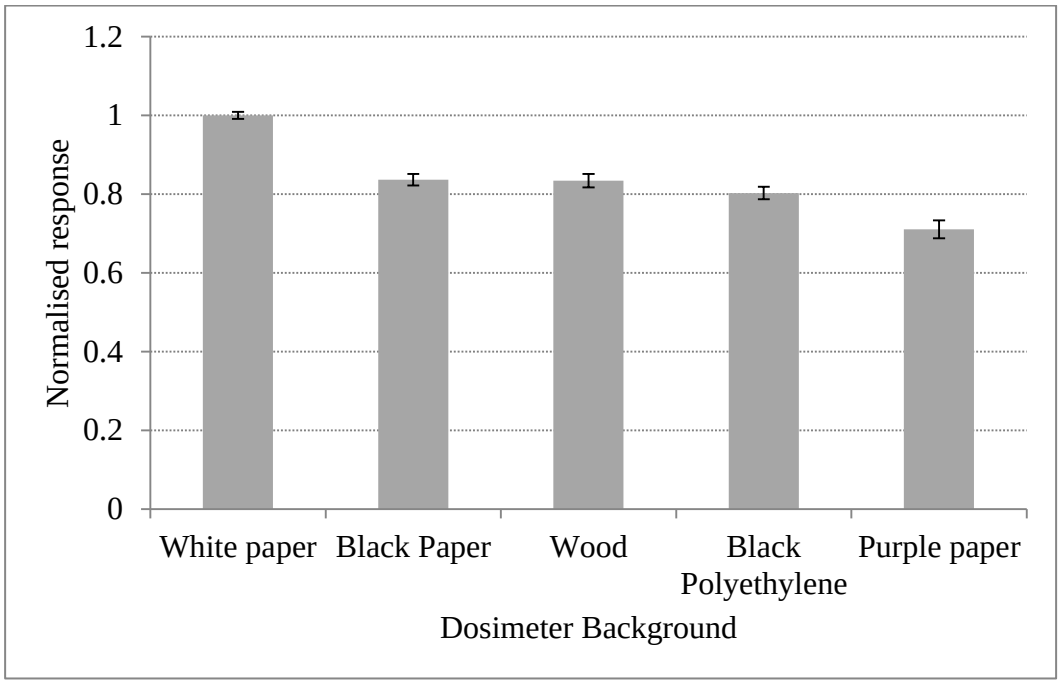

Figure 4.18: The response of PVC dosimeters irradiated evenly over different backgrounds.

In general, darker backgrounds had less effect on the absorbance. This is in agreement with previous research (Lester & Parisi 2002; Riva et al. 2009) that reported less UV reflectivity of dark colours than light ones. The maximum response was for the white paper background. Responses for white and purple backgrounds differed by about 30%. In addition, a slight effect of the material type is noticed by the 5% discrepancy in the response of dosimeters irradiated with black polyethylene and black paper. The results indicate that similar materials and colours should be employed for both calibrating dosimeters and measuring dosimeters to avoid any backscattering effect.

4.2.7 Erythemal dose response curves

Figure 4.19 shows the erythemal dose response curves of the PVC dosimeter obtained for different seasons. The dose-response relationship was represented by a best fit to a second-degree polynomial function. The best fit of the data for all curves is almost similar and very close to linear. The average deviation of the experimental points from the regression was about 15%. The greatest deviation was observed for fitted function values less than 120 SED with an average of about 32%. For higher exposures, the average deviation of the experimentally determined exposures was about 12% from those calculated by the fitted function.

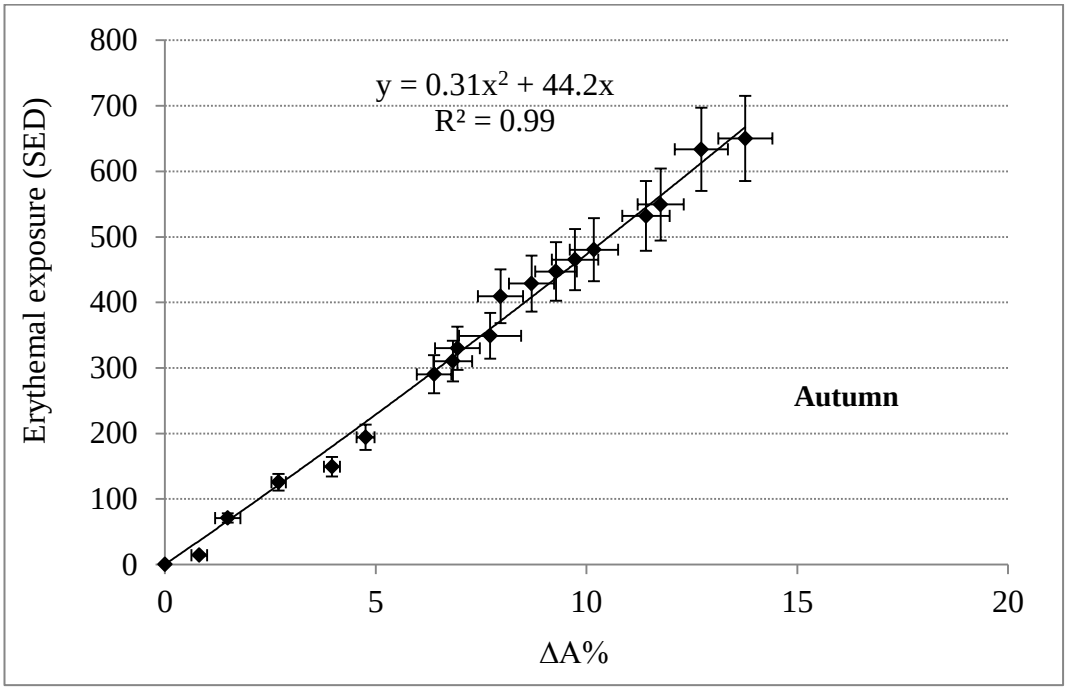

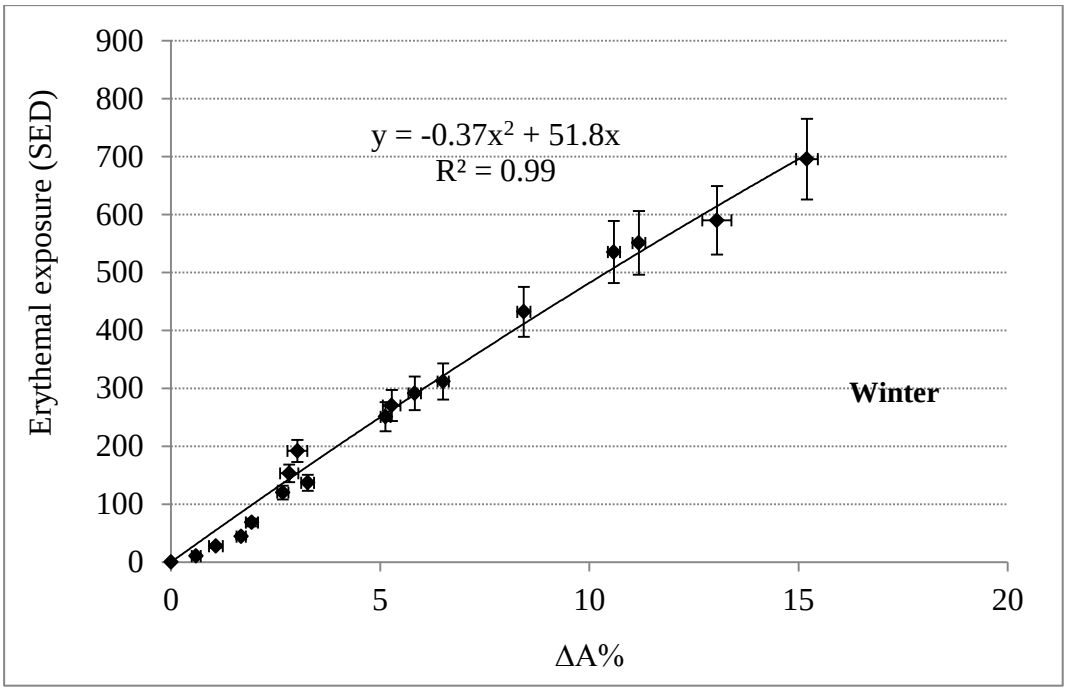
Erythemal exposure (SED)
900
800
700
600
500
400
300
200
100
0
y = -0.37x² + 51.8x
R² = 0.99
Winter
0
5
10
15
20
ΔA%

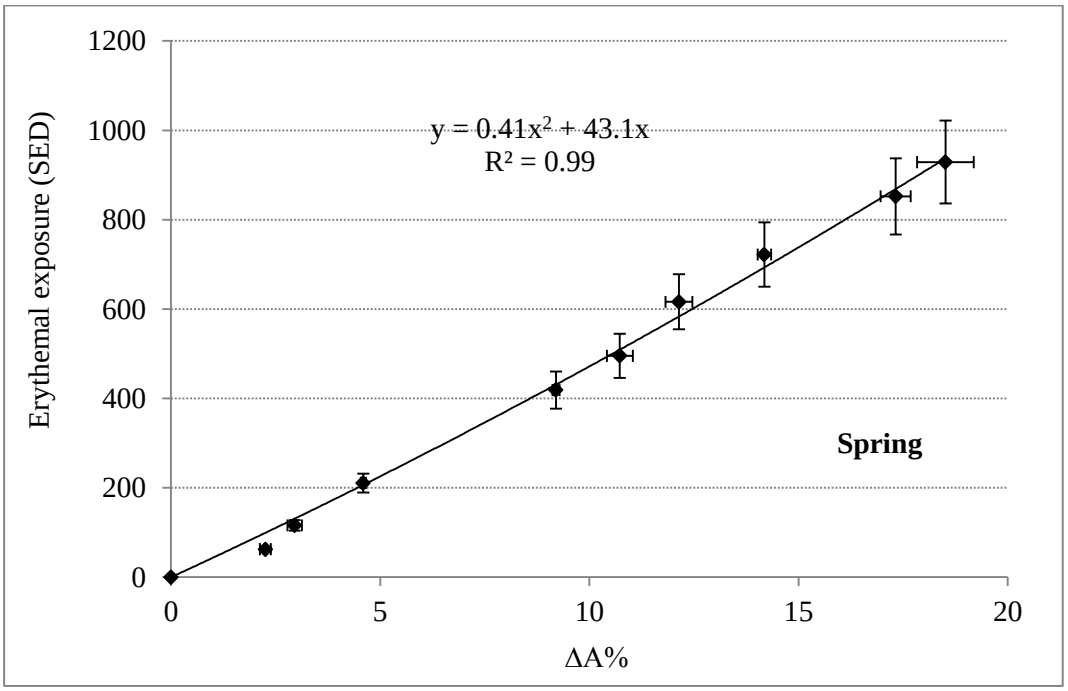
Erythemal exposure (SED)
1200
1000
800
600
400
200
0
y = 0.41x² + 43.1x
R² = 0.99
Spring
0
5
10
15
20
ΔA%

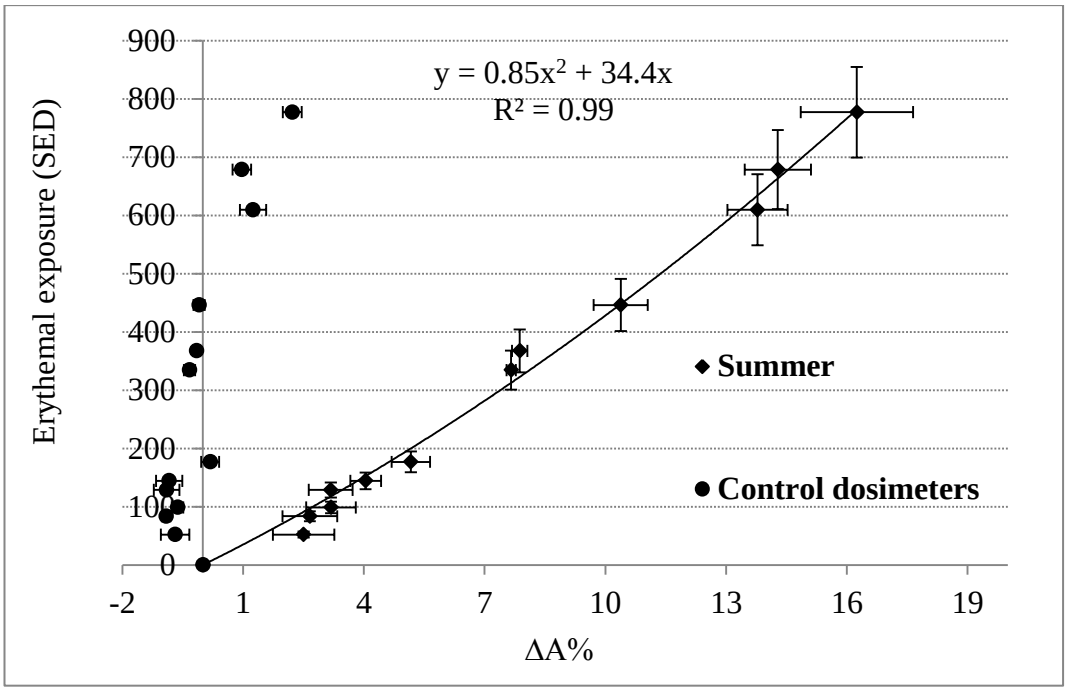

Figure 4.19: Solar erythemal UV dose response curves of the PVC dosimeter. The summer curve includes the response of the control dosimeters. The x error bars represent the standard error of the measured absorbance while the y error bars represent 10% accuracy of the Biometer .

Control dosimeters used during summer calibration (when the temperature is the highest) showed an absorbance change of ±1%, except for one point where the change was 2%. This change is within the experimental error of the absorbance measurements, which means there was no evidence of significant effect of ambient temperature on the measured response. The maximum measured cumulative exposure was about 900 SED, obtained during the spring calibration (28 days of exposure), with no signs of saturation or substantial deviation from the general trend of the curve indicating that the dosimeter is able to measure even higher doses.

The combined data of all seasons is shown in Figure 4.20. The curve could be used as a standard dose response curve for the different seasons.

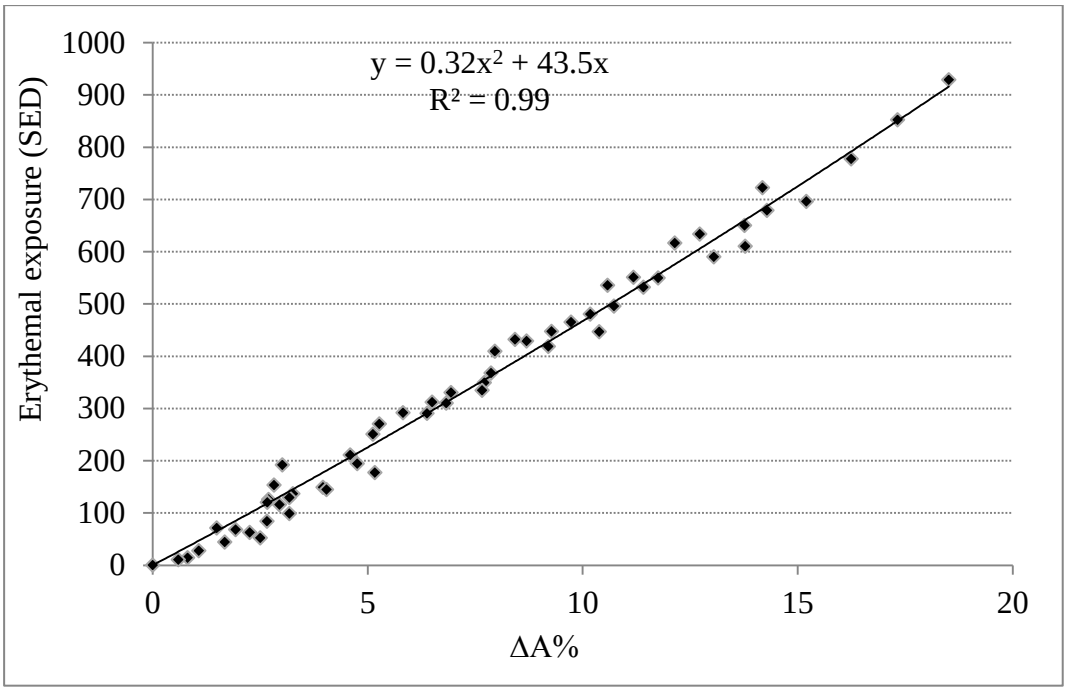

Figure 4.20: Combined dose response curve of the PVC dosimeter for the four seasons.

4.2.8 Threshold dose

Figure 4.21 shows the dose response curve of PVC dosimeters subjected to a total broadband UV dose of 6 SED using the solar simulator. A fluctuation in response is apparent for doses less than 2 SED. After that, the response starts to change monotonically. A dose of 3 SED can be considered as the lower threshold dose of the dosimeter.

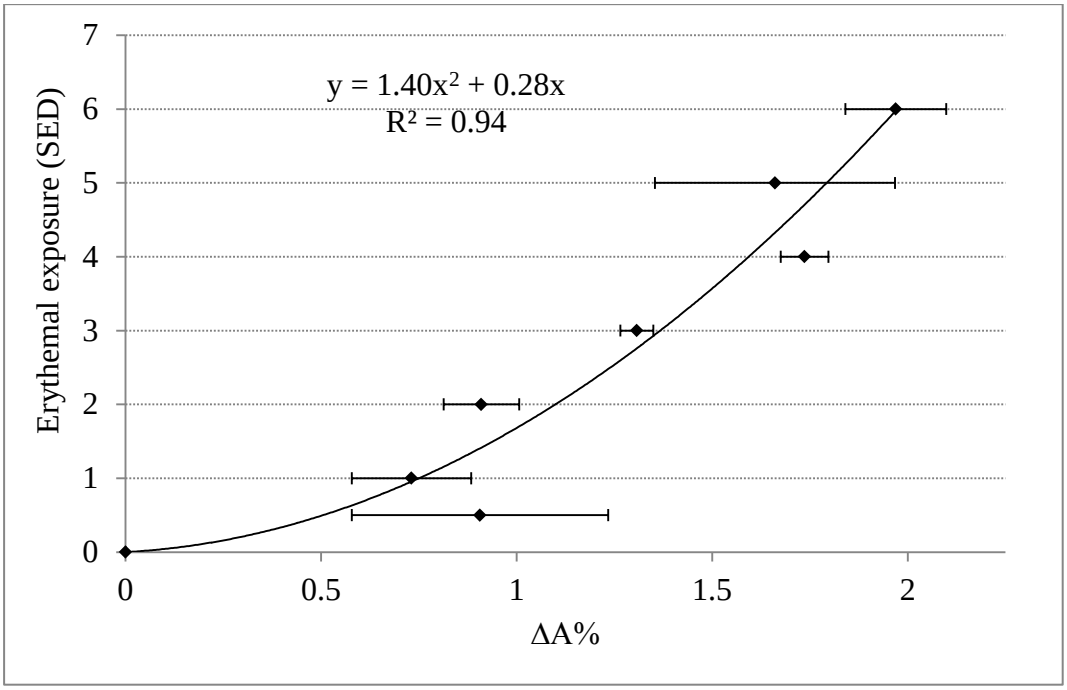

Figure 4.21: The response of PVC dosimeter to small doses.

4.2.9 Dark reaction

The dark reaction induced absorbance change of PVC dosimeters, measured after exposure had ceased, is illustrated in Figure 4.22 and 4.23. It can be seen from these figures that there was no evidence of incremental change. ΔA% fluctuated within the experimental error of the measured absorbance, ± 3%, up to about 70 days after terminating the exposure. For both groups of dosimeters, irradiated by 3.5 MJ/m^2 and 1.75 MJ/m^2, there is no clear dark reaction or dependent change on post-exposure time or temperature.

Furthermore, negligible fluctuation in post-exposure absorbance change was also independent of the radiant exposure. Figure 4.24 reveals that PVC dosimeters receiving different exposures, stored at similar temperatures after exposure, show similar behaviour of post-exposure absorbance as a function of time.

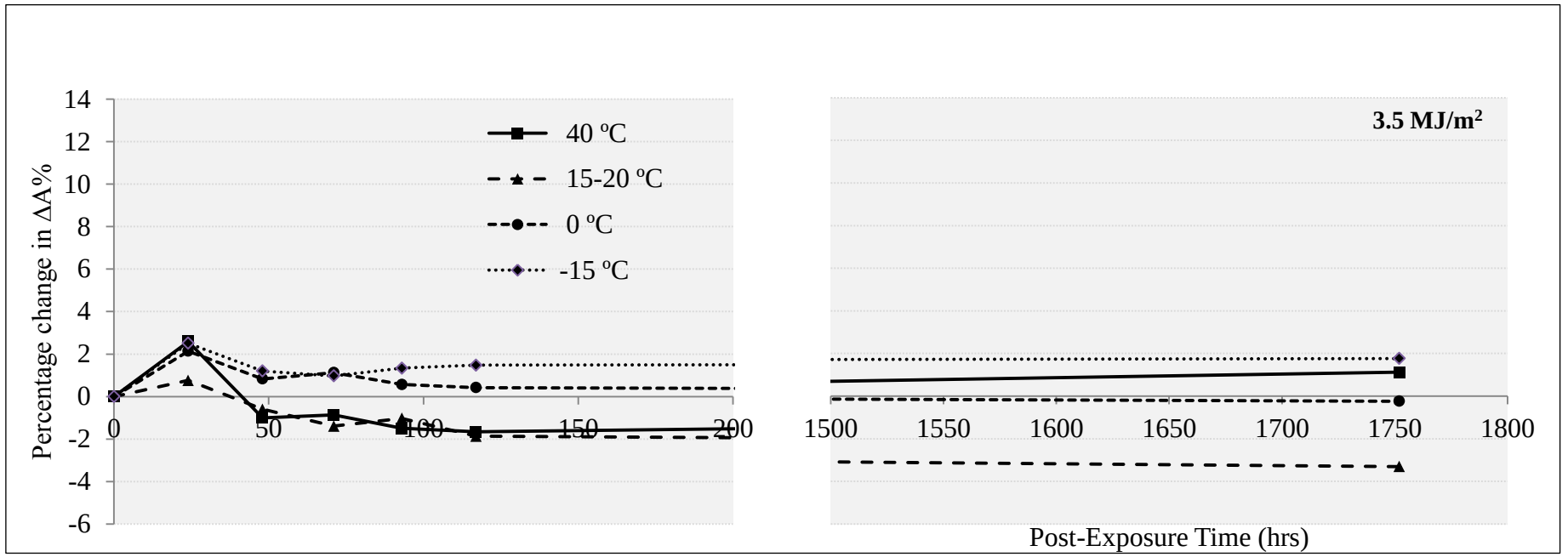

Figure 4.22: The dark reaction induced change of PVC dosimeters exposed to 3.5 MJ/m^2 of broadband UV and stored after exposure at different temperatures.

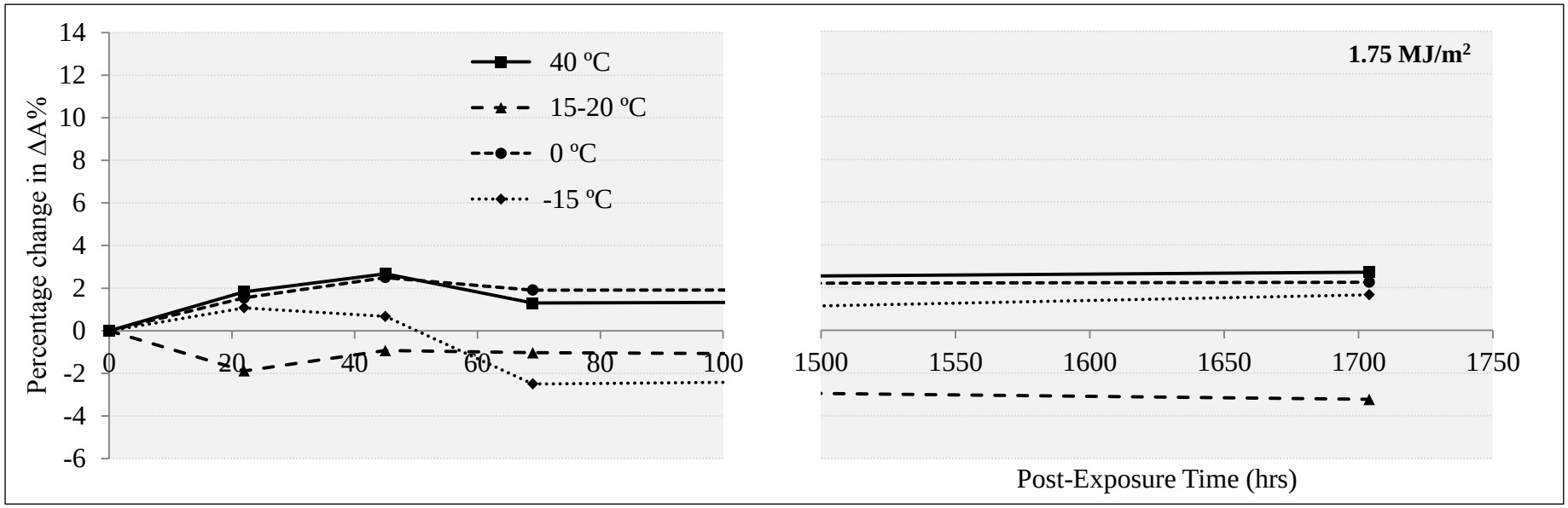

Figure 4.23: The dark reaction induced change of PVC dosimeters exposed to 1.75 MJ/m^2 of broadband UV and stored after exposure at different temperatures.

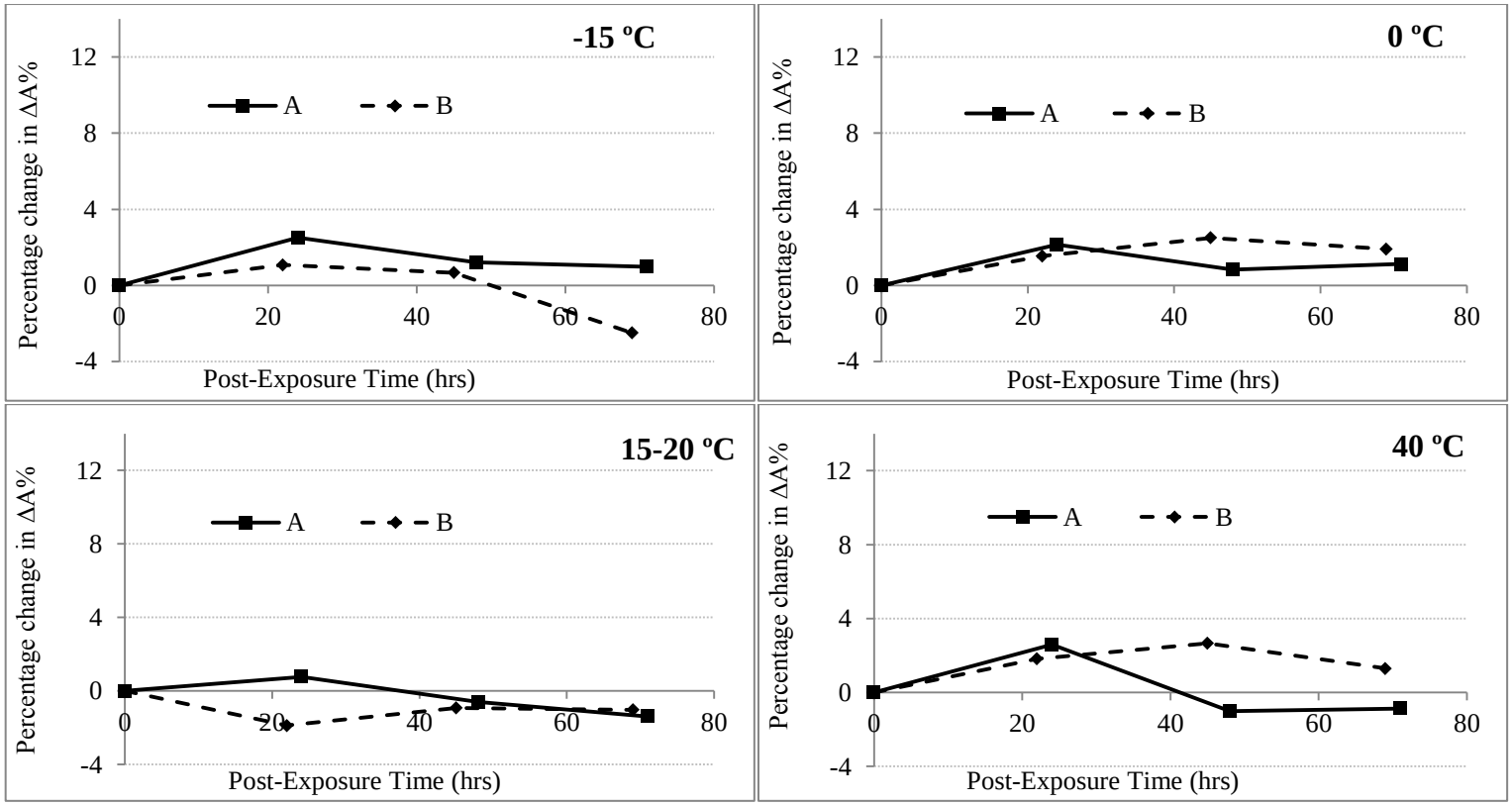

Figure 4.24: The dark reaction induced change of two groups of PVC dosimeters (A, B) subjected to two different exposures and stored at the same temperature after terminating the exposure. (A) dosimeters irradiated by 3.5 MJ/m^2 and (B) dosimeters irradiated by 1.75 MJ/m^2.

Chapter 5

Employment of the PVC dosimeter in anatomical exposure measurements

5.1 Introduction.

5.2 Materials and methods.

5.3 Results and discussion.

5.1 Introduction

The experimental investigation of the dosimetric properties in previous chapters has proven that the PVC dosimeter can be calibrated to quantify solar erythemally effective exposures that are significantly greater than those that can be measured by the PS and PPO chemical dosimeters. The exposure limit of the PS dosimeter is about 30 SED (Diffey 1987) and the PPO dosimeter is about 300 SED (Lester et al. 2003).

An outdoor test was carried out in order to evaluate the reliability of the PVC dosimeter in personal solar UV exposure measurements during an extended period of time. The ability of the PVC dosimeter to deliver reliable measurements was evaluated by comparing the results obtained by one set of PVC dosimeters with the results concurrently obtained by three sets of PPO dosimeters, and also with the results reported in similar studies.

5.2 Materials and methods

PVC dosimeters of thickness of 16 μm were prepared from 10% PVC/THF solution using the polymer casting table as described previously. PPO dosimeters were kindly provided by Professor Alfio Parisi. The 40 μm PPO dosimeters were cast using 0.12 mixing ratio of PPO and chloroform as described by Lester et al. (2003).

The PVC and PPO dosimeters were employed to monitor the erythemally effective exposure that reaches five anatomical sites using four head form manikins rotating at a constant velocity of one revolution per minute. This velocity may be regarded as equivalent to random motion during outdoor activities (Diffey et al. 1977b).

Figure 5.1: The experimental set-up for the anatomical exposure measurements showing the PVC and PPO dosimeters attached to chosen spots on manikins that were mounted on a rotating platform.

Two dosimeters of each type were attached to each of the following sites: vertex, nose, shoulder, chin and neck (Figure 5.1). The exposures were carried out for 12 consecutive days during summer 2013 at a private property near the University of Southern Queensland (27.56 °S 151.95 °E 690 m). The site of the exposures was an unshaded lawn surrounded by a house and fence, with partial shading before 08:00 and after 18:00 EST.

The calibration curves for the two dosimeters were determined at the time of the anatomical exposure measurements by exposing a number of PVC and PPO dosimeters on a horizontal unshaded plane near the erythemally weighted UV meter and regularly recording the UV-induced response of the two dosimeters as a function of the UV exposure.

The ambient erythemally effective exposure and, therefore, measured personal exposure are expressed in units of SED following CIE (1998).

The UV-induced response of the PPO dosimeters was quantified by the change in the optical absorbance at 320 nm (Lester et al. 2003) measured using the Shimadzu spectrophotometer, while the PVC response was taken as the percentage change in the 1064 cm^{-1} peak intensity (Amar & Parisi 2012), measured using the FTIR spectrophotometer.

Due to the fact that PPO dosimeters are saturated after about five days of exposure to solar UV radiation (Lester et al. 2003), the PPO dosimeters used for measurement and calibration were replaced every four days of exposure.

At the end of the exposures, the measured absorbance change within the PVC and PPO dosimeters were converted into exposure doses in SED using the calibration curves concurrently established.

Finally, the anatomical exposure measured by one set of PVC dosimeters (10 dosimeters) was compared with that measured using three sets of PPO dosimeters (30 dosimeters).

5.3 Results and Discussion

The PVC and PPO calibration curves determined at the same time as the field measurements, and employed to convert the measured absorbance change of the measuring dosimeters to exposure dose, are presented in Figure 5.2 and Figure 5.3, respectively.

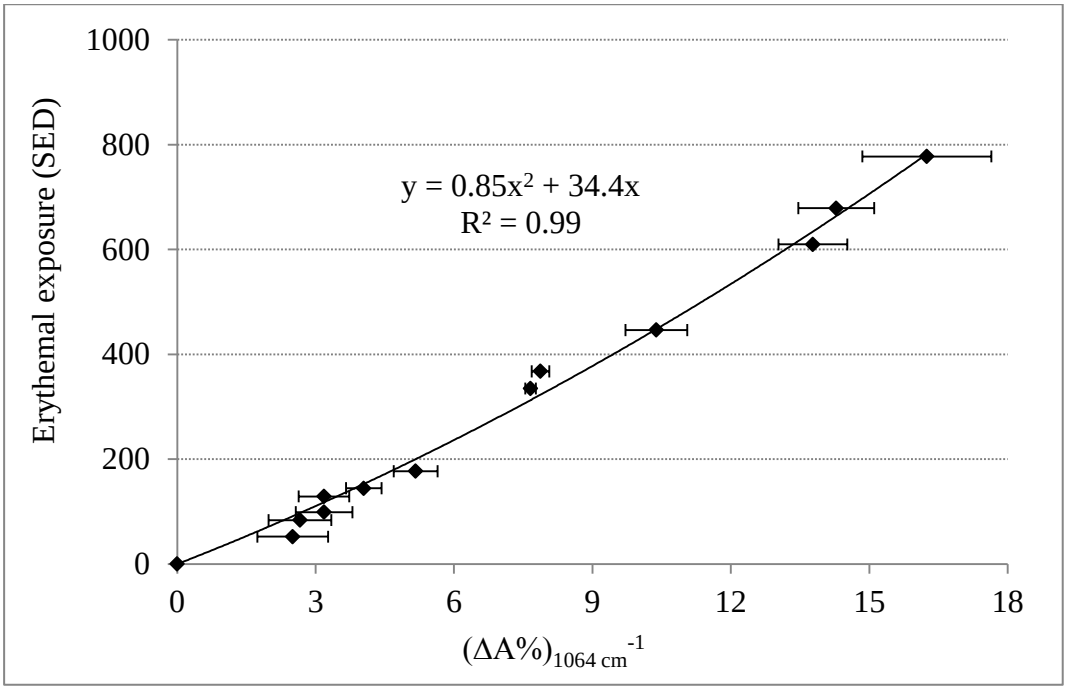

Figure 5.2: The dose response curve of the PVC based dosimeter. The error bars are the standard error in the measured absorbance of the dosimeters.

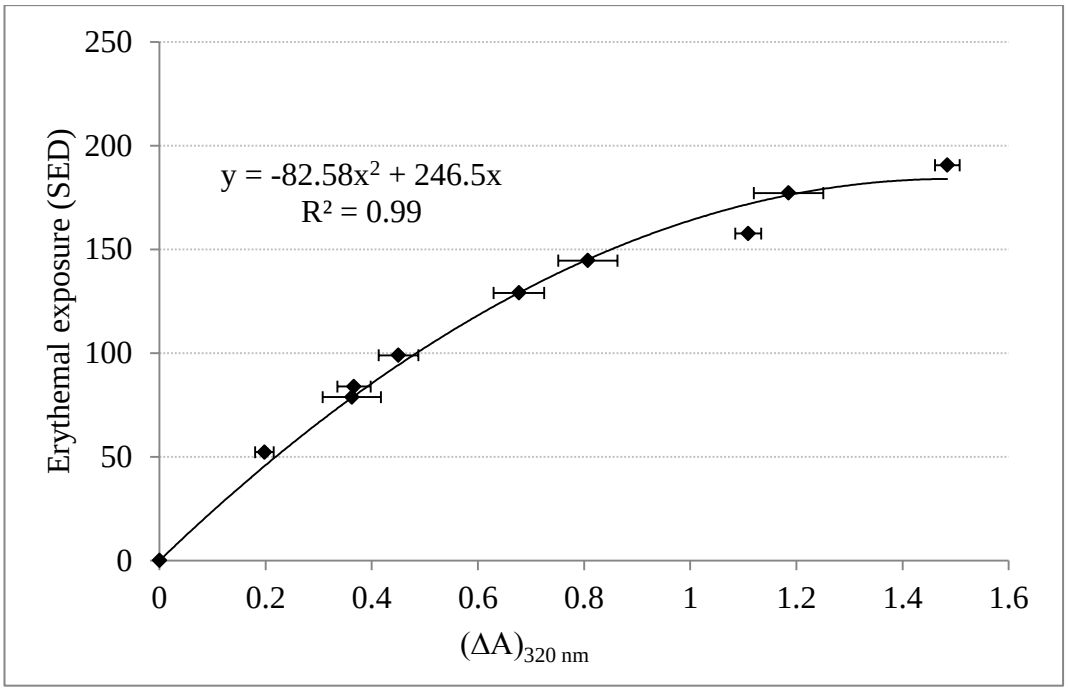

Figure 5.3: The dose response curve of the PPO based dosimeter. The error bars are the standard error in the measured absorbance of the dosimeters.

A comparison between the doses received by the five investigated anatomical sites during 12 consecutive days in summer as measured using the PVC and PPO dosimeters are presented in Figure 5.4. The agreement between the results was best for the vertex, nose and shoulder. However, there was a slight discrepancy between the two dosimeter types for doses measured at the chin and back of the neck.

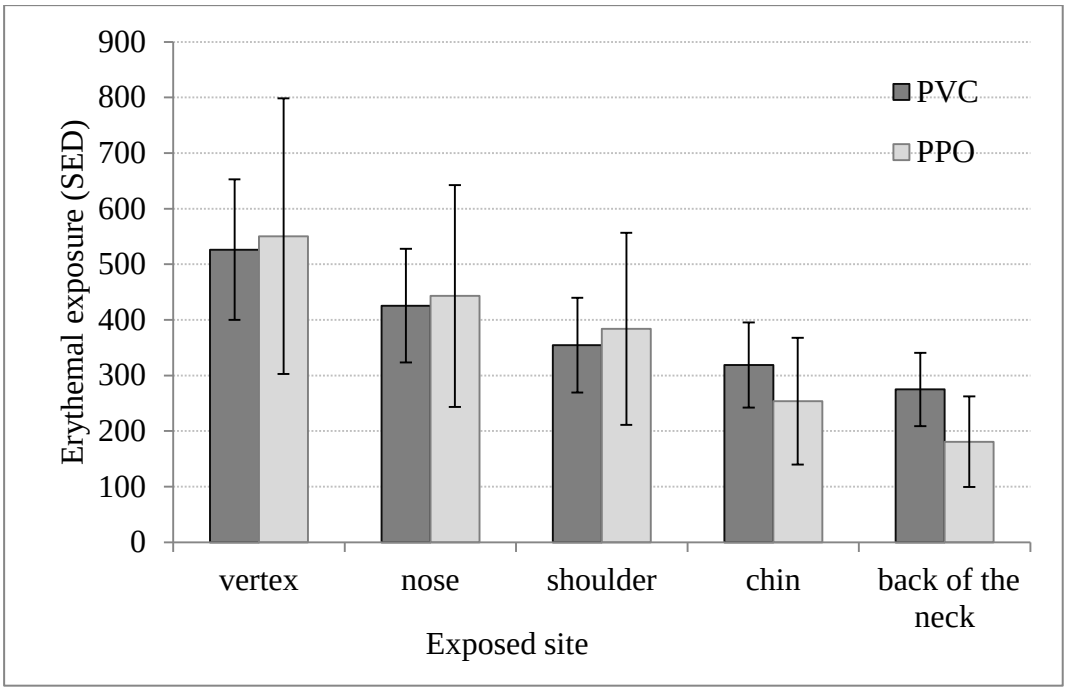

Figure 5.4: Doses received by five anatomical sites due to exposure to solar radiation for 12 days as measured by PVC and PPO dosimeters.

The error bars in Figure 5.4 represent a measurement uncertainty of 15% for each set of PPO dosimeters (Lester et al. 2003), and 24% for the PVC dosimeter. The uncertainty was estimated as described below.

As for all measured quantities, the UV dose measured by the PVC dosimeter has a level of uncertainty (variability) that needs to be communicated along with the measured value. One method of estimating the measurement uncertainty of passive dosimeters relies on the concept that:

"*when propagating the error in a measurement of A through nonlinear function,* $Z = f(A)$ *, the uncertainty in* Z *is a function of both* A *and its uncertainty* α_A *…… A calculus-based approximation for the uncertainty propagation for a single-variable function is* $\alpha_Z = \left|\frac{dZ}{dA}\right|\alpha_A$". (Hughes & Hase 2010).

This was the methodology employed by Tate et al. (1980) to estimate the uncertainty in the measured UV dose using nalidixic acid film dosimeter.

The established calibration function for PVC dosimeters used for measuring the anatomical exposure (Figure 5.2) is:

$$y = 0.85x^2 + 34.4x \qquad (5.1)$$

where, in this instance, the absorbance change is denoted by x rather than ΔA%, and y is the associated UV dose in SED units (instead of *H*).

The derivative of 5.1 is:

$$\frac{dy}{dx} = 2 \times 0.85x + 34.4 \Rightarrow dy = (1.7x + 34.4)dx \qquad (5.2)$$

where $dx = \alpha_x.x$, α_x *is* the average deviation of the absorbance change (reproducibility) of the dosimeter which was previously (4.2.1) determined as 2.5%.

The measured anatomical UV dose and the related uncertainty in the current study are shown in Table 5.1:

Table 5.1: The uncertainty in the estimated anatomical exposures measured by PVC dosimeters.

Exposure site	**x**	**y (SED)**	**(dy/y)%**
vertex	11.85	527	21
nose	9.95	426	21
shoulder	8.53	355	22
chin	7.79	320	22
back of the neck	6.85	276	22

The average uncertainty of dose measurements was about 22%. This uncertainty in the measured dose is due to the absorbance uncertainty. To take into account the uncertainty in the Biometer data (10%) used to establish the calibration curve, the combined standard uncertainty (U_C) was calculated after (Castrup 2010) by:

U_C =*Positive square root of the sum of the square uncertainties*

$$U_C = +\sqrt{u_1^2 + u_2^2 + u_3^2 + ...etc.} \qquad (5.3)$$

where u_i are the statistically independent uncertainty components.

$$U_C = \sqrt{22^2 + 10^2} = 24\%$$

Although 24% uncertainty can be considered high, it is still comparable with that of other chemical UV dosimeters. For instance, the PPO uncertainty was reported to be 15% (Lester et al. 2003); and the PS uncertainty was found to be 10% for ΔA_{330} up to 0.3 and about 30% for $\Delta A_{330} = 0.4$ (Diffey 1987).

Another methodology for estimating the dosimeter uncertainty depends on calculating the deviation of the experimental data used in constructing the calibration curve from the best fit of the data. The average deviation of the experimental points from the regression in Figure 5.2 was about 10%. The greatest deviation was observed for fitted function values less than 120 SED with an average of about 20%. For higher exposures, the average deviation of the experimentally determined exposures was about 6% from those calculated by the fitted function. The maximum uncertainty in the dosimeter measurements can then be considered to be 20%, which is close to that calculated by the calculus-based approximation.

The exposure ratio (ER), which is defined as the ratio between the personal UV exposure on a selected anatomical site and the corresponding ambient UV exposure measured on a horizontal plane, can be considered in this study as the fraction of the ambient UV exposure received on the vertex (Schmalwieser et al. 2010b). This ratio was calculated from the data obtained by the PVC dosimeter and is presented in Table 5.2.

Table 5.2: The UV exposure relative to the vertex at five anatomical sites as measured using the PVC dosimeter after 12 consecutive days of exposure in summer at Toowoomba, QLD.

Anatomical site	**Exposure Ratio (ER)**
Vertex	1.00
Nose	0.81
Shoulder	0.67
Chin	0.61
Back of the neck	0.52

The results are consistent with the generalization of earlier studies where the shoulders generally receive two-thirds of the dose relative to the vertex while vertical sites of the body receive roughly half of the vertex dose. For instance, Diffey et al. (1977b) employed the PS dosimeter on a rotating manikin to measure the UV exposure received by some anatomical sites under three different weather conditions and found that the ER of the shoulder was 0.68 ± 0.10, 0.75 ± 0.09 and 0.80 ± 0.07 for clear sky, light cloud cover and heavy cloud cover, respectively. In the same study, the ER of the mid lumbar spine (vertical orientation) was 0.51 ± 0.07, 0.43 ± 0.10 and 0.47 ± 0.08, respectively, for the same weather conditions respectively. Another study conducted by Sobolewski et al. (2008) reported that the daily mean dose measured by a broadband meter placed horizontally is half of the dose measured on a vertical receiver randomly oriented towards the sun.

Chapter 6

Discussion of Results

An initial objective of this research was to introduce a novel chemical UV dosimeter with simple preparation and readout processes suitable for measuring large doses of solar UV radiation. This objective was fulfilled by the development and characterisation of a chemical UV dosimeter employing unstabilised solvent cast polyvinyl chloride (PVC) thin film. The PVC dosimeter was found to be capable of monitoring up to at least three weeks of continuous exposure to solar UV radiation under clear sky conditions at subtropical sites in summer (900 SED). This is about five times the dose capacity of the PPO dosimeter (Lester et al. 2003) and twenty times that of the PS dosimeter (Diffey 1987). Most importantly, the experimental findings presented in this research have shown that the PVC dosimeter satisfies the basic requirements for a reliable long-term UV dosimeter.

A simple readout technique was employed with the PVC dosimeter to estimate UV doses. It was found in this project that the UV induced changes within the PVC thin film can be quantified using infrared spectroscopy, particularly the change in the 1064 cm^{-1} peak intensity. This change occurs in a monotonic manner; hence, this peak was used to quantify UV-induced change in the PVC film.

PVC dosimeters were constructed using commercially available materials by employing an uncomplicated solvent cast polymer technique. PVC sheets were cast from PVC/THF solution using a polymer casting table.

Overall, 16 µm PVC films prepared from 10% PVC/THF solution proved to have long-term durability and to be able to withstand extreme weather conditions during outdoor applications. This study showed that this thickness and concentration are the optimal parameter levels for PVC dosimeter construction.

Spectral response curves of the PVC dosimeter, measured using cut-off filters, narrow band-pass filters and an irradiation monochromator, showed close qualitative agreement. The greatest response of the PVC dosimeter was in the UVB band and decreased with wavelength to about 340 nm in the UVA. The cut-off filter technique showed no response of PVC to wavelengths longer than 345 nm (Figure 4.8). The maximum response was to wavelengths between 292 and 312 nm and dropped to about one half and one quarter of this value for the 315–332 nm and 324–346 nm bands, respectively. The same band, approximately, is dominant in the spectral curve determined by narrow band-pass filters (Figure 4.9), where longer bands showed less response than that measured by cut-off filters. This might be because the bands with the cut-off filters are wider and interfere with each other with more chance for a synergistic effect. In line with these results, the maximum in the response curve determined using monochromatic radiation was at 290 nm and the response decreased exponentially with wavelength, independent of temperature and exposure dose (Figure 4.10).

Figure 6.1 compares the spectral response curve of the PVC dosimeter measured using the irradiation monochromator with those of PS (CIE 1993), PPO (Parisi et al. 2010b) dosimeters and the CIE erythemal action spectrum (CIE 1998).

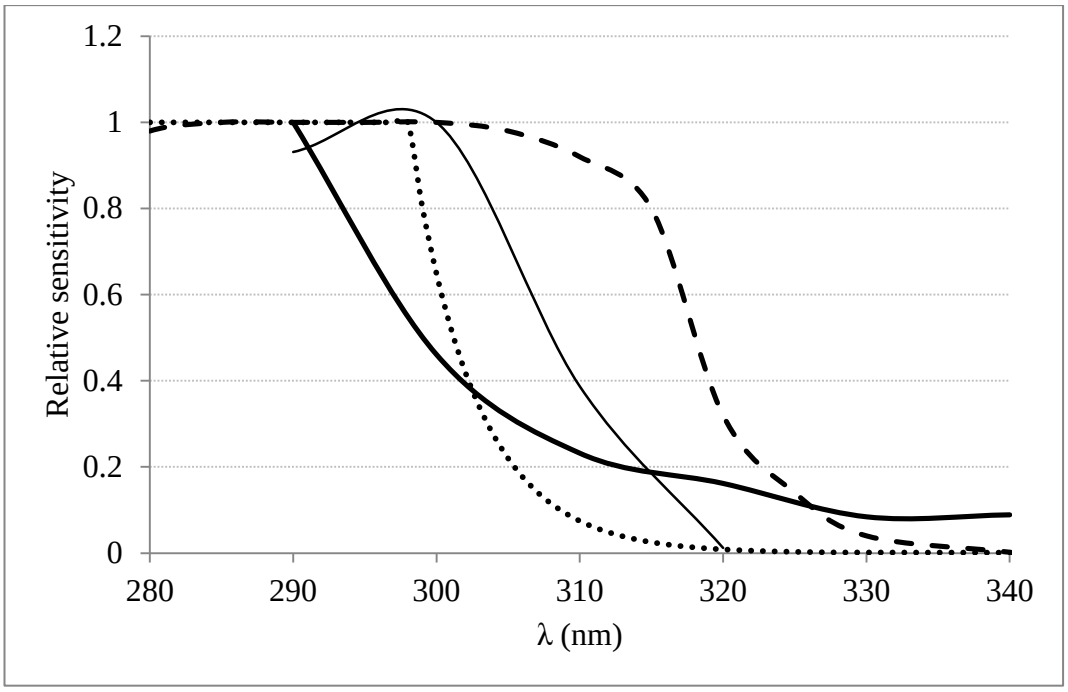

Figure 6.1: Spectral response of 16 µm PVC dosimeter (thick line) compared to the erythemal action spectrum (CIE 1998) (dotted line), PS spectral response (CIE 1993) (dashed line) and the PPO spectral response (Parisi et al. 2010b) (thin line).

It can be noticed from Figure 6.1 that none of the three responses exactly matches the erythemal response. The PVC response coincides with the eythemal response at 304 nm. The difference between the two curves is less than 37% at the shorter wavelengths while at longer wavelengths the PVC response is considerably higher than that of the erythemal response. However, similar to the way that the PS and PPO dosimeters are used for measuring erythemal exposures provided that the dosimeters are calibrated for the season and conditions of the field measurements (Casale et al. 2009; Parisi 2004; Parisi et al. 1996a; Siani et al. 2008), it is expected that the PVC dosimeter can be calibrated for the appropriate seasonal and field conditions to measure long term erythemal UV exposures.

PVC dosimeters subjected to equal exposures showed a high reproducibility in their response to UV exposure. The response was within 2.5% of its mean, with a maximum deviation of 5% for exposures less than 2.5 MJ/m^2 (Figure 3). This is on a level with the reported reproducibility of the PS and PPO dosimeters (Table 6.1).

The response of the PVC dosimeter is independent of irradiation temperature in the range of up to 45 ºC (Figure 4.12, 4.13 and 4.14). Temperature independency was established using three different exposures over the range of 5–45 ºC. The average deviation from the mean response was about 4.5%, which is an acceptable value considering the 3% variation in the lamp output, 5% reproducibility and an uncertainty of about 1% for the absorbance measurements. Furthermore, no clear relationship was found between the dose response and dose-rate for the tested irradiances (Figure 4.15 and 4.16). The time-irradiance reciprocity was tested for two different exposures. The Bunsen-Roscoe law was obeyed, in general, for the two

exposures over a wide range of irradiances. The response over the irradiance range (3–53 W/m^2) deviated within an average of 6% from the mean with no clear trend or dependency of the response on the supplied irradiance. The temperature and dose rate independence of the PVC dosimeter allow its deployment under different weather conditions with various ambient temperatures and solar irradiances.

In addition, the general shape of the angular response of the PVC film was similar to the cosine function with a tendency to exhibit smaller efficiency at large angles (Figure 4.17). The difference between the normalised response of the PVC dosimeter and cosine function was less than 6.5% for angles up to 40º, but it reached 40% for angles ≥60º. This is higher than the cosine error reported for the PS and PPO dosimeters (Table 6.1). However, it is generally known that no radiation detector is perfect in this regard (Michalsky et al. 1995) and the angular response of even modern electronic instruments is a significant uncertainty source that affects spectral UV irradiance measurements.

No dark reaction was observed during the investigation of the post-exposure behaviour of the PVC dosimeter. This is an advantage that the PVC dosimeter has over PS and PPO dosimeters, and it allows the PVC dosimeter to be used in remote and inhospitable places, leaving the post-exposure absorbance measurements to more convenient time and conditions. Post-exposure absorbance of PS dosimeters, for instance, is determined either immediately after exposure or at a particular time, usually 24 hours, after exposure. This is due to the increasing change of absorbance with post-exposure time. The PS absorbance at 24 hours, 1 week and three months after exposure is 4%, 5% and 7% higher than that determined immediately after exposure, respectively (Diffey 1987) and, therefore, the establishment of a set routine for post-exposure measurements is required for PS dosimeters to minimise any inconsistencies due to this dark reaction.

The minimum detectible dose for the PVC dosimeter was determined as 3 SED. Although this threshold is higher than those of other chemical UV dosimeters, it is not necessarily a disadvantage, as the dosimeter is proposed for high doses accumulated during prolonged exposures.

The results also demonstrated the necessity of calibrating the PVC film with background material matched to the colour and texture of the experimental exposures in order to eliminate any response due to backscattering radiation (Figure 4.18). Colour and material mismatch may result in relative uncertainties of up to two or three decades in the measured UV dose.

The establishment of the PVC dose response curves underlined not only the high dose capacity of the dosimeter, but also the suitability of the dosimeter to be used in a range of environmental conditions. The dose response curves indicate that the PVC dosimeter can measure more than 900 SED of exposure. This is equivalent to about three weeks of continuous exposure under clear sky conditions during summer at subtropical sites. Furthermore, in contrast to the PS dose response which varies with the seasons (Casale et al. 2006), the PVC dose response curves obtained during

different seasons have similar pattern. Casale et al. (2006) related the variability of the PS dose response curves to the total ozone amount and the solar zenith angle. Follow up research would be required to investigate the effect of these factors on the PVC dosimeter.

The performance of the dosimeter was investigated by measuring the anatomical exposure over 12 consecutive days. The results were comparable with those measured concurrently using the PPO dosimeter and in a reasonable agreement with the results reported in earlier similar studies. The results support the positive overall evaluation of the PVC dosimeter as a reliable means of measuring prolonged UV exposures.

The uncertainty of the PVC measurements was estimated to be 24% as derived from the calculus-based approximation for uncertainty propagation, assuming an uncertainty in the measured absorbance change of about 2.5% and taking into account the 10% uncertainty for the biometer employed to construct the calibration curve. This calculated uncertainty is higher than those reported for other chemical UV dosimeters. However, the comparison could be unrealistic as various methodologies were used in other studies; hence different error components were included in calculating the uncertainties of different dosimeters. For instance, Diffey (1989) employed the calculus-based approximation and assumed an uncertainty of 0.01 in the average optical absorbance change up to 0.4 while ignoring the error related to the calibration curve to derive an average uncertainty of 8% in PS dosimeter measurements. Tate et al. (1980) also calculated uncertainty using the calculus-based approximation but the standard deviation of measured absorbance was also the only error component considered when assessing the efficacy of a Nalidixic Acid based chemical UV dosimeter; reported uncertainty was about 20% for a measured dose of 40 KJ/m^2. Lester et al. (2003) estimated an uncertainty of 15% in PPO measurements, but did not report the methodology used for this estimation.

One limitation of the present research is that measurement uncertainty was not determined experimentally. Although the theoretical methodologies used are certified and can give a reliable estimation of the uncertainty, comparing the dose measured by the proposed new dosimeter with concurrently measured dose using a calibrated electronic device is the optimal way to validate dosimeter measurements. Seckmeyer et al. (2012) compared UV doses measured by polysulphone (PS) with measurements obtained using a reference spectroradiometer (RS) and found that PS showed mean absolute deviations of 26% with a maximum deviation of 44%. However, these observed large deviations were based only on one calibration curve carried out at Hannover (Seckmeyer et al. 2012). This uncertainty is much higher than that estimated theoretically and reported in other studies and emphasises the usefulness of the experimental investigation of the uncertainty of new dosimeters. The experimental approach for calculating PVC uncertainty was not applied due to the unavailability of the necessary equipment; this is an area that warrants further research.

The comprehensive assessment and evaluation of the proposed new chemical UV dosimeter (PVC) verified its applicability for continuous long-term monitoring of erythemally effective doses of solar UV radiation. The dosimetric characteristics and measurement uncertainty of the PVC dosimeter are comparable with those of PPO and PS dosimeters (Table 6.1), with the added advantage of a far higher dose capacity for the PVC dosimeter.

Table 6.1: A comparison of the dosimetric properties of the PVC, PPO and PS dosimeters.

	PVC **(Amar & Parisi 2013b; 2013a)**	**PPO** (Lester et al. 2003)	**PS** (Casale et al. 2012; Davis et al. 1976; Diffey 1987; Kollias et al. 2003; Krins et al. 2000)
Sensitivity	Primarily to UVB	Primarily to UVB	Primarily to UVB
Dose Capacity (SED)	> 900	~ 300	~ 30
Reproducibility (response variation)	2.5% average variation (5% maximum)	6.5%	5%
Temperature dependency	Independent 4.6% variation in the response within the range 5-45 ºC	Independent < 2% variation in the response within the range 1.5-50 ºC	Independent
Dose-rate dependency	Independent 6.4% variation within the range 3-53 W/m^2	Independent 4% variation in the response within the range 2.1-11.7 W/m^2 + Slight dependency 13% variation in the response within the range 1-3.7 W/m^2	Independent 5% variation in the response within the range 0.56-3.4 W/m^2
Angular response (% deviation from the cosine function)	< 6.5% for angles up to 40º increasing to up to 40% for angles ≥ 60º	< 6.2% for angles up to 40º increasing to up to 13.2% for angles ≥ 60º	Independent for angles up to 70º
Dark reaction induced change after exposure	Negligible No clear trend	~ 3.4% per night Dependent on temperature	4% after 24 hours 5% after a week

Chapter 7

Conclusions

7.1 Realization of the research objectives

7.2 Further research

7.3 Final conclusion

7.1 Realization of the research objectives

The research aim was to develop and characterise a new chemical UV dosimeter suitable for estimating the UV doses accumulated over long periods of time (weeks) through a single measurement. The review of the literature and the results of the conducted pilot study determined solvent cast unstabilised polyvinyl chloride (PVC) as a possible candidate for this purpose. Therefore, the subsidiary objectives of this research were to investigate and determine the physical and dosimetric properties of the proposed PVC dosimeter.

A comparison of the preparation process and physical properties of PVC films cast from different concentrations of PVC/THF solution revealed that 10% is the optimum concentration for casting high quality PVC films with sufficient durability. In addition, investigation of PVC films cast with different thicknesses showed that the 16 µm thickness is the best compromise between physical quality, sensitivity to UV and linearity of the dose response curve. Furthermore, experimental investigation of the UV response of PVC films dried for different lengths of time showed that drying the films for about 25 days at 50 ºC is a requirement to minimise any possible effects of temperature on the dosimeter performance.

The reproducibility of the dosimeter was evaluated for exposures up to 27 MJ/m^2 of broadband UV radiation. The dosimeter response varied within ±2% for exposures higher than 2.5 MJ/m^2. The variation was more for lower exposures (±5% at 1 MJ/m^2) and the reproducibility was then established to be 2.5%. Three different techniques were employed to determine the dosimeter spectral response. Results showed that the dosimeter responds mainly to the UVB waveband with a maximum response at 290 nm and decreasing exponentially with wavelength up to about 340 nm independent of temperature and exposure dose. The established spectral response curve of the dosimeter is comparable with those of the PS and PPO dosimeters, but slightly different from the erythemal action spectrum and so the dosimeter can be used to measure erythemally effective exposure when calibrated using the UV source of interest.

The effect of ambient temperature on the dosimeter response to UV radiation was investigated using three different exposures over a wide range of temperatures. The average deviation of the response over the range of 5–45 ºC was about 4.5%. In addition, the dosimeter response was found to be reasonably independent of dose rate. The dose rate independency was tested for two different exposures over the irradiance range (3–53 W/m^2) and the average deviation of the response was about 6% from the mean. Furthermore, the response of the dosimeter as a function of the incident angle of radiation was examined using a UV solar simulator with a collimated beam of radiation. The dosimeter exhibits a cosine like response with less than 6.5% error for angles up to 40º, but the error reached 40% for angles ≥60º.

No significant change due to dark reaction was observed on the dosimeter response after terminating the exposure. Dosimeters subjected to different exposures and stored at different temperatures after exposure showed negligible change (within

the experimental error range) in the post-exposure response over periods up to about 70 days.

The erythemally effective dose response curve of the PVC dosimeter was established for each season and it was found that the erythemal dose capacity of the dosimeter is more than 900 SED. This result demonstrates that the PVC dosimeter can measure at least three weeks of full day exposure to solar UV radiation under clear sky conditions in summer at subtropical sites, without the need to replace the dosimeter. In addition, the dosimeter suitability for long-term personal exposure measurements was evaluated in a field trial. The results showed that the PVC dosimeter could provide reliable exposure estimates using a single dosimeter, decreasing the cost, effort and measurement uncertainty.

Two dosimetric properties of the proposed dosimeter need further clarification, as determined in this research. The first property is the high threshold dose (3 SED) that the dosimeter can detect, although this could be considered as an insignificant aspect as the dosimeter was introduced to measure several hundred SEDs. The second one is the relatively high uncertainty (24%) of the measured dose compared to the reported uncertainties for other chemical UV dosimeters. However, the dose measured using a single PVC dosimeter is accompanied by a much lower uncertainty than that of the same dose measured using a series of short-term exposure dosimeters (e.g. PS) as the uncertainty in the latter case is the dosimeter's uncertainty times the number of employed dosimeters.

7.2 Further research

Some complementary studies, such as the examples detailed below, could be conducted to further enhance the understanding of the physical and dosimetric properties and also the performance of the proposed PVC dosimeter.

- Although the experimental investigation in this research showed that the PVC dosimeter satisfies the demanding requirements and the long-term UV exposure field measurements conducted by the PVC dosimeter were compatible with those obtained by the PPO dosimeter and similar to the findings of earlier studies, it would be worthwhile to perform further side-by-side comparative long-term solar UV exposure measurements with the PVC dosimeter and other types of personal UV dosimeters, especially the electronic dosimeters. Comparison of measurements with the PVC dosimeter to those obtained using accurate electronic dosimeters helps to further evaluate the reliability of the measurements of the proposed dosimeter and clarify its usefulness, limitation and operating characteristics under various situations.
- Since the dosimeter has not shown any signs of saturation and maintained its robustness even after a month of continuous exposure to solar UV radiation, it would be worthwhile to investigate the suitability of the dosimeter for measurements over longer periods. Determination of the maximum dose capacity completes the picture of the optical properties of the dosimeter. The establishment of seasonal or annual calibration curves, if possible, would be a great contribution to the UV dosimetry field.
- Considering the fact that the PVC dosimeter responds mainly to the UVB band and some biological action spectra, other than erythema, are characterised by the dominant effect of UVB wavelengths, it seems that there is a possibility to calibrate the dosimeter to exposures weighted to other biological responses to solar UV radiation. For instance, the PVC dosimeter could be investigated for the exposures weighted for the production of vitamin D in human skin where the effect peaks in UVB wavelengths (Bouillon et al. 2006) (Figure 2.4). DNA damage is also caused mainly by UVB (Figure 2.2) and it could also be worthwhile to calibrate the dosimeter for this biological effect.
- Some chemical dosimeters have shown great potential for use in aquatic ecosystems. The PS and PPO dosimeters, for example, were successfully calibrated and deployed for underwater UV measurements (Dunne 1999; Frost et al. 2006; Schouten et al. 2007; Schouten et al. 2008). In a similar way, the PVC dosimeter could be investigated for assessment of the exposure of aquatic ecosystems in underwater measurements for extended periods. The underwater durability and the dosimetric properties such as spectral response, cosine response, dose response curves, and temperature and dose-rate independency of the dosimeter would have to be studied.

7.3 Final conclusion

Chemical UV dosimeters have been widely used in human UV exposure research. The introduced new PVC dosimeter provides an additional tool for this area of research with a competitive advantage in terms of enhanced capacity for long-term measurements. Applications of the PVC dosimeter are in all fields of research in which other chemical dosimeters are employed. Such applications include determination of anatomical personal UV exposure in different environments and evaluation of protection strategies against solar UV radiation. The potential application of the new dosimeter is likely to be in research related to latent responses caused by doses accumulated over long periods. The dosimeter is expected to improve cumulative annual personal UV exposure estimates required to analyse the correlation between UV exposure and chronic UV induced responses. Measurements conducted over long periods (weeks) take into account variations in the solar spectrum due to changing atmospheric conditions and therefore will provide a more precise evaluation of the annual exposure. The PVC dosimeter developed in this research therefore has the potential to make significant contributions to the UV-related research.

References

ABS (Australian Bureau of Statistics) 2013, *Causes of Death Australia 2011*, viewed 25/08/2013, http://www.abs.gov.au/ausstats/abs@.nsf/Lookup/3303.0main+features100012012.

Alexandrescu, DT, Maslin, B, Kauffman, CL, Ichim, TE & Dasanu, CA 2013, 'Malignant melanoma in pigmented skin: Does the current interventional model fit a different clinical, histologic, and molecular entity?', *Dermatologic Surgery*, vol. 39, no. 9, pp. 1291-303.

Allen, MW & McKenzie, RL 2005, 'Enhanced UV exposure on a ski-field compared with exposures at sea level', *Photochemical and Photobiological Sciences* vol. 4, no. 5, pp. 429-37.

Allen, MW & McKenzie, RL 2010, 'Electronic UV dosimeters for research and education', *proceedings of the NIWA UV Workshop*, Queenstown, 7-9 April, Paper 11.

Amar, A & Parisi, AV 2012, 'Investigation of unstabilized polyvinyl chloride (PVC) for use as a long-term UV dosimeter: preliminary results', *Measurement Science and Technology*, vol. 23, no. 8, pp. 1-7.

Amar, A & Parisi, AV 2013a, 'Spectral response of solvent-cast polyvinyl chloride (PVC) thin film used as a long-term UV dosimeter', *Journal of Photochemistry and Photobiology B: Biology*, vol. 125, pp. 115-20.

Amar, A & Parisi, AV 2013b, 'Optical properties of a long dynamic range chemical UV dosimeter based on solvent cast polyvinyl chloride (PVC)', *Journal of Photochemistry and Photobiology B: Biology*, vol. 128, pp. 92-9.

Andrady, AL & Searle, ND 1989, 'Photodegradation of rigid PVC formulations. II. Spectral sensitivity to light-induced yellowing by polychromatic light', *Journal of Applied Polymer Science*, vol. 37, no. 10, pp. 2789-802.

Andrews, DG 2000, *An introduction to atmospheric physics*, Cambridge University Press, Cambridge UK.

ASCC 2008, *Guidance notes for the protection of workers from the ultraviolet radiation in sunlight*, Australian Safety and Compensation Council, Canberra.

Aun, M, Eerme, K, Ansko, I, Veismann, U & Lätt, S 2011, 'Modification of spectral ultraviolet doses by different types of overcast cloudiness and atmospheric aerosol', *Photochemistry and Photobiology*, vol. 87, no. 2, pp. 461-9.

Azzam, N & Dovrat, A 2004, 'Long-term lens organ culture system to determine age-related effects of UV irradiation on the eye lens', *Experimental Eye Research*, vol. 79, no. 6, pp. 903-11.

Bais, AF & Lubin, D 2006, 'Surface ultraviolet radiation: Past and future', *proceedings of the Scientific assessment of ozone depletion: 2006, global ozone research and monitoring project report no. 50*, World Meteorology Organisation, Geneva.

Barnard, WF & Wenny, BN 2009, 'Ultraviolet radiation and its interaction with air pollution', in W Gao, et al. (eds), *UV radiation in global climate change*, Springer, New York, pp. 221-326.

Baum, GA 1967, 'Outdoor exposure of organotin-stabilized rigid PVC', *proceedings of the Weatherability of plastic materials: Symposium held at National Bureau of Standards* Interscience Publishers, Gaithersburg, Maryland, February 8-9, 1967, p. 189.

Beadle, PC, Burton, JL & Leach, JF 1980, 'Correlation of seasonal variation of 25-hydroxycalciferol with UV radiation dose', *British Journal of Dermatology*, vol. 103, no. 3, pp. 289-93.

Bens, G 2008, 'Sunscreens', in J Reichrath (ed.), *Sunlight, Vitamin D and Skin Cancer*, Dermatology Clinic, The Saarland University Hospital, Saarland, vol. 624, pp. 137-61.

Bentham 1997, *A guide to spectroradiometry instruments and applications for the ultraviolet*, Reading, UK.

Bérces, A, Fekete, A, Gáspár, S, Gróf, P, Rettberg, P, Horneck, G & Rontó, G 1999, 'Biological UV dosimeters in the assessment of the biological hazard from environmental radiation', *Journal of Photochemistry and Photobiology B: Biology*, vol. 53, no. 1–3, pp. 36-43.

Berre, B & Lala, D 1989, 'Investigation on photochemical dosimeters for ultraviolet radiation', *Solar Energy*, vol. 42, no. 5, pp. 405-16.

Bouillon, R, Eisman, J, Garabedian, M, Holick, M, Kleinschmidt, J, Suda, T, Terenetskaya, I & Webb, AR 2006, *Action spectrum for the production of previtamin D_3 in human skin*, Technical Report 174, Commission Internationale de l'Éclairage, Vienna.

Braun, D 2004, 'Poly (vinyl chloride) on the way from the 19th century to the 21st century', *Journal of Polymer Science Part A: Polymer Chemistry*, vol. 42, no. 3, pp. 578-86.

Butson, MJ, Cheung, T, Peter, K, Abbati, D & Greenoak, GE 2000, 'Ultraviolet radiation dosimetry with radiochromic film', *Physics in Medicine and Biology*, vol. 45, no. 7, pp. 1863-8.

Calbó, J, Pagès, D & González, J-A 2005, 'Empirical studies of cloud effects on UV radiation: A review', *Reviews of Geophysics*, vol. 43, no. 2, pp. 1-28.

Cañada, M, Cañada, J, Moreno, J & Gurrea, G 2014, 'Personal UV exposure for different outdoor sports', *Photochemical & Photobiological Sciences*, vol. 13, no. 4, pp. 671-9.

Carli, P, Crocetti, E, Chiarugi, A, Salvini, C, Nardini, P, Zipoli, G & Simeone, E 2008, 'The use of commercially available personal UV-meters does cause less safe tanning habits: a randomized-controlled trial', *Photochemistry and Photobiology*, vol. 84, no. 3, pp. 758-63.

Casale, G, Siani, AM & Colosimo, A 2009, 'Polysulphone dosimetry: a tool for personal exposure studies', *Biophysics and Bioengineering Letters*, vol. 2, no. 1, pp. 1-14.

Casale, GR, Borra, M, Colosimo, A, Colucci, M, Militello, A, Siani, AM & Sisto, R 2006, 'Variability among polysulphone calibration curves', *Physics in Medicine and Biology*, vol. 51, no. 17, pp. 4413-27.

Casale, GR, Siani, AM, Diemoz, H, Kimlin, MG & Colosimo, A 2012, 'Applicability of the polysulphone horizontal calibration to differently inclined dosimeters', *Photochemistry and Photobiology*, vol. 88, no. 1, pp. 207-14.

Castrup, S 2010, 'Comparison of methods for establishing confidence limits and expanded uncertainties', *proceedings of the Measurement Science Conference*, California, pp. 1-23.

Chang, NB, Feng, R, Gao, Z & Gao, W 2010, 'Skin cancer incidence is highly associated with ultraviolet-B radiation history', *International Journal of Hygiene and Environmental Health*, vol. 213, no. 5, pp. 359-68.

CIE 1984, *Determination of the spectral responsivity of optical radiation detectors*, 064-1984, Commission Internationale de L'Eclairage, Paris.

CIE 1993, 'CIE Publication No. 98-1992: Personal dosimetry of UV radiation ', *Color Research & Application*, vol. 18, no. 3, pp. 226-7.

CIE 1998, *Erythema reference action spectrum and standard erythema dose*, CIE 007/E-1998, Commission Internationale de l'Éclairage, Vienna.

CIE 2014, *Rationalizing nomenclature for UV doses and effects on humans*, 211, Commission Internationale de l'Éclairage, Vienna.

Cockell, CS, Scherer, K, Horneck, G, Rettberg, P, Facius, R, Gugg-Helminger, A, Driscoll, C & Lee, P 2001, 'Exposure of arctic field scientists to ultraviolet radiation evaluated using personal dosimeters', *Photochemistry and Photobiology*, vol. 74, no. 4, pp. 570-8.

Davis, A, Deane, GH & Diffey, BL 1976, 'Possible dosimeter for ultraviolet radiation', *Nature*, vol. 261, no. 5556, pp. 169-70.

De Gruijl, F & Van der Leun, J 1994, 'Estimate of the wavelength dependency of ultraviolet carcinogenesis in humans and its relevance to the risk assessment of a stratospheric ozone depletion', *Health Physics*, vol. 67, no. 4, pp. 319-25.

Diaz, JH 2013, 'Sun exposure behavior and protection: recommendations for travelers', *Journal of Travel Medicine*, vol. 20, no. 2, pp. 108-18.

Diffey, BL, Davis, A, Johnson, M & Harrington, TR 1977a, 'A dosimeter for long wave ultraviolet radiation', *British Journal of Dermatology*, vol. 97, no. 2, pp. 127-30.

Diffey, BL, Kerwin, M & Davis, A 1977b, 'The anatomical distribution of sunlight', *British Journal of Dermatology*, vol. 97, no. 4, pp. 407-10.

Diffey, BL & Davis, A 1978, 'A new dosemeter for the measurement of natural ultraviolet radiation in the study of photodermatoses and drug photosensitivity', *Physics in Medicine and Biology*, vol. 23, no. 2, pp. 318-23.

Diffey, BL 1987, 'A comparison of dosimeters used for solar ultraviolet radiometry', *Photochemistry and Photobiology*, vol. 46, no. 1, pp. 55-60.

Diffey, BL 1989, 'Ultraviolet radiation dosimetry with polysulphone film', in BL Diffey (ed.), *Radiation measurement in Photobiology*, Academic press limitted, pp. 134-59.

Diffey, BL 1991, 'Solar ultraviolet radiation effects on biological systems', *Physics in Medicine and Biology*, vol. 36, no. 3, pp. 299-328.

Diffey, BL & Cheeseman, J 1992, 'Sun protection with hats', *British Journal of Dermatology*, vol. 127, no. 1, pp. 10-2.

Diffey, BL, Gibson, CJ, Haylock, R & McKinlay, AF 1996, 'Outdoor ultraviolet exposure of children and adolescents', *British Journal of Dermatology*, vol. 134, no. 6, pp. 1030-4.

Diffey, BL, Jansen, CT, Urbach, F & Wulf, HC 1997, 'The standard erythema dose: A new photobiological concept', *Photodermatology Photoimmunology and Photomedicine*, vol. 13, no. 1-2, pp. 64-6.

Diffey, BL 2002a, 'Sources and measurement of ultraviolet radiation', *Methods*, vol. 28, no. 1, pp. 4-13.

Diffey, BL 2002b, 'What is light?', *Photodermatology, Photoimmunology and Photomedicine*, vol. 18, no. 2, pp. 68-74.

Downs, N & Parisi, AV 2008, 'Patterns in the received facial UV exposure of school children measured at a subtropical latitude', *Photochemistry and Photobiology*, vol. 84, no. 1, pp. 90-100.

Downs, N & Parisi, AV 2009, 'Measurements of the anatomical distribution of erythemal ultraviolet: a study comparing exposure distribution to the site incidence of solar keratoses, basal cell carcinoma and squamous cell carcinoma', *Photochemical & Photobiological Sciences*, vol. 8, no. 8, pp. 1195-201.

Dunne, RP 1999, 'Polysulphone film as an underwater dosimeter for solar ultraviolet-B radiation in tropical latitudes', *Marine Ecology Progress Series*, vol. 189, pp. 53-63.

Estupiñán, JG, Raman, S, Crescenti, GH, Streicher, JJ & Barnard, WF 1996, 'Effects of clouds and haze on UV-B radiation', *Journal of Geophysical Research: Atmospheres*, vol. 101, no. D11, pp. 16807-16.

Fernando, SS, Christensen, PA, Egerton, TA & White, JR 2007, 'Carbon dioxide evolution and carbonyl group development during photodegradation of polyethylene and polypropylene', *Polymer Degradation and Stability*, vol. 92, no. 12, pp. 2163-72.

Field, LD 1995, *Organic structures from spectra*, 2 edn, John Wiley, Chichester.

Floyd, L, Newmark, J, Cook, J, Herring, L & McMullin, D 2005, 'Solar EUV and UV spectral irradiances and solar indices', *Journal of Atmospheric and Solar-Terrestrial Physics*, vol. 67, no. 1, pp. 3-15.

Foyo-Moreno, I, Alados, I, Olmo, FJ & Alados-Arboledas, L 2003, 'The influence of cloudiness on UV global irradiance (295-385 nm)', *Agricultural and Forest Meteorology*, vol. 120, no. 1-4, pp. 101-11.

Frederick, JE, Snell, HE & Haywood, EK 1989, 'Solar ultraviolet radiation at the earth's surface', *Photochemistry and Photobiology*, vol. 50, no. 4, pp. 443-50.

Frost, PC, Mack, A, Larson, JH, Bridgham, SD & Lamberti, GA 2006, 'Environmental controls of UV-B radiation in forested streams of northern Michigan', *Photochemistry and Photobiology*, vol. 82, no. 3, pp. 781-6.

Gies, P & Mackay, C 2004, 'Measurements of the solar UVR protection provided by shade structures in New Zealand primary schools', *Photochemistry and Photobiology*, vol. 80, no. 2, pp. 334-9.

Gies, P, Javorniczky, J, Roy, C & Henderson, S 2006, 'Measurements of the UVR protection provided by hats used at school', *Photochemistry and Photobiology*, vol. 82, no. 3, pp. 750-4.

Gies, P, Elix, R, Lawry, D, Gardner, J, Hancock, T, Cockerell, S, Roy, C, Javorniczky, J & Henderson, S 2007, 'Assessment of the UVR protection provided by different tree species', *Photochemistry and Photobiology*, vol. 83, no. 6, pp. 1465-70.

Grant, WB & Holick, MF 2005, 'Benefits and requirements of vitamin D for optimal health: a review', *Alternative Medicine Review*, vol. 10, no. 2, pp. 94-111.

Gróf, P, Gaspar, S & Ronto, G 1996, 'Use of uracil thin layer for measuring biologically effective UV dose', *Photochemistry and Photobiology*, vol. 64, no. 5, pp. 800-6.

Gueymard, CA 2004, 'The sun's total and spectral irradiance for solar energy applications and solar radiation models', *Solar Energy*, vol. 76, no. 4, pp. 423–53.

Gupta, D, Kumar, S, Kalsi, P, Manchanda, V & Mittal, V 2012, 'γ-Ray modifications of optical/chemical properties of a PVC polymer', *Radiation Effects and Defects in Solids*, vol. 167, no. 2, pp. 149-56.

Haigh, JD 2007, 'The Sun and the Earth's Climate', *Living Reviews in Solar Physics*, vol. 4, no. 2, pp. 1614-4961.

Hansen, JE & Travis, LD 1974, 'Light scattering in planetary atmospheres', *Space Science Reviews*, vol. 16, no. 4, pp. 527-610.

Heisler, GM & Grant, RH 2000a, *Ultraviolet radiation, human heaith, and the urban forest*, USDA Forest Service General Technical Report No. 268, Northeastern Research Station, Newtown Square, PA.

Heisler, GM & Grant, RH 2000b, 'Ultraviolet radiation in urban ecosystems with consideration of effects on human health', *Urban Ecosystems*, vol. 4, no. 3, pp. 193-229.

Herlihy, E, Gies, P, Roy, CR & Jones, M 1994, 'Personal dosimetry of solar uv radiation for different outdoor activities', *Photochemistry and Photobiology*, vol. 60, no. 3, pp. 288-94.

Hirt, RC & Searle, N 1967, 'Energy characteristics of outdoor and indoor exposure sources and their relation to the weatherability of plastics', *proceedings of the Applied Polymer Symposia*, DTIC Document, pp. 61-83.

Hockberger, PE 2002, 'A history of ultraviolet photobiology for humans, animals and microorganisms', *Photochemistry and Photobiology*, vol. 76, no. 6, pp. 561-79.

Holick, MF 2008, 'Sunlight, UV-radiation, vitamin D and skin cancer: how much sunlight do we need?', *Advances in Experimental Medicine and Biology*, vol. 624, pp. 1-15.

Holman, CDJ, Gibson, IM, Stephenson, M & Armstrong, BK 1983, 'Ultraviolet irradiation of human body sites in relation to occupation and outdoor activity: field studies using personal UVR dosimeters', *Clinical and Experimental Dermatology*, vol. 8, no. 3, pp. 269-77.

Horváth, R, Kerékgyártó, T, Csúcs, G, Gáspár, S, Illyés, P, Rontó, G & Papp, E 2001, 'The effect of UV irradiation on uracil thin layer measured by optical

waveguide lightmode spectroscopy', *Biosensors and Bioelectronics*, vol. 16, no. 1–2, pp. 17-21.

Hu, L-W, Gao, Q, Xu, W-Y, Wang, Y, Gong, H-Z, Dong, G-Q, Li, J-H & Liu, Y 2010, 'Diurnal variations in solar ultraviolet radiation at typical anatomical sites', *Biomedical and Environmental Sciences*, vol. 23, no. 3, pp. 234-43.

Huffman, RE 1992, *Atmospheric ultraviolet remote sensing*, Academic Press, Boston.

Hughes, I & Hase, T 2010, *Measurements and their uncertainties: a practical guide to modern error analysis*, Oxford University Press.

ICNIRP 2004, 'Guidelines on limits of exposure to ultraviolet radiation of wavelengths between 180 nm and 400 nm (incoherent optical radiation)', *Health Physics*, vol. 87, no. 2, pp. 171-86.

IEC 2007, *Photovoltaic devices – Part 9: Solar simulator performance requirements*, International Electrotechnical Commission, Geneva.

Ilic-Popovic, J 1966, *The use of polyvinyl-chloride film for electron beam dosimetry*, Risø 141, Research Establishment Risø, Danish Atomic Energy Commission, Roskilde, Denmark.

Ilyas, M 1987, 'Effect of the cloudiness on solar ultraviolet radiation reaching thesurface', *Atmospheric Environment*, vol. 21, no. 6, pp. 1483-4.

ISO 2007, *Space environment (natural and artificial)-Process for determining solar irradiances*, International Organization for Standardization, Geneva.

Izewska, J & Rajan, G 2005, 'Radiation dosimeters', in EB Podgorsak (ed.), *Radiation Oncology Physics*, International atomic energy agency, Vienna, pp. 71-6.

Jankowski, JJ, Kieber, DJ, Mopper, K & Neale, PJ 2000, 'Development and intercalibration of ultraviolet solar actinometers', *Photochemistry and Photobiology*, vol. 71, no. 4, pp. 431-40.

Jeong, J 2007, 'PHOTOVOLTAICS-Enhancements enable solar simulators to shed light on new photovoltaic designs-Advances to Class A solar simulators allow measurement of parameters, including current voltage, quantum efficiency, and efficiency of conversion from incident photon to charge carrier, during photovoltaic-cell design validation and certification testing', *Laser Focus World*, vol. 43, no. 3, p. 71.

Juzeniene, A, Brekke, P, Dahlback, A, Andersson-Engels, S, Reichrath, J, Moan, K, Holick, MF, Grant, WB & Moan, J 2011, 'Solar radiation and human health', *Reports on Progress in Physics*, vol. 74, no. 6, p. 066701.

Kaczmarek, H, Drag, R, Świątek, M & Ołdak, D 2002, 'The influence of UV-irradiation on poly (vinyl chloride) modified by poly (vinyl acetate)', *Surface Science*, vol. 507, pp. 877-82.

Kaczmarek, H, Kowalonek, J & Ołdak, D 2003, 'The influence of UV-irradiation on poly (vinyl chloride) modified by iron and cobalt chlorides', *Polymer Degradation and Stability*, vol. 79, no. 2, pp. 231-40.

Kaczmarek, H, Podgórski, A & Bajer, K 2005, 'Photochemical reactions in poly (vinyl chloride)/poly (vinyl alcohol) blends', *Journal of Photochemistry and Photobiology A: Chemistry*, vol. 171, no. 2, pp. 187-95.

Kattan, M, al Kassiri, H & Daher, Y 2011, 'Using polyvinyl chloride dyed with bromocresol purple in radiation dosimetry', *Applied Radiation and Isotopes*, vol. 69, no. 2, pp. 377-80.

Kemp, TJ & McIntyre, RA 2006a, 'Transition metal-doped titanium (IV) dioxide: characterisation and influence on photodegradation of poly (vinyl chloride)', *Polymer Degradation and Stability*, vol. 91, no. 1, pp. 165-94.

Kemp, TJ & McIntyre, RA 2006b, 'Influence of transition metal-doped titanium (IV) dioxide on the photodegradation of polyethylene', *Polymer Degradation and Stability*, vol. 91, no. 12, pp. 3020-5.

Kerr, JB 2005, 'Understanding the factors that affect surface ultraviolet radiation', *Optical Engineering*, vol. 44, no. 4, pp. 1-9.

Kimlin, MG, Parisi, AV & Wong, JCF 1998, 'Quantification of personal solar UV exposure of outdoor workers, indoor workers and adolescents at two locations in Southeast Queensland', *Photodermatology, Photoimmunology and Photomedicine*, vol. 14, no. 1, pp. 7-11.

Kimlin, MG 2003, 'Techniques for assessing human UV exposures', *proceedings of the Ultraviolet Ground- and Space-based Measurements, Models, and Effects III*, JR Slusser, et al. (eds.), Proc. SPIE, San Diego, pp. 197-206.

Kohler, R 1998, 'Photometric and radiometric quantitie', in C DeCusatis (ed.), *Handbook of Applied Photometry*, Optical Society of America and Springer-Verlag, New York, pp. 33-53.

Kollias, N, Baqer, A, Sadiq, I, Gillies, R & Ou-Yang, H 2003, 'Measurement of solar UVB variations by polysulphone film ', *Photochemistry and Photobiology*, vol. 78, no. 3, pp. 220-4.

Krins, A, Bolsée, D, Dörschel, B, Gillotay, D & Knuschke, P 2000, 'Angular dependence of the efficiency of the UV sensor polysulphone film', *Radiation Protection Dosimetry*, vol. 87, no. 4, pp. 261-6.

Kuhn, H, Braslavsky, S & Schmidt, R 2004, 'Chemical actinometry (IUPAC technical report)', *Pure and Applied Chemistry*, vol. 76, no. 12, pp. 2105-46.

Larena, A, Jiménez de Ochoa, S & Dominguez, F 2006, 'Dynamic-mechanical analysis of the photo-degradation of long glass fibre reinforced polypropylene: Mechanical properties' changes', *Polymer Degradation and Stability*, vol. 91, no. 4, pp. 940-6.

Lavker, RM, Gerberick, GF, Veres, D, Irwin, CJ & Kaidbey, KH 1995, 'Cumulative effects from repeated exposures to suberythemal doses of UVB and UVA in human skin', *Journal of the American Academy of Dermatology*, vol. 32, no. 1, pp. 53-62.

Lester, RA & Parisi, AV 2002, 'Spectral ultraviolet albedo of roofing surfaces and human facial exposure', *International Journal of Environmental Health Research*, vol. 12, no. 1, pp. 75-81.

Lester, RA, Parisi, AV, Kimlin, MG & Sabburg, J 2003, 'Optical properties of poly(2,6-dimethyl-1,4-phenylene oxide) film and its potential for a long-term solar ultraviolet dosimeter', *Physics in Medicine and Biology*, vol. 48, no. 22, pp. 3685-98.

Long, CS, Miller, AJ, Lee, H-T, Wild, JD, Przywarty, RC & Hufford, D 1996, 'Ultraviolet index forecasts issued by the National Weather Service', *Bulletin of the American Meteorological Society*, vol. 77, no. 4, pp. 729-48.

Madronich, S 1993, 'The atmospheric and UV-B radiation at the ground level', in AR Young (ed.), *Environmental UV photobiology*, Plenum Press, New York, pp. 1-39.

Mai, HH, Duong, ND & Kojima, T 2004, 'Dyed polyvinyl chloride films for use as high-dose routine dosimeters in radiation processing', *Radiation Physics and Chemistry*, vol. 69, no. 5, pp. 439-44.

Maláč, J, Šimůnková, E & Zelinger, J 1969, 'Properties of PVC. I. Properties of PVC films prepared by casting and by precipitation', *Journal of Polymer Science Part A-1: Polymer Chemistry*, vol. 7, no. 7, pp. 1893-904.

Martin, JW, Chin, JW & Nguyen, T 2003, 'Reciprocity law experiments in polymeric photodegradation: a critical review', *Progress in Organic Coatings*, vol. 47, no. 3, pp. 292-311.

Martin, KG & Tilley, RI 1971, 'Influence of radiation wavelength on photooxidation of unstabilized PVC', *British Polymer Journal*, vol. 3, no. 1, pp. 36-40.

Martin, KG 1973, 'Monitoring ultraviolet radiation with polyvinylchloride', *British Polymer Journal*, vol. 5, no. 6, pp. 443-50.

McCluney, WR 1994, *Introduction to radiometry and photometry*, Artech House, Boston.

McKenzie, R, Liley, B, Johnston, P, Scragg, R, Stewart, A, Reeder, AI & Allen, MW 2013, 'Small doses from artificial UV sources elucidate the photo-production of vitamin D', *Photochemical & Photobiological Sciences*, vol. 12, no. 9, pp. 1726-37.

McMichael, JR, Veledar, E & Chen, SC 2013, 'UV radiation protection by handheld umbrellas', *JAMA Dermatology* vol. 149, no. 6, pp. 757-8.

Melnikova, IN 2005, *Short-wave solar radiation in the earth's atmosphere: calculation, observation, interpretation*, Springer, Berlin.

Michalsky, J, Harrison, L & Berkheiser III, W 1995, 'Cosine response characteristics of some radiometric and photometric sensors', *Solar Energy*, vol. 54, no. 6, pp. 397-402.

Miller, A & Liqing, X 1985, *Properties of commercial PVC films with respect to electron dosimetry*, Risø National Laboratory.

Moehrle, M, Korn, M & Garbe, C 2000, 'Bacillus subtilis spore film dosimeters in personal dosimetry for occupational solar ultraviolet exposure', *International Archives of Occupational and Environmental Health*, vol. 73, no. 8, pp. 575-80.

Moehrle, M, Dennenmoser, B & Garbe, C 2003, 'Continuous long-term monitoring of UV radiation in professional mountain guides reveals extremely high exposure', *International Journal of Cancer*, vol. 103, no. 6, pp. 775-8.

Moise, A, Gies, H & Harrison, S 1999, 'Estimation of the annual solar UVR exposure dose of infants and small children in tropical Queensland, Australia', *Photochemistry and Photobiology*, vol. 69, no. 4, pp. 457-63.

Moran, DJ & Hollows, FC 1984, 'Pterygium and ultraviolet radiation: a positive correlation', *British Journal of Ophthalmology*, vol. 68, no. 5, pp. 343-6.

Morys, M & Berger, D 1993, 'Accurate measurements of biologically effective ultraviolet radiation', *proceedings of the International Symposium on High latitude Optics*, International Society for Optics and Photonics, Norway, July 1993, pp. 152-61.

Munakata, N, Morohoshi, F, Hieda, K, Suzuki, K, Furusawa, Y, Shimura, H & Ito, T 1996, 'Experimental correspondence between spore dosimetry and spectral photometry of solar ultraviolet radiation', *Photochemistry and Photobiology*, vol. 63, no. 1, pp. 74-8.

Munakata, N 1999, 'Comparative measurements of solar UV radiation with spore dosimetry at three European and two Japanese sites', *Journal of Photochemistry and Photobiology B: Biology*, vol. 53, no. 1–3, pp. 7-11.

Munakata, N, Makita, K, Bolsee, D, Gillotay, D & Horneck, G 2000, 'Spore dosimetry of solar UV radiation: applications to monitoring of daily irradiance and personal exposure', *Advances in Space Research*, vol. 26, no. 12, pp. 1995-2003.

Naggar, SE, Gustat, H, Magister, H & Rochlitzer, R 1995, 'An electronic personal UV-B-dosimeter', *Journal of Photochemistry and Photobiology B: Biology*, vol. 31, no. 1–2, pp. 83-6.

Newport n.d., *Cornerstone™ 260 1/4 m Monochromator*, viewed 05/10/2013, http://www.newport.com/Cornerstone153-260-1-4-m-Monochromator/375108/1033/info.aspx#tab_Specifications.

Norval, M, Lucas, RM, Cullen, AP, de Gruijl, FR, Longstreth, J, Takizawa, Y & van der Leun, JC 2011, 'The human health effects of ozone depletion and interactions with climate change', *Photochemical & Photobiological Sciences* vol. 10, no. 2, pp. 199-225.

O'Riordan, DL, Stanton, WR, Eyeson-Annan, M, Gies, P & Roy, C 2000, 'Correlations between reported and measured ultraviolet radiation exposure of mothers and young children', *Photochemistry and Photobiology*, vol. 71, no. 1, pp. 60-4.

O'Shea, JG 1996, 'Environmental factors in the epidemiology and aetiology of malignant tumours of the eye', *Clinical and Experimental Optometry*, vol. 79, no. 5, pp. 177-85.

Parisi, AV, Kimlin, MG, Wong, JCF & Fleming, R 1996a, 'The effects of body size and orientation on ultraviolet radiation exposure', *Photodermatology, Photoimmunology and Photomedicine*, vol. 12, no. 2, pp. 66-72.

Parisi, AV, Wong, JCF & Galea, V 1996b, 'A method for evaluation of UV and biologically effective exposures to plants', *Photochemistry and Photobiology*, vol. 64, no. 2, pp. 326-33.

Parisi, AV & Kimlin, MG 2000, 'Effect of meal break times on solar UV exposure to schoolchildren in a Southeast Queensland summer month', *Environmetrics*, vol. 11, no. 5, pp. 563-70.

Parisi, AV & Wong, JCF 2000, 'An estimation of biological hazards due to solar radiation', *Journal of Photochemistry and Photobiology B: Biology*, vol. 54, no. 2-3, pp. 126-30.

Parisi, AV & Kimlin, MG 2003, 'Extending the dynamic range of polysulphone for measuring UV exposures', *proceedings of the Optical Science and Technology, SPIE's 48th Annual Meeting*, International Society for Optics and Photonics, pp. 188-96.

Parisi, AV 2004, 'Solar UV radiation measurements with polysulphone', *Chemistry in Australia*, vol. 71, no. 2, pp. 16-8.

Parisi, AV & Kimlin, MG 2004, 'Personal solar UV exposure measurements employing modified polysulphone with an extended dynamic range', *Photochemistry and Photobiology*, vol. 79, no. 5, pp. 411-5.

Parisi, AV, Sabburg, J & Kimlin, MG 2004, *Scattered and filtered solar UV measurements*, Kluwer Academic, Dordrecht.

Parisi, AV, Schouten, PW, Downs, NJ & Turner, J 2010a, 'Solar UV exposures measured simultaneously to all arbitrarily oriented leaves on a plant', *Journal of Photochemistry and Photobiology B: Biology*, vol. 99, no. 2, pp. 87-92.

Parisi, AV, Schouten, PW & Turnbull, DJ 2010b, 'UV dosimeter based on polyphenylene oxide for the measurement of UV exposures to plants and humans over extended periods', *proceedings of the NIWA 2010 UV Workshop: UV Radiation and its Effects - an Update 2010*, Queenstown, New Zealand, 7-9 May 2010 pp. 78-9.

Patrick, S 2005, *Practical guide to polyvinyl chloride*, Rapra Technology Limited, Shrewsbury, UK.

Persson, L 1991, 'On the boundary between ionizing and nonionizing radiation', *Health Physics*, vol. 60, no. 5, pp. 929-32.

Platt, U, Pfeilsticker, K & Vollmer, M 2007, 'Radiation and optics in the atmosphere', in F Träge (ed.), *Springer Handbook of Lasers and Optics*, Springer, New York, pp. 1165-203.

Powers, JG & Gilchrest, BA 2012, 'What you and your patients need to know about vitamin D', *Seminars in Cutaneous Medicine and Surgery*, vol. 31, no. 1, pp. 2-10.

Prasad, AV, Thanki, P & Singh, R 1997, 'Photo-and thermooxidative degradation of polyethylene-polypropylene blends: Comparison of oxidation products', *Journal of Macromolecular Science, Part A: Pure and Applied Chemistry*, vol. 34, no. 2, pp. 349-59.

Qiang, F 2003, 'Radiation (Solar)', in JR Holton, et al. (eds), *Encyclopedia of atmospheric sciences 5*, Academic Press, Amsterdam, pp. 1859–63.

Qin, H, Zhang, S, Liu, H, Xie, S, Yang, M & Shen, D 2005, 'Photo-oxidative degradation of polypropylene/montmorillonite nanocomposites', *Polymer*, vol. 46, no. 9, pp. 3149-56.

Rabe, JH, Mamelak, AJ, McElgunn, PJ, Morison, WL & Sauder, DN 2006, 'Photoaging: mechanisms and repair', *Journal of the American Academy of Dermatology*, vol. 55, no. 1, pp. 1-19.

Rasheed, R, Mansoor, H, Yousif, E, Hameed, A, Farina, Y & Graisa, A 2009, 'Photostabilizing of PVC films by 2-(aryl)-5-[4-(aryloxy)-phenyl]-1, 3, 4-oxadiazole compounds', *European Journal of Scientific Research*, vol. 30, no. 3, pp. 464-77.

Reinisch, RF, Gloria, HR & Wilson, DE 1966, 'A kinetic study of the photodegradation of poly(vinyl chloride) film in vacuum', *American Chemical Society Preprint*, vol. 7, no. 1, pp. 1-29.

Rettberg, P & Cockell, CS 2004, 'Biological UV dosimetry using the DLR-biofilm', *Photochemical & Photobiological Sciences*, vol. 3, no. 8, pp. 781-7.

Rhodes, LE, Webb, AR, Fraser, HI, Kift, R, Durkin, MT, Allan, D, O'Brien, SJ, Vail, A & Berry, JL 2010, 'Recommended summer sunlight exposure levels can produce sufficient (> or = 20 ng/ml) but not the proposed optimal (> or = 32 ng/ml) 25 (OH)D levels at UK latitudes', *Journal of Investigative Dermatology*, vol. 130, no. 5, pp. 1411-8.

Rigel, EG, Lebwohl, M, Rigel, AC & Rigel, DS 2003a, 'Daily UVB exposure levels in high-school students measured with digital dosimeters', *Journal of the American Academy of Dermatology*, vol. 49, no. 6, pp. 1112-4.

Rigel, EG, Lebwohl, MG, Rigel, AC & Rigel, DS 2003b, 'Ultraviolet radiation in alpine skiing: magnitude of exposure and importance of regular protection', *Archives of Dermatology*, vol. 139, no. 1, pp. 60-2.

Riva, A, Algaba, I, Pepió, M & Prieto, R 2009, 'Modeling the effects of color on the UV protection provided by cotton woven fabrics dyed with azo dyestuffs', *Industrial & Engineering Chemistry Research*, vol. 48, no. 22, pp. 9817-22.

Roberts, JE 2011, 'Ultraviolet radiation as a risk factor for cataract and macular degeneration', *Eye & Contact Lens*, vol. 37, no. 4, pp. 246-9.

Rontó, G, Gáspár, S & Bérces, A 1992, 'Phages T7 in biological UV dose measurements', *Journal of Photochemistry and Photobiology B: Biology*, vol. 12, no. 3, pp. 285-94.

Rontó, G, Bérces, A, Fekete, A, Kovács, G, Gróf, P & Lammer, H 2004, 'Biological UV dosimeters in simulated space conditions', *Advances in Space Research*, vol. 33, no. 8, pp. 1302-5.

Ross, AC, Manson, JE, Abrams, SA, Aloia, JF, Brannon, PM, Clinton, SK, Durazo-Arvizu, RA, Gallagher, JC, Gallo, RL, Jones, G, Kovacs, CS, Mayne, ST, Rosen, CJ & Shapses, SA 2011, 'The 2011 report on dietary reference intakes for calcium and vitamin D from the Institute of Medicine: what clinicians need to know', *Journal of Clinical Endocrinology and Metabolism*, vol. 96, no. 1, pp. 53-8.

Sabaa, MW, Oraby, EH, Abdel Naby, AS & Mohamed, RR 2005, 'Anthraquinone derivatives as organic stabilizers for rigid poly (vinyl chloride) against photo-degradation', *European Polymer Journal*, vol. 41, no. 11, pp. 2530-43.

Sabburg, JM & Parisi, AV 2006, 'Spectral dependency of cloud enhanced UV irradiance', *Atmospheric Research*, vol. 81, no. 3, pp. 206-14.

Schafer, JS, Saxena, VK, Wenny, BN, Barnard, W & De Luisi, JJ 1996, 'Observed influence of clouds on ultraviolet-B radiation', *Geophysical Research Letters*, vol. 23, no. 19, pp. 2625-8.

Schmalwieser, AW, Enzi, C, Wallisch, S, Holawe, F, Maier, B & Weihs, P 2010a, 'UV exposition during typical lifestyle behavior in an urban environment', *Photochemistry and Photobiology*, vol. 86, no. 3, pp. 711-5.

Schmalwieser, AW, Cabaj, A, Schauberger, G, Rohn, H, Maier, B & Maier, H 2010b, 'Facial solar UV exposure of Austrian farmers during occupation', *Photochemistry and Photobiology*, vol. 86, no. 6, pp. 1404-13.

Schnabel, W 1981, *Polymer degradation: principles and practical applications*, Hanser International, Munich.

Schouten, PW, Parisi, AV & Turnbull, DJ 2007, 'Application of poly (2, 6-dimethyl-1, 4-phenylene oxide) film for the long-term measurement of underwater solar UVB', *proceedings of the UV Conference "One Century of the UV Radiation Research"*, Davos,

Schouten, PW, Parisi, AV & Turnbull, DJ 2008, 'Field calibrations of a long-term UV dosimeter for aquatic UVB exposures', *Journal of Photochemistry and Photobiology B: Biology*, vol. 91, no. 2-3, pp. 108-16.

Schouten, PW, Parisi, AV & Turnbull, DJ 2009, 'Applicability of the polyphenylene oxide film dosimeter to high UV exposures in aquatic environments', *Journal of Photochemistry and Photobiology B: Biology*, vol. 96, no. 3, pp. 184-92.

Schouten, PW, Parisi, AV & Turnbull, DJ 2010, 'Usage of the polyphenylene oxide dosimeter to measure annual solar erythemal exposures', *Photochemistry and Photobiology*, vol. 86, no. 3, pp. 706-10.

Schouten, PW & Parisi, AV 2012, 'Underwater deployment of the polyphenylene oxide dosimeter combined with a neutral density filter to measure long-term solar UVB exposures', *Journal of Photochemistry and Photobiology B: Biology*, vol. 112, pp. 31-6.

Schwartz, GG & Hanchette, CL 2006, 'UV, latitude, and spatial trends in prostate cancer mortality: all sunlight is not the same (United States)', *Cancer Causes and Control*, vol. 17, no. 8, pp. 1091-101.

Seckmeyer, G, Klingebiel, M, Riechelmann, S, Lohse, I, McKenzie, RL, Liley, JB, Allen, MW, Siani, AM & Casale, GR 2012, 'A critical assessment of two types of personal UV dosimeters', *Photochemistry and Photobiology*, vol. 88, no. 1, pp. 215-22.

Sekelj, S, Dekaris, I, Kondža-Krstonijević, E, Gabrić, N, Predović, J & Mitrović, S 2007, 'Ultraviolet light and pterygium', *Collegium Antropologicum*, vol. 31, no. 1, pp. 45-7.

Serrano, MA, Canada, J & Moreno, JC 2010, 'Erythemal ultraviolet exposure of cyclists in Valencia, Spain', *Photochemistry and Photobiology*, vol. 86, no. 3, pp. 716-21.

Serrano, MA, Canada, J & Moreno, JC 2011, 'Solar UV exposure of primary schoolchildren in Valencia, Spain', *Photochemical & Photobiological Sciences*, vol. 10, no. 4, pp. 523-30.

Setlow, RB 1974, 'The wavelengths in sunlight effective in producing skin cancer: a theoretical analysis', *Proceedings of the National Academy of Sciences*, vol. 71, no. 9, pp. 3363-6.

Shi, W, Zhang, J, Shi, XM & Jiang, GD 2008, 'Different photodegradation processes of PVC with different average degrees of polymerization', *Journal of Applied Polymer Science*, vol. 107, no. 1, pp. 528-40.

Shimadzu 1994, *User's system guide uv-1601 Shimadzu recording spectrophotometer*, Shimadzu Corporation, Japan.

Siani, AM, Casale, GR, Diémoz, H, Agnesod, G, Kimlin, MG, Lang, CA & Colosimo, A 2008, 'Personal UV exposure in high albedo alpine sites', *Atmospheric Chemistry and Physics*, vol. 8, no. 14, pp. 3749-60.

Siani, AM, Casale, GR, Sisto, R, Borra, M, Kimlin, MG, Lang, CA & Colosimo, A 2009, 'Short-term UV exposure of sunbathers at a Mediterranean Sea site', *Photochemistry and Photobiology*, vol. 85, no. 1, pp. 171-7.

Siani, AM, Casale, GR, Sisto, R, Colosimo, A, Lang, CA & Kimlin, MG 2011, 'Occupational exposures to solar ultraviolet radiation of vineyard workers in Tuscany (Italy)', *Photochemistry and Photobiology*, vol. 87, no. 4, pp. 925-34.

Sliney, DH & Chaney, E 2006, 'Basic concepts of radiation', in F Ghetti, et al. (eds), *Environmental UV radiation impact on ecosystems and human health and predictive models*, Springer, Dordrecht, pp. 5-23.

Sliney, DH 2007, 'Radiometric quantities and units used in photobiology and photochemistry: Recommendations of the Commission Internationale de l'Eclairage (International Commission on Illumination)', *Photochemistry and Photobiology*, vol. 83, no. 2, pp. 425-32.

Smith, BC 1996, *Fundamentals of Fourier transform infrared spectroscopy*, CRC Press, Boca Raton.

Sobolewski, P, Jaroslawski, J & Stebel, K 2008, 'Measurements of UV radiation on rotating vertical plane at the ALOMAR Observatory (69° N, 16° E), Norway, June 2007', *Atmospheric Chemistry and Physics*, vol. 8, no. 12, pp. 3033-43.

Steeneken, SF, Buma, AG & Gieskes, WW 1995, 'Changes in transmission characteristics of polymethylmethacrylate and cellulose (III) acetate during exposure to ultraviolet light', *Photochemistry and Photobiology*, vol. 61, no. 3, pp. 276-80.

Sun, SF 2004, *Physical chemistry of macromolecules: Basic principles and issues*, 2 edn, John Wiley & Sons, Hoboken, New Jersey.

Tarrant, AWS 1989, 'Basic principles of light measurements', in BL Diffey (ed.), *Radiation measurement in Photobiology*, Academic Press Limited, London, pp. 1-21.

Tate, TJ, Diffey, BL & Davis, A 1980, 'An ultraviolet radiation dosimeter based on the photosensitising drug, Nalidixic acid', *Photochemistry and Photobiology*, vol. 31, no. 1, pp. 27-30.

Terenetskaya, I 2000, 'Spectral monitoring of biologically active solar UVB radiation using an in vitro model of vitamin D synthesis', *Talanta*, vol. 53, no. 1, pp. 195-203.

Terenetskaya, I 2003, 'Solar UV-B dosimetry in situ with 'D-dosimeter': effect of ozone depletion on the Vitamin D synthetic capacity of sunlight', *Agricultural and Forest Meteorology*, vol. 120, no. 1–4, pp. 45-50.

Torikai, A & Hasegawa, H 1999, 'Accelerated photodegradation of poly (vinyl chloride)', *Polymer Degradation and Stability*, vol. 63, no. 3, pp. 441-5.

Turnbull, DJ & Schouten, PW 2007, 'Development of a long term solar UVA dosimeter', *proceedings of the UV Conference "One Century of the UV Radiation Research"*, Davos, pp. 53-4.

Turnbull, DJ & Schouten, PW 2008, 'Utilising polyphenylene oxide for high exposure solar UVA dosimetry', *Atmospheric Chemistry and Physics*, vol. 8, no. 10, pp. 2759-62.

Turner, J, Parisi, AV & Turnbull, DJ 2009, 'Dosimeter for the measurement of plant damaging solar UV exposures', *Agricultural and Forest Meteorology*, vol. 149, no. 8, pp. 1301-6.

Vázquez, M & Hanslmeier, A 2006, *Ultraviolet radiation in the solar system*, vol. 331, Springer.

Vecchia, P, Hietanen, M, Stuck, BE, Deventer, EV & Niu, S 2007, *Protecting workers from ultraviolet radiation*, International Commission on Non-Ionizing Radiation Protection ICNIRP 14/2007, Oberschleißheim, Germany.

Weatherhead, B, Tanskanen, A & Stevermer, A 2005, 'Ozone and ultraviolet radiation', in ACIA (ed.), *Arctic Climate Impact Assessment - Scientific Report*, Cambridge University Press, pp. 151-82.

Webb, AR & Holick, MF 1988, 'The role of sunlight in the cutaneous production of vitamin D_3', *Annual Review of Nutrition*, vol. 8, no. 1, pp. 375-99.

Webb, AR, Pilbeam, C, Hanafin, N & Holick, MF 1990, 'An evaluation of the relative contributions of exposure to sunlight and of diet to the circulating concentrations of 25-hydroxyvitamin D in an elderly nursing home population in Boston', *The American Journal of Clinical Nutrition*, vol. 51, no. 6, pp. 1075-81.

Webb, AR 1995, 'Measuring UV radiation: a discussion of dosimeter properties, uses and limitations', *Journal of Photochemistry and Photobiology B: Biology*, vol. 31, no. 1, pp. 9-13.

Webb, AR & Engelsen, O 2006, 'Calculated ultraviolet exposure levels for a healthy vitamin D status', *Photochemistry and Photobiology*, vol. 82, no. 6, pp. 1697-703.

Weihs, P, Webb, AR, Hutchinson, SJ & Middleton, GW 2000, 'Measurements of the diffuse UV sky radiance during broken cloud conditions', *Journal of Geophysical Research: Atmospheres (1984–2012)*, vol. 105, no. D4, pp. 4937-44.

Weihs, P, Schmalwieser, A, Reinisch, C, Meraner, E, Walisch, S & Harald, M 2013, 'Measurements of personal UV exposure on different parts of the body during various activities', *Photochemistry and Photobiology*, vol. 89, no. 4, pp. 1004-7.

WHO 1979, *Environmental health criteria 14: Ultraviolet radiation*, World Health Organization, Geneva.

WHO 1994, *Environmental health criteria 160: Ultraviolet radiation*, World Health Organization, Geneva.

Wiles, D & Carlsson, D 1980, 'Photostabilisation mechanisms in polymers: A review', *Polymer Degradation and Stability*, vol. 3, no. 1, pp. 61-72.

Wirth, H & Andreas, H 1977, 'The stabilization of PVC against heat and light', *Pure and Applied Chemistry*, vol. 49, no. 5, pp. 627-48.

Wlodarczyk, J, Whyte, P, Cockrum, P & Taylor, H 2001, 'Pterygium in Australia: a cost of illness study', *Clinical & Experimental Ophthalmology*, vol. 29, no. 6, pp. 370-5.

Wong, JCF, Fleming, RA, Carter, SJ, Ring, IT & Vishvakarman, D 1992, 'Measurement of human exposure to ultraviolet-B solar radiation using a CR-39 dosimeter', *Health Physics*, vol. 63, no. 4, pp. 457-61.

Wulf, HC & Gniadecka, M 1996a, 'CaF_2:Dy and CaF_2 crystal-based UV dosimeters', *Skin Research and Technology*, vol. 2, no. 3, pp. 108-13.

Wulf, HC & Gniadecka, M 1996b, 'Electronic UV dosimeters', *Skin Research and Technology*, vol. 2, no. 3, pp. 103-7.

Wypych, G 2008, *PVC: Degradation & Stabilization*, 2 edn, ChemTec Publishing, Toronto.

Wypych, J 1985, *Polyvinyl chloride degradation*, Elsevier Science Publishers, Amsterdam.

Yam, J & Kwok, A 2014, 'Ultraviolet light and ocular diseases', *International Ophthalmology*, vol. 34, no. 2, pp. 383-400.

Yan, W, Zhang, L-L, Yan, L, Zhang, F, Yin, N-B, Lin, H-B, Huang, C-Y, Wang, L, Yu, J, Wang, D-M & Zhao, Z-M 2013, 'Transcriptome analysis of skin photoaging in Chinese females reveals the involvement of skin homeostasis and metabolic changes', *PLoS ONE*, vol. 8, no. 4, pp. 1-10.

Ye, X, Pi, H & Guo, S 2010, 'A novel route for preparation of PVC sheets with high UV irradiation resistance', *Journal of Applied Polymer Science*, vol. 117, no. 5, pp. 2899-906.

Yi, C, Sun, Y, Pi, H & Guo, S 2011, 'Low-temperature UV irradiation induced the color change kinetics and the corresponding structure development of PVC film', *Journal of Applied Polymer Science*, vol. 122, no. 4, pp. 2588-93.

Zhang, X, Pi, H & Guo, S 2012, 'The effect of high intensity UV irradiation on color behavior of poly (vinyl chloride)', *Journal of Macromolecular Science, Part B*, vol. 51, no. 7, pp. 1303-21.

Zweifel, H, Maier, RD & Schiller, M 2009, *Plastics additives handbook*, 6 edn, Hanser-Gardner Publications, Ohio, USA.

Appendix A – Pilot Study

A.1 Introduction

The deterioration of some synthetic polymers (plastics) during outdoors application has long been a subject of intensive study. UV radiation has been identified as the main factor in this deterioration. The proposed mechanism, in general, is that the energy of UV radiation is high enough to initiate the formation of free radicals within the polymer by the breakage of some of its molecular bonds and then to activate a series of complex reactions that lead to a severe change in the microstructure and bulk properties of the polymer (Schnabel 1981). Research that has been conducted to minimise this effect of UV radiation is a reliable source of information for polymers that can be tested for use as UV dosimeters. UV-induced changes in unstabilized polymers such as poly (Vinyl Chloride) (PVC), polyethylene (PE), polypropylene (PP) and cellulose acetate (CA) have been reported in the literature.

Previous studies have confirmed the susceptibility of unstabilised PVC sheets to photo-degradation (Kaczmarek et al. 2003; Kemp & McIntyre 2006a; Martin & Tilley 1971; Rasheed et al. 2009; Shi et al. 2008; Ye et al. 2010). Changes have been reported in the IR absorption spectra of unstabilised PVC samples after exposure to UV radiation for periods up to 15 days. Also, the photo-degradation of PE and PP have been studied by infrared spectroscopy (Fernando et al. 2007; Kemp & McIntyre 2006b; Larena et al. 2006; Prasad et al. 1997; Qin et al. 2005) and chemical changes in these polymers have been confirmed. Moreover, CA, which has been employed in UV research as a UVC cut-off filter, experiences changes in its optical transmission after lengthy exposure to UV radiation (Parisi et al. 1996b; Steeneken et al. 1995), indicating that it could be suitable as a UV monitor.

Therefore, PVC, PE, PP and CA have been nominated to be investigated for use as long-term UV dosimeters.

A.2 Investigation of candidate polymers

To investigate the response of candidate polymers to UV radiation, PVC dosimeters were constructed at the University of Southern Queensland, Toowoomba, Australia from a 40 µm thin film. The 40 µm thickness was selected as it has been identified in previous research (Davis et al. 1976; Lester et al. 2003) as a suitable thickness for PS and PPO dosimeters that balances the durability of the chemical dosimeter and its sensitivity to UV radiation.

PVC thin film sheets were prepared by dissolving a suitable amount of PVC powder (Aldrich Chemical Company, Inc., catalogue number 34675-6) in 50 ml of Tetrahydrofuran for 24 hours. A polymer casting-table was employed to spread the

solution into a thin layer, leaving a thin film polymer sheet, after evaporation of the solvent at room temperature.

PP and PE sheets were purchased from Dolphin Plastics and Packaging, Warana, Qld, while CA sheets were purchased from Artery, Tasmania.

Dosimeters were fabricated by cutting the polymer sheets into 2 cm width square pieces. Each piece was attached by tape to a 3 cm width hard plastic square holder with a 1.8 cm × 1.2 cm aperture (Figure A.1).

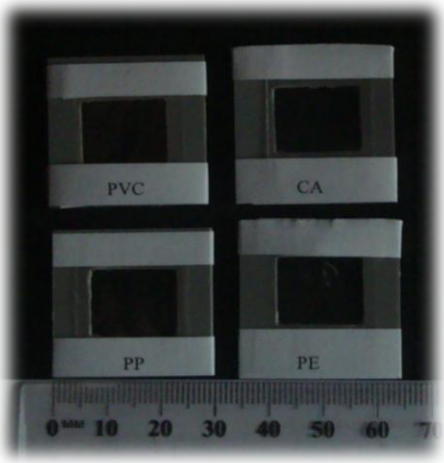

Figure A.1: The shape and dimensions of fabricated dosimeters

A UV fluorescent lamp (model Philips TL40/12, supplier Lawrence and Hansen, Toowoomba) was employed to examine the response of the candidate polymers to UV radiation. The output of this lamp is predominantly UVB with a lower output in the UVA. The spectral irradiance of the lamp on the exposure site was measured using a portable spectroradiometer (model USB4000, Ocean Optics). The pre exposure IR absorption spectra for a set of 35 PVC, PP, PE and CA dosimeters were obtained within the range 400–4000 cm^{-1} using a Fourier Transform Infrared (FTIR) spectrophotometer (IRPrestige-21/FTIR-8400S, Shimadzu Co., Kyoto). Following that, the dosimeters were placed on a black board and subjected to even and continuous exposure at room temperature for different periods of time; the UV spectral irradiance was recorded at 1–5 hours intervals. The exposure time of dosimeters ranged between one hour and 248 hours. The post exposure IR absorption spectra were measured immediately.

The analysis and comparison of the recorded IR spectra showed that exposure-related changes in some peaks of PVC's spectra were proportional to exposure time. There was no detectable change with accumulative trend in IR spectra of PP, PE and CA dosimeters. These polymers were purchased from a commercial supplier and there was originally some concern that they may contain UV absorption additives or stabilizers.

To confirm the encouraging preliminary results of PVC, nine PVC dosimeters were placed on the exposure area at 7 cm from the UV fluorescent lamp; for control, three of them were covered with opaque cardboard, which prevents all wavelengths from reaching the dosimeters, and three with a UV cut-off filter (Llumar, Scotchline, Australia) that blocks wavelengths <400 nm from reaching the dosimeters. The pre-exposure IR absorption spectra of the dosimeters were measured and then the dosimeters were exposed to the lamp at a controlled temperature (22 ± 1 ◦C) for more than 300 h, receiving a total UV exposure dose of about 12 MJ m^{-2}. The dosimeters were removed from exposure for the measurement of the IR absorption spectra at various exposure time intervals. The recorded IR absorption spectra were then compared and analysed.

Further investigation in an outdoor environment was undertaken for the PVC dosimeters. Three PVC dosimeters were exposed to solar radiation over 23 non-consecutive days (because of weather conditions) on a horizontal unshaded plane on the roof of a USQ building between 31st January 2011 and 7th April 2011. The maximum temperature during the exposure days ranged between 20 and 30 ◦C; and the sky was almost clear of clouds on 14 d, 7 d were partly cloudy and 2 were mostly cloudy accompanied by light showers (<1 mm). The erythemal solar UV doses were measured near the dosimeters' site by a calibrated erythemal UV meter (model 501 Biometer, Solar Light Co., PA, USA), recording the cumulative erythemal UV dose every 5 min. For the 23 exposure days, the IR absorption spectra were measured in the early morning prior to exposure for the day and then the dosimeters were exposed for 5–7 h until late afternoon with the post-exposure IR absorption spectra being immediately recorded at the end of the exposure. The dosimeters were then covered and kept in a UV-free environment until the next exposure day.

A.3 Results and conclusions

The comparison of the IR absorption spectra of the PVC dosimeters that were exposed to the UV fluorescent lamp showed two major changes. These are the appearance (and then an increase) of the 1724 cm^{-1} peak and the decrease in the 1064 cm^{-1} peak (Figure A.2).

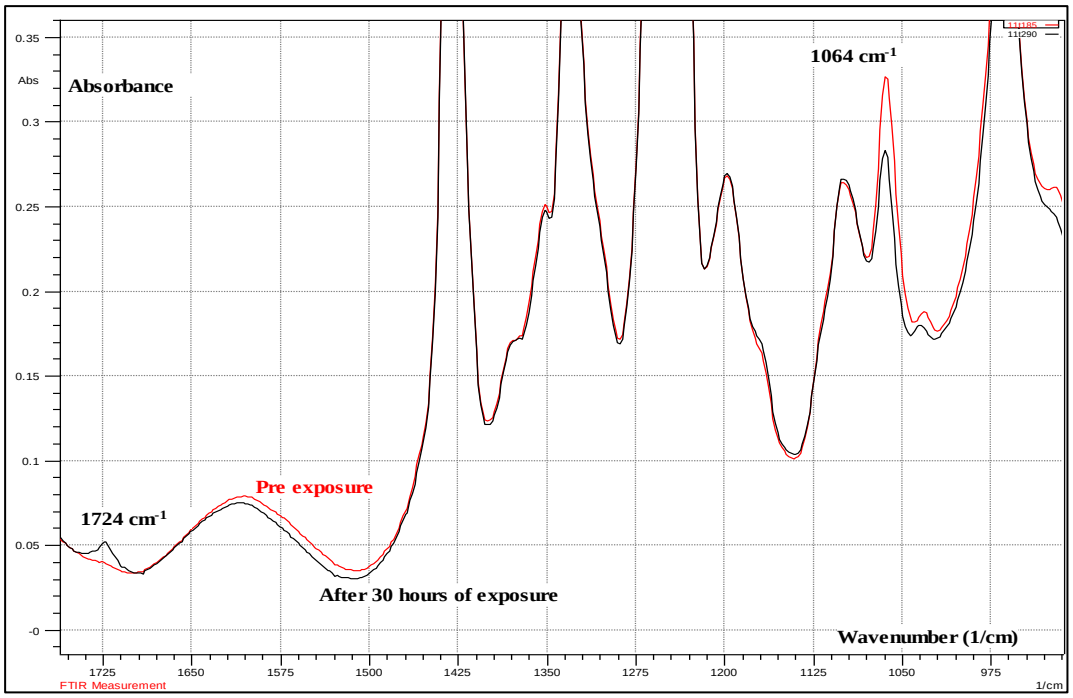

Figure A.2: Changes in 1724 cm^{-1} and 1064 cm^{-1} peaks of IR absorption spectrum of the PVC dosimeter due to 30 hours of exposure to artificial UV radiation.

There was a fluctuation in the change of the 1724 cm^{-1} peak with no clear trend. The 1064 cm^{-1} peak showed a monotonic decrease as the radiant exposure increased (Figure A.3) and, therefore, has been chosen as an indicator to quantify the UV-induced changes in the PVC dosimeter.

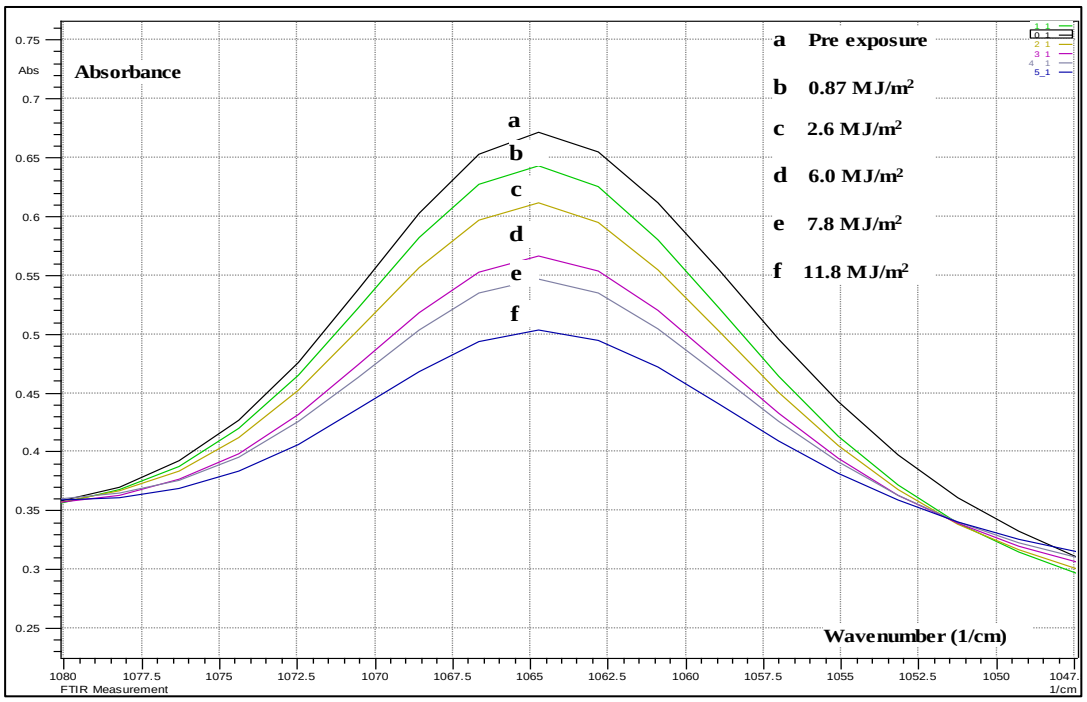

Figure A.3: Changes in the 1064 cm^{-1} peak of IR absorption spectrum of the PVC dosimeter due to exposure to artificial UV radiation.

For the laboratory investigation, the initial absorbance of the nine dosimeters at 1064 cm^{-1} ($A^{initial}$) was measured immediately before the first exposure. The post exposure absorbance (A_t^{final}) , where t is the length of exposure period, of the dosimeters was also measured at regular time intervals as well as the spectral irradiance of the UV lamp at the dosimeters' position.

The change in the absorption intensity $(\Delta A)_t$ at 1064 cm^{-1} of the dosimeters after a period t of exposure was calculated by $(\Delta A)_t = A^{initial} - A_t^{final}$ and averaged for each group of dosimeters. The change was then related to the corresponding unweighted UV radiant exposure over 280–400 nm in MJ/m^2, along with the absorbance changes that occurred at the same time in the control dosimeters (Figure A.4).

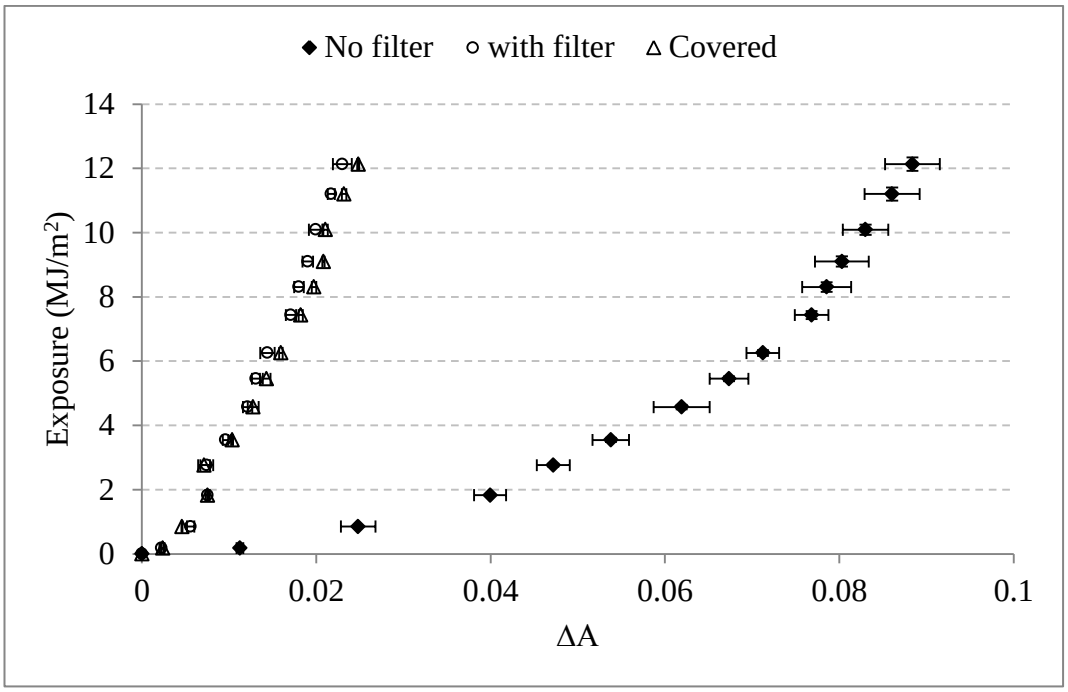

Figure A.4: The change in 1064 cm^{-1} peak intensity of the PVC dosimeter with the increase of unweighted exposure received from the artificial UV in (MJ/m^2).

As can be seen in Figure A.4, there was a regular increase in the absorbance change of the UV-irradiated dosimeters with an increase in radiant exposure. The unexposed dosimeters showed a slight absorbance change which could be attributed to thermal degradation. This change can be disregarded since it is small and already included in the total change of the exposed dosimeters. The curve that represents the dosimeters which have been covered with the UV cut-off filter is the same as that of the unexposed dosimeters, indicating that the dosimeters did not respond to the radiation for wavelengths beyond the UV band (> 400 nm). The short error bars of the averaged measurements reflect the high reproducibility of dosimeters that received the same dose or experienced the same conditions.

Each of the three PVC dosimeters, which were simultaneously exposed to solar UV radiation for 23 days, showed a gradual decrease in the absorption intensity at 1064 cm^{-1} as the exposure time was increased. The change (ΔA) and percentage change (ΔA)% in the absorption intensity of the dosimeters at 1064 cm^{-1} were calculated and averaged, and then related to the corresponding UV exposure dose in SED (Standard Erythema Dose = 100 J/m^2), as shown in Figure A.5 and Figure A.6.

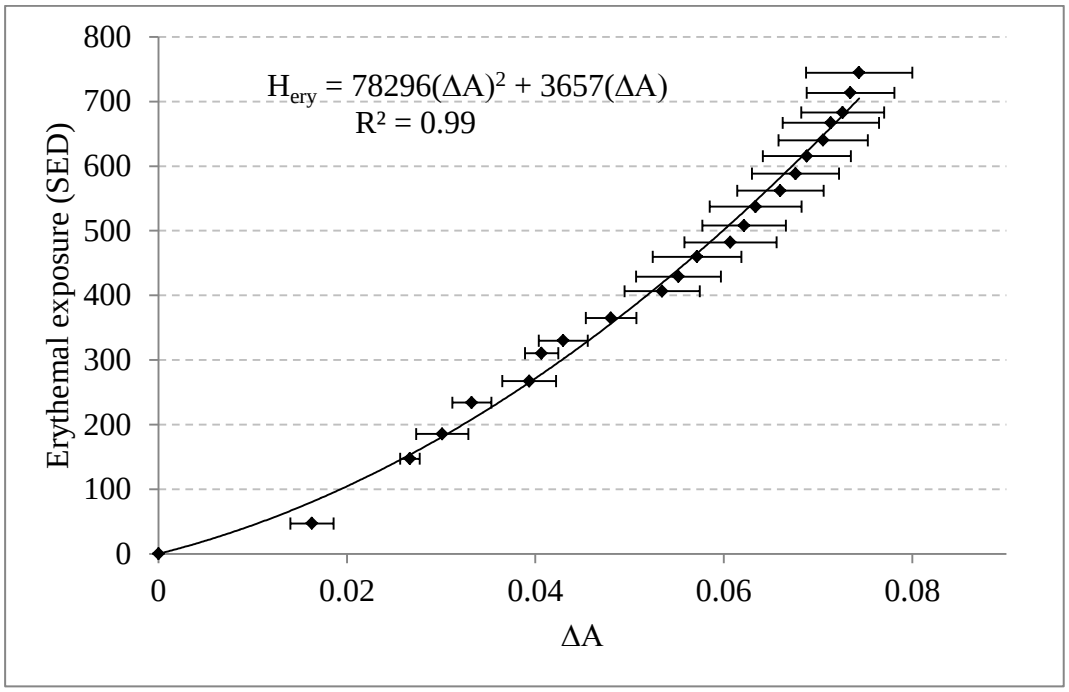

Figure A.5: Dose response of the PVC dosimeter to solar radiation. The error bars show the standard error of each point.

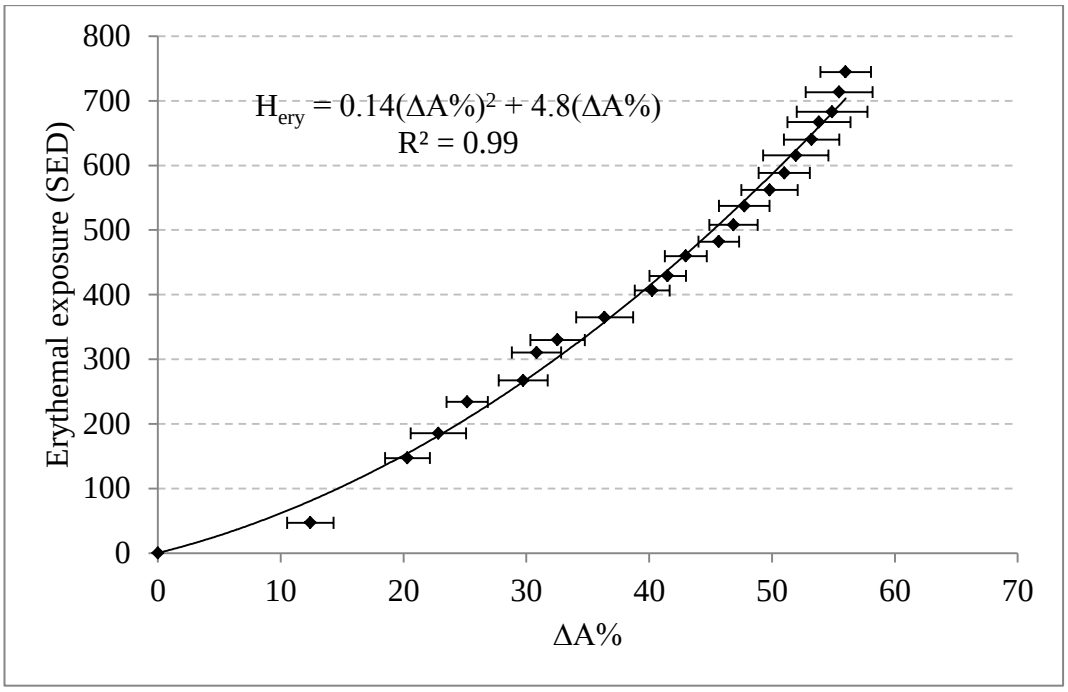

Figure A.6: The percentage change in 1064 cm^{-1} peak intensity of the PVC dosimeter with the increase of erythemal exposure to solar UV.

The comparison of the two figures shows that the deviation from the mean value of the absorbance change could be reduced by using the percentage change instead of the absolute change. The reason is that the change depends not only on the UV exposure but also on the initial absorbance. After 23 days of exposure, the dosimeters were subjected to a total dose of 745 SED, which is equivalent to about two to three weeks of exposure under clear sky conditions in summer at subtropical sites and, as they were not saturated, this pilot study indicates that the dosimeters may be able to respond to longer exposures.

The preliminary results of the response of PVC to UV radiation indicate that the PVC based UV dosimeter can be calibrated to measure hundreds of hours of exposure to an artificial UV source and also at least three weeks of exposure to solar UV radiation. This large dose capacity encourages further investigation on the physical and dosimetric properties of the proposed PVC dosimeter.